



National Library of Canada

Cataloguing Branch
Canadian Theses Division

Ottawa, Canada
K1A 0N4

Bibliothèque nationale du Canada

Direction du catalogage
Division des thèses canadiennes

NOTICE

The quality of this microfiche is heavily dependent upon the quality of the original thesis submitted for microfilming. Every effort has been made to ensure the highest quality of reproduction possible.

If pages are missing, contact the university which granted the degree.

Some pages may have indistinct print especially if the original pages were typed with a poor typewriter ribbon or if the university sent us a poor photocopy.

Previously copyrighted materials (journal articles, published tests, etc.) are not filmed.

Reproduction in full or in part of this film is governed by the Canadian Copyright Act, R.S.C. 1970, c. C-30. Please read the authorization forms which accompany this thesis.

**THIS DISSERTATION
HAS BEEN MICROFILMED
EXACTLY AS RECEIVED**

AVIS

La qualité de cette microfiche dépend grandement de la qualité de la thèse soumise au microfilmage. Nous avons tout fait pour assurer une qualité supérieure de reproduction.

S'il manque des pages, veuillez communiquer avec l'université qui a conféré le grade.

La qualité d'impression de certaines pages peut laisser à désirer, surtout si les pages originales ont été dactylographiées à l'aide d'un ruban usé ou si l'université nous a fait parvenir une photocopie de mauvaise qualité.

Les documents qui font déjà l'objet d'un droit d'auteur (articles de revue, examens publiés, etc.) ne sont pas microfilmés.

La reproduction, même partielle, de ce microfilm est soumise à la Loi canadienne sur le droit d'auteur, SRC 1970, c. C-30. Veuillez prendre connaissance des formules d'autorisation qui accompagnent cette thèse.

**LA THÈSE A ÉTÉ
MICROFILMÉE TELLE QUE
NOUS L'AVONS REÇUE**

NETWORK MODELS FOR BRAKE PIPE LEAKAGE

Chun-Tat KWAN

A RESEARCH THESIS
IN THE
FACULTY OF ENGINEERING

• Chun-Tat KWAN 1977

Present in Partial Fulfilment of the Requirements for the
Degree of MASTER OF ENGINEERING

at

Concordia University

Sir George Williams Campus

Montreal, Quebec

June, 1977

C O N C O R D I A U N I V E R S I T Y

SIR GEORGE WILLIAMS CAMPUS

FACULTY OF ENGINEERING

GRADUATE STUDIES

RESEARCH THESIS

This is to certify that the Research Thesis prepared

by _____ CHUN-TAT KWAN

Entitled NETWORK MODELS FOR BRAKE PIPE LEAKAGE

Complies with the regulations of this University and meets the accepted standards with respect to originality and quality.

For the degree of:

MASTER OF ENGINEERING

Signed by the examining committee:

____ Supervisor

____ Supervisor

Chairman

Approved, for and on behalf of the Dean of Engineering

Secretary for Engineering Graduate Studies

NETWORK MODELS FOR BRAKE PIPE LEAKAGE

Chun-Tat KWAN

ABSTRACT

Network models for brake pipe leakage are presented in this thesis. The models are classified according to their treatment of leakage flow. The models show that the effects of leakage on the pressure gradient and brake pipe taper depend on the position of the leak. Rear leakage has larger effect than front leakage.

Leakage detection and leakage measurements which are used as safe road operation criteria are also analytically discussed.

The models are compared to an electrical experimental circuit and a scaled down brake pipe experimental model. The agreement between the analytical and experimental results are good. The largest discrepancies in the experiment on the scaled down brake pipe model occur in the rear end are less than 17 percent of the brake pipe tapers.

ACKNOWLEDGEMENTS

The author thanks his supervisors, Dr. Silas Katz, and Dr. R.H.M. Cheng for their guidance, suggestions, and helpful comments throughout both this research and the writing of this thesis.

The author wishes to acknowledge the university for the facilities provided through the Fluid Control Center, where this work has been conducted.

Many thanks are due to Mr. S. Hibbert of Canadian National Research Centre for the many discussions on the subject matter.

The formatting of this typescript was done by using the 'TYPESET'-- a test formatting program implemented in the computer system of the university.

This study has been supported by a research grant from the National Research Council of Canada.

TABLE OF CONTENTS

	page
Abstract.....	i
Acknowledgements.....	ii
Table of Contents.....	iii
List of Figures.....	vi
Nomenclature.....	ix

CHAPTER 1

INTRODUCTION

1.1	Freight Train Pneumatic Braking System Design and Operation	1
1.2	Brake Pipe and Its Leakage.....	2
1.3	Measurements of Leakage.....	3
1.4	Leakage Effects on Train Operation.....	6
1.5	Objective of the Thesis.....	8

CHAPTER 2

SIGNAL VARIABLES AND BASIC ELEMENTS FOR BRAKE

PIPE NETWORK MODELS

2.1	Signal Variables of the Brake Pipe Network Model....	10
2.2	Basic Elements of the Brake Pipe Network Model.....	11

CHAPTER 3

BRAKE PIPE LEAKAGE MODELS

3.1	Introduction.....	16
3.2	Flow Sink Leakage Models.....	16
3.2.1	Model with Flow Sink Leakage, Laminar-Incompressible Flow.....	17
3.2.2	Model with Flow Sink Leakage, Turbulent-Compressible Flow.....	24
3.3	Resistance Leakage Model.....	29
3.3.1	Model with Resistance Leakage, Laminar- Incompressible Flow.....	29
3.3.2	Model with Resistance Leakage, Turbulent- Compressible Flow.....	33
3.4	Numerical Technique for Solving the Models.....	38
3.5	Summary.....	39

CHAPTER 4

LEAKAGE DETECTION AND LEAKAGE MEASUREMENTS

4.1	Leakage Detection.....	41
4.2	Pressure Drop Measurement.....	42
4.3	Leakage Flow Measurement.....	47
4.4	Correlation Between the Two Leakage Measurements....	49
4.5	Summary.....	51

CHAPTER 5

EXPERIMENTAL INVESTIGATION

5.1	Introduction to Experimental Models.....	52
5.2	Experiments on the Electrical Model.....	53
5.2.1	Tests on Electrical Experimental Model.....	53
5.2.2	Results of Experiments on Electrical Model.....	54
5.3	Experiment on the Brake Pipe Scaled Down Model.....	54
5.3.1	Test Set-up for Pressure-Flow Characteristic on the Pipe-Bend Combination.....	55
5.3.2	Pipe-Bend Combination Tests and Results.....	55
5.3.3	Test Set-up for Pressure-Flow Characteristic on the Orifice.....	56
5.3.4	Orifice Test and Results.....	57
5.3.5	Test Set-up for the Scaled Down Brake Pipe Model....	58
5.3.6	Brake Pipe Leakage Tests and Results.....	59

CHAPTER 6

CONCLUSION AND SUGGESTION ON FURTHER WORK

6.1	Conclusion.....	63
6.2	Further Suggestion.....	66
	References.....	68
	Figures.....	72
	Appendixes.....	109

LIST OF FIGURES

FIGURE	page
1.1 Brake Pipe Gradient with Various Amounts of Brake Leakage in a Typical Train with Excessive Leakage.....	72
1.2 Brake Pipe vs Train Length.....	73
1.3 Comparison on Different Leakage Test by Air Brake Association.....	74
2.1 Simplified Configuration of the Brake (a,b,c) Pipe Models.....	75
3.1 Flow Sink Leakage Model.....	76
3.2 Pressure Gradient Curves for Flow Sink Laminar-Incompressible Flow Model.....	77
3.2.a Dimensionless Pressure Gradient Curves for Flow Sink Leakage, Laminar-Incompressible Flow Model....	78
3.3 Pressure Gradient Curves for Flow Sink Leakage, Turbulent-Compressible Flow Model.....	79
3.3.a Dimensionless Pressure Gradient Curves for Flow Sink Leakage, Turbulent-Compressible Flow Model....	80
3.4 Resistance Leakage Flow Model.....	81
3.5 Pressure Gradient for Resistance Leakage, Laminar-Incompressible Flow Model.....	82
3.6 Pressure Gradient Curves for the Resistance Leakage, Turbulent-Incompressible Flow Model.....	83

3.6.a	Dimensionless Pressure Gradient Curves for Resistance Leakage, Turbulent-Compressible Flow Model.....	84
3.7	Pressure Gradient Curve for Simplified Equations...	85
3.8	Brake Pipe Gradient vs Train Length.....	86
4.1(a;b)	Pressure Gradient and Leakage Flow Curves.....	87
4.2	Pressure Drop vs Leakage.....	88
4.3	Pressure Drop vs Car Length.....	89
4.4	Leakage Flow vs No. Of Car.....	90
4.5	Leakage Flow vs Car Length.....	91
4.6	Pipe Taper vs Leakage Flow and Leakage Drop.....	92
5.1.a	Photograph of the Electrical Panel.....	93
5.1.b	Circuit for the Electrical Panel.....	94
5.2	Flow Sink Leakage, Laminar-Incompressible Flow Model Experiment on Electrical Panel.....	95
5.3	Resistance Leakage, Laminar-Incompressible Flow Model Experiment on Electrical Panel.....	96
5.4	Set-up for Pipe-Bend Combination Test.....	97
5.5	Pressure-Flow Characteristics of the Pipe-Bend Combinations.....	98
5.6	Set-up for Orifice Test.....	99
5.7	Pressure-Flow Characteristics of the Orifices.....	100
5.8	Schematic Drawing of the Brake Pipe Experimental Model.....	101
5.9	Photograph of the Brake Pipe Experiment.....	102
5.10	Pressure Gradient Curve ($P_0=60$ PSIG).....	103
5.11	Pressure Gradient Curve ($P_0=30$ PSIG).....	104

5.12	Leakage Detection.....	105
5.13	Leakage Detection.....	106
5.14	Taper vs No. of Car ($P_0=60$ PSIG).....	107
5.15	Taper vs No. of Car ($P_0=30$ PSIG).....	108

NOMENCLATURE

- a effective cross section area of orifices, in^2 .
- A cross section area of the brake pipe, in^2 .
- C_d discharge coefficient.
- d diameter of the brake pipe, in.
- d_o orifice diameter, in.
- d_{oi} diameter of the leakage orifice at the i th car, in.
- f friction factor.
- g_c gravitation constant, $386 \text{ lbm-in/lbf-sec}^2$.
- h_l loss of static pressure head due to fluid flow, ft.
- I electrical current, amp.
- i car number (position in n car train).
- K constant in nozzle flow formula, $\sqrt{O}R/\text{sec}$.
- K_1 resistance constant for laminar-incompressible flow in the pipe, $\text{lbf-sec/in}^2\text{-lbm}$.
- K_2 resistance constant for turbulent-compressible flow in the pipe, $\text{lbf}^2\text{-sec}^2/\text{in}^4\text{-lbm}^2$.
- K_3 prescribed leakage flow from a flow sink element, lbm/sec .
- l length of car and connecting hose, in.
- m mass flow rate, lbm/sec .
- m_i the in-line leakage flow at the i th car, lbm/sec .
- m_{Li} the leakage flow through the flow sink element

at the i th car, lbm/sec .
 M mass, lbm .
 n total number of cars in a train.
 p' pressure in the brake pipe after 15 psi pressure reduction is made in the pressure drop measurement, psia .
 p_i brake pipe pressure in the i th car, psia .
 p_0 absolute pressure in the locomotive, psia .
 R gas constant, $\text{lbf-in/lbm-}^\circ\text{R}$.
 R_e Reynold number.
 R_i leakage resistance in the i th car, $\text{lbf-sec/in}^2\text{-lbm}$.
 R_T leakage resistance for the whole train, $\text{lbf-sec/in}^2\text{-lbm}$.
 t time, sec .
 T absolute temperature, $^\circ\text{R}$.
 V voltage, volt .
 v volume, in^3 .
 v mean velocity of fluid, ft/sec .
 γ ratio of specific heat at constant pressure to specific heat at constant volume.
 ρ density, lbm/in^3 .
 μ viscosity, lbf-sec/in^2 .
 α i/n , i is the number of cars, n is the total number of cars in a train.
 Δp pressure drop, psi .

CHAPTER 1

INTRODUCTION

1.1 FREIGHT TRAIN PNEUMATIC BRAKING SYSTEM DESIGN AND OPERATION

The automatic air brake system was introduced to freight trains over 100 years ago. During the train operation, the application and release of the train brake is controlled by means of the changes in brake system pressure.

In the locomotive, there is a manually operated device called an "automatic brake valve". The engineman can position the handle of the valve to control the flow of air into and out of the system as braking power or to generate a control signal for braking activities.

A brake pipe, used to connect the air brake equipment on the locomotive units to those on the cars, is designed for supplying braking power as well as transmitting control signal to the cars.

Every car in the train is equipped with friction brake shoes. The retardation force is developed when a normal force to the frictional surface is produced by admitting pressurized air into a local brake cylinder. The valve that admits air to the car brake cylinders is designated as an AB or ABD valve. The feature of this valve is that it causes

the brakes to operate in service or emergency applications in response to the rate of brake pipe pressure reduction. A complete description of the train operation is given in (1) and (2).

1.2 BRAKE PIPE AND ITS LEAKAGE

The brake pipe, an important part of an automatic air brake system, consists of a series of lengths of 1.25 in. pipes, branch pipes, angle cocks, cutout cocks, dirt collectors, and hose couplings used for connecting the locomotive and the cars.

Because of numerous joining points, shock action due to train movement and contraction of metal fittings at low temperature, all cars and locomotive air brake system have unavoidable leakage to some degree. It occurs primarily at the various pipe joints, fittings, gaskets, and seals in devices, as well as at hoses and hose couplings (3)(4)(5).

Leakage has existed since the creation of air brake systems in spite of continuing efforts that have been made to reduce it. It will continue to exist into the foreseeable future. Therefore, it is important that the effects of leakage are understood so as to establish effective operating procedures for safe brake operation.

1.3 MEASUREMENT OF LEAKAGE

Since the entire braking system of a freight train is operated with compressed air, information regarding the leakage in the system is an indication of braking capability (6) (7). Thus there are two existing methods of determining leakage in the system, the "PRESSURE DROP" and "PRESSURE FLOW" measurements.

PRESSURE DROP MEASUREMENT

At any initial terminal, there are rules requiring to examine the condition of the braking system of a made-up train. This procedure is called "initial terminal test". One criterion associated with brake pipe leakage measurement is included in the test. The "pressure drop" measurement, expressed as psi/min, is the measurement of the rate of pressure drop when the compressed air supply is cut off. This criterion requires that the train is charged to within 15 psi of the setting of the feed valve and also the pressure at the last car is not less than 60 psi. A 15 psi brake pipe reduction is made from the locomotive and the subsequent pressure drop in the brake pipe must not exceed 5 psi/min. It is noted that the expression, psi/min, has been conventionally used to represent the degree of brake pipe leakage in the previous document.

LEAKAGE FLOW MEASUREMENT

The leakage measurement, expressed as CFM (cubic feet per minute), is a steady state measurement of the amount of

air flow into the whole system required to maintain a fixed pressure in the presence of leakage. Since many shortcomings have been found with the pressure drop criterion such as delays occurred on short and medium length train, it is believed that the leakage flow measurement provides better information of brake conditions as well as simplifies the testing procedure. A new criterion has been suggested but it is still in the experimental stage. This requires that the differential pressure between locomotive and the last car (i.e. taper of the brake pipe) should not exceed 15 psi and the leakage flow indicated in the flowmeter mounted in the locomotive should not exceed 60 CFM for any train length.

Leakage existing throughout the train reduces brake pipe pressure as distances from the locomotive increase. The difference in brake pipe pressure in the locomotive and that at any point in the train is called brake pipe gradient. The difference in brake pipe pressure between the locomotive and the last car of the train is called taper (8) (9).

The brake pipe gradient curve, usually used by brake system engineer to represent informations of leakage condition, is believed to be caused by factors such as location and magnitude of leaks, train length, and feed valve setting (10). In the following, two figures which are normally used for braking system studies are introduced. It is noted that in these reproduced figures, the degree of

leakage is expressed in terms of psi/min because such leakage is determined by the "pressure drop" measurement and these units are conventionally used in this manner in all relevant documents.

Figure 1.1, reproduced from ref(2), is the pressure gradient curves of a train with leakage of 5 psi/min. When the leakage is evenly distributed through the train, the gradient in brake pressure on a 100-car train is 2.5 psi and on the train of 150 cars results in 7 psi gradient. When the leakage is concentrated in the rear third of the train, the same 5 psi/min leakage results in larger gradients as shown in three dotted curves for three different car lengths. Although the ~~50-car~~ train is not affected very much, the taper for 100 and 150-car train are approximately double. The 100-car train has increased to 6 psi taper and the 150-car train to 13 psi. The figure shows a well-known phenomenon that the effect of leakage at the rear of the train is more significant to the brake pipe gradient than leakage in the front.

Figure 1.2, reproduced from ref(7), shows how the train length and brake pipe leakage affect the taper. Leakage evenly distributed throughout a train of 150 cars (approximate 9000.0 ft.) with brake pipe leakage 5 psi/min and 3 psi/min are shown in two solid lines, while leakage concentrated at rear third are shown in dotted lines. The figure shows that the taper for a 150-car train with 3

psi/min uniformly distributed leakage is 6 psi. With the leakage concentrated at the rear third, the taper is 9 psi. The taper becomes double when the same leakage is concentrated at the rear third and it would not satisfy the criterion which requires allowable taper of less than 15 psi. It is evident that leakage location affects the train brake taper significantly.

1.4 LEAKAGE EFFECTS ON TRAIN OPERATION

During the train operation, a great amount of compressed air is wasted in maintaining the leakage in the system. Besides economical considerations, leakage has significant effect on the braking performance (11)(12). The locations and sizes of leakages affect the pressure distribution and gradient. The concentration of leakage at the rear end is more serious and can produce twice the gradient in the train. Experience has shown that the practical limit for satisfactory brake control on trains depends on leakage or gradient. Too much leakage on a train causes erratic brake response because this may reduce the ability of the brake valve to maintain control of the brake pipe pressure. Unwanted application and release may result or brakes may not respond. Also, a sudden increase in leakage can cause a pressure drop inducing cars to apply their brakes. This, in turn, increases the train drag and energy required.

Since many of the inadequacies in the operation of the system are caused by excessive leakage, it is necessary to detect and correct efficiently the major leaks which are randomly distributed. Many tests have been conducted by the Air Brake Association in an effort to investigate the location and causes of leakage on cars. The following is a brief review of the tests.

In 1925, a series of "SOAP SUDS TEST" were made on trains. The location and degree of leakage were recorded for each car (3). In 1950, the same conventional leakage tests were made and the pipe thoroughly soaped and the leakage location recorded. These tests were conducted on approximately 500 cars (10). The most recent leakage test was made in the winter of 1975 and was performed by listening for the leaks. The test was conducted by crews of men walking along the train and recording all the audible leaks, their locations and causes. Figure 1.3, reproduced from ref (10), summarizes the findings of the three tests. The figures given in the right-hand columns show the percentage of total cars checked that had leakage. The specific location of leakage is categorized. For example, in 1925, 71 % of all cars checked had leakage around the hose or hose gasket. In 1950, 16.7% did, and in the recent cold weather tests in 1975, 71.1% had audible leaks in this location. The three left-hand columns show what percentage of leaks were located at the various points and the total

number of leaks. For example, in 1925, 17% of the 10634 leaks found were at the hose and hose gasket, in 1950, 19.8 percent were at this location, and the recent test shows 31.8%.

The table shows that results from the three tests are different. It is believed to be the consequence of the following facts:

1. The brake pipe assembly of the tests were different. In the last 50 years, the braking system has been continually improved and the leakage has been reduced.

2. There may be difference in interpretation for leakage. Soaping each car will certainly detect more leakage because some leaks are too small to detect by noise detectors.

3. Due to contraction of metal, conducting the test in winter will detect more leaks.

1.5 OBJECTIVES OF THE THESIS

The acquired knowledge appearing in the studies of brake pipe is of a practical nature. A lot is known about leakage through experimental investigation. This has been applied to the establishment of criteria for safe road operation. There has been no attempt to approach the brake pipe leakage problem analytically which is essential to the thorough understanding of the phenomena. The purpose of this thesis

is to suggest several time independent network models for brake pipe leakage. Some experiments regarding these models are also illustrated. The detection and the measurement of leakage are also analytically discussed in accordance with the network model. It is believed that these models provide a valuable supplement to existing practical know-how.

This thesis is divided into six chapters. In the first and this present chapter, an introduction on train operation and leakage in the air brake system is given. The second chapter contains a brief discussion of fluid circuit theory. With this as a background the third chapter is devoted to the introduction of the resistance type network models for brake pipe leakage and also its solution with numerical technique. The application of the analytical models to leakage detection and leakage measurement is introduced in chapter four. In the fifth chapter, the experimental investigation conducted on the electrical network model and laboratory brake pipe model are compared to its theoretical predictions. In the last chapter, the conclusion and some suggestions for further work are given.

CHAPTER 2

SIGNAL VARIABLES AND BASIC ELEMENTS FOR BRAKE PIPE NETWORK MODELS

The physical configuration of the brake pipe is a combination of a series of lengths of 1.25 in. pipes, branch pipes, angle cocks, cutout cocks, dirt collectors, hoses and hose couplings. When the brake pipe is charged with compressed air, the leakage will generate a leakage flow in the pipes and resistance to the flow causes the pressure gradient. For the purpose of convenience, the brake pipe configuration is simplified into a form which consists of a series of pipes with leakage holes in between (see figure 2.1.a). This new physical model can provide a means for analysis of the brake pipe with circuit theory. In this thesis, the brake pipe will be modelled under different flow conditions (turbulent or laminar flow) and different leakage conditions (resistance leakage or flow sink leakage). To develop such network models, one must first relate the physical system to an equivalent circuit and determine the signal variables. The next section shows how to choose the through variable and across variable of the equivalent circuit.

2.1 SIGNAL VARIABLES OF THE BRAKE PIPE NETWORK MODEL

A. THE THROUGH VARIABLE

Since in any kind of circuit theory, the flow into a node must equal to the flow out. It is apparent that the through variable must obey the continuity equation, and therefore the mass flow rate has been chosen as through variable for this analysis.

B. THE ACROSS VARIABLE

There are many ways to choose the across variable in fluid system under various conditions (13) (14). In our case, absolute static pressure is taken as fluid potential, because it provides the ease of measurement and availability of well known functional relations between the pressure and mass flow for pipe flow (15) (16). Sometimes when there are significant changes in sectional area, large amount of heat exchanges, or Mach Number between terminals, the choice of static pressure may lead to large errors. But in case of the brake pipe, these changes are so small that their effects are negligible.

2.2 BASIC ELEMENTS OF BRAKE PIPE NETWORK MODELS

In formulating the equations that describe a physical circuit model, it is necessary to specify the characteristics of the elements expressed as the relation between the across variable and through variable. Since the steady state flow is dealt with in these brake pipe models, the basic elements are restricted to resistive type components only. The resistive models, for fluid

components, are complicated by the effect of laminar or turbulent flow and incompressible or compressible flow through the pipes. Actually, the behavior of the flow in brake pipes is more turbulent-compressible than laminar-incompressible. However, both models are applied to demonstrate the extreme conditions. There are four basic elements used in the brake pipe network models for various physical configurations and these are introduced as follows (see figure 2.1.b and 2.1.c):

1. RESISTIVE ELEMENT FOR BRAKE PIPE WITH LAMINAR-INCOMPRESSIBLE FLOW

In the case of laminar incompressible flow through a uniform duct, the pressure drop along a line is proportional to the mass flow. Thus, the resistive element for brake pipe has the following functional form (17): (see appendix I for derivation)

$$P_i - P_{i+1} = K_1 \dot{m} \quad (2.1)$$

where
$$K_1 = \frac{128 \mu l}{\pi \rho d^4}$$

and P_i , P_{i+1} are the brake pipe pressure in the i^{th} and $i+1^{\text{th}}$ car, in psia, μ is viscosity in lbf-sec/in²,

l is the length of pipe and connecting hose, ρ is density in lbm/in^3 , and d is diameter of brake pipe in inch.

2. RESISTIVE ELEMENT FOR BRAKE PIPE TURBULENT-COMPRESSIBLE FLOW

In the case of turbulent-compressible flow through a uniform duct, the difference in the square of the pressures of two points varies approximately as the square of the mass flow. Thus, the turbulent-compressible elemental model for brake pipe has the following form (18) (19): (see appendix 1 for derivation)

$$p_i^2 - p_{i+1}^2 = K_2 \dot{m}^2 \quad (2:2)$$

where
$$K_2 = \frac{16 f R T}{\pi^2 d^5 g_c}$$

and f is friction factor, R is gas constant in $\text{lb-f-in/lbm-}^\circ\text{R}$, T is temperature in $^\circ\text{R}$, and g_c is the gravitation constant in $386 \text{ lbm-in/lbf-sec}^2$.

For practical purposes, when the difference between p_i and p_{i+1} is less than 3 psi, equation 2.2 can be approximated as:

$$p_i + p_{i+1} = \frac{K_2}{2 p_{i+1}} m^2 \quad (2.2.a)$$

3. RESISTIVE ELEMENT FOR CHOKED ORIFICE

The mass flow rate of a choked flow through an orifice to atmosphere is proportional to the up-stream pressure. The elemental model for this resistance leakage flow can be expressed as: (see appendix 2 for derivation)

$$p_i = R_i m_{Li} \quad (2.3)$$

where

$$R_i = \frac{4\sqrt{T}}{0.532 \pi C_d d_{oi}^2}$$

and p_i is the absolute pressure in the i^{th} car, C_d is the discharge coefficient, d_{oi} is the leakage nozzle diameter at the i^{th} car.

4. IDEAL FLOW SINK FOR LEAKAGE

In our leakage flow in each brake pipe, another elemental model called ideal flow sink is chosen. The expression is (20):

$$m_{Li} = K_3 \quad (2.4)$$

where K_3 is a prescribed constant independent of brake

pipe pressure in lbm/sec.

CHAPTER 3

BRAKE PIPE LEAKAGE MODELS

3.1 INTRODUCTION

In this chapter, the brake pipe leakage network will be modelled by using the basic elements mentioned previously. The section of pipe and the total leakage in each individual car provide a convenient lump. Thus, the number of lumps represents the number of cars. Each lump contains two network elements. They are the shunt element to ground representing the leakage and the series element representing the piping and the connecting hose in each car.

According to the leakage condition, the models are classified into two types. They are the leakage resistance type and flow sink leakage type. The laminar-incompressible, and turbulent-compressible in-line flow relation are also applied to each type. Therefore, there are four configurations of the brake pipe model to be introduced in this chapter.

At the end of this chapter, an iterative computer technique is also introduced for the solutions of the models in accordance with the mathematical expression.

3.2 FLOW SINK LEAKAGE MODELS

Figure 3.1 shows the flow sink leakage lumped model. In this case, the network is modelled by using the flow sink shunt elements (equation 2.4) and two resistive series elements (equation 2.1 and equation 2.2). When equation 2.1 is used to model the series element, the flow in the brake pipe has the laminar-incompressible relation. The network is linear and easily treated analytically. When equation 2.2 is used, the flow has the turbulent-compressible relation, and the network is non-linear. In general, most non-linear analyses of fluid network are performed by computational means (21) (22). As mentioned before, the flow sink leakage is a prescribed constant and is assumed independent of brake pipe pressure. It is not necessary to consider how this might be accomplished physically in the brake pipe system. As a concept, it is useful in the analysis.

3.2.1 MODEL WITH FLOW SINK LEAKAGE, LAMINAR-INCOMPRESSIBLE FLOW

When the series resistance is modelled by the laminar-incompressible relation, one may specify equation 2.1 for the i^{th} lump as:

$$P_i - P_{i+1} = K_i m_i \quad (3.1)$$

where the subscript i refers to the car position along an n

car train. The continuity at each node of the model may be written as:

$$m_i = m_{i+1} + m_{L(i+1)} \quad (3.2)$$

The total flow in the i^{th} car is equal to the sum of the leakage flows in all the cars that come after. Thus equation 3.1, can be expressed as:

$$p_i - p_{i+1} = K_1 \left[m_{L(i+1)} + m_{L(i+2)} + \dots + m_{Ln} \right] \quad (3.3)$$

and in summation form, this can be written as:

$$p_i - p_{i+1} = K_1 \sum_{j=1}^{n-i} m_{L(i+j)} \quad (3.4)$$

where j is a summation index.

If n sections are summed up together, the locomotive-rear end pressure difference can be expressed as:

$$p_o - p_n = K_1 \left[\sum_{j=1}^n m_{L(n+1-j)} + \sum_{j=1}^{n-1} m_{L(n+1-j)} + \dots + \sum_{j=1}^1 m_{L(n+1-j)} \right] \quad (3.5)$$

where p_0 = locomotive pressure, p_n = local pressure at n^{th} car.

Equation 3.5 may also be written in a more compact form as:

$$p_0 - p_n = K_1 \sum_{j=1}^n j m_{Lj} \quad (3.6)$$

Also, the relation between the pressure at any location and the locomotive pressure for specified leakage in each car can be written as:

$$p_0 - p_i = -K_1 m_L \left[\sum_{j=1}^{n-i} j m_{Lj} - \sum_{j=1}^{n-i} j m_{L(i+j)} \right] \quad (3.7)$$

This equation can now be applied to obtain the pressure gradient for specified leakage distributions.

A. UNIFORM LEAKAGE

In this case all the flow from the flow sink element are equal (i.e. $m_L = m_{L2} \dots \dots \dots m_{Ln}$), equation 3.7 is simplified as:

$$p_0 - p_i = -K_i m_L \left[\sum_{j=1}^{n-i} j - \sum_{j=1}^n j \right] \quad (3.8)$$

The summations in equation 3.8 are merely the sums of a number of consecutive integers. Thus, it can be algebraically expressed as:

$$p_0 - p_i = K_i m_L \left[\frac{i(2n-i+1)}{2} \right] \quad (3.9)$$

This equation may also be expressed in non-dimensional form. Some of the terms considered insignificant are omitted during the normalization. For example, terms like $1/n^2$ and $1/n^3$ are omitted from the right hand side of the following normalized equations.

An approximate normalized form of this equation is:

$$\frac{p_0 - p_i}{K_i m_L n^2} = \frac{\alpha(2-\alpha)}{2} \quad (3.9.a)$$

where $\alpha = i/n$, i = number of car, n = total number of cars.

B. LEAKAGE DISTRIBUTED IN REAR HALF

The total leakage from the pipe is made the same as in the uniform case. However, it is distributed equally only in the rear half of the brake pipe. The leakage specification is $m_{L1} = m_{L2} \dots m_{L(n/2)} = 0$ and $m_{L(n/2+1)} = m_{L(n/2+2)} = \dots = 2m_L$. The equation 3.7 is again used to determine the pressure gradient of train.

$$p_o - p_i = -2K_1 m_L \left[\sum_{j=n/2+1}^n (j-i) - \sum_{j=n/2+1}^n j \right]$$

$$0 < i \leq n/2 \quad (3.10.1)$$

and

$$p_o - p_i = -2K_1 m_L \left[\sum_{j=i+1}^n (j-i) - \sum_{j=n/2+1}^n j \right]$$

$$n/2 < i \leq n \quad (3.10.2)$$

Again, this equation can be simplified to an algebraical form as:

$$p_0 - p_i = K, m_L n i, \quad 0 < i \leq \frac{1}{2} \quad (3.11.1)$$

$$p_0 - p_i = K, m_L \left[\frac{n}{2} \left(\frac{n}{2} + 1 \right) - (n-i)(n-i+1) \right]$$

$$\frac{n}{2} < i \leq n \quad (3.11.2)$$

An approximate normalized form of equation 3.11 is:

$$\frac{p_0 - p_i}{K, m_L n^2} = \alpha, \quad 0 < \alpha \leq \frac{1}{2} \quad (3.11.1.a)$$

$$\frac{p_0 - p_i}{K, m_L n^2} = \frac{3}{4} + (1 - \alpha)^2$$

$$\frac{1}{2} < \alpha \leq 1 \quad (3.11.2.a)$$

C. LEAKAGE DISTRIBUTED IN REAR THIRD

In this case, $m_{L(2n/3)} = \dots m_{Ln} = 3m_L$. Equation 3.7 is applied and after simplification, one gets:

$$p_0 - p_i = K_1 m_L n i, \quad 0 < i \leq \frac{2}{3} \quad (3.12.1)$$

$$p_0 - p_i = K_1 m_L \left[\frac{n(\frac{5n}{3} + 1) - 3(n-i)(n-i+1)}{2} \right] \quad (3.12.2)$$

$$\frac{2}{3} < i \leq n$$

An approximate normalized form of this equation is:

$$\frac{p_0 - p_i}{K_1 m_L n^2} = \alpha, \quad 0 < \alpha \leq \frac{2}{3} \quad (3.12.1.a)$$

$$\frac{p_0 - p_i}{K_1 m_L n^2} = \frac{5}{6} + 3(1-\alpha)^2$$

$$\frac{2}{3} < \alpha \leq 1 \quad (3.12.2.a)$$

Figure 3.2 shows some typical results obtained from equations 3.9, 3.11, and 3.12 for 50, 100 and 150 car trains. The value of $K_1 m_L$ is somewhat arbitrarily selected as 0.001 psi. This value is believed to represent

the order of magnitude that might be expected in an actual brake pipe. Figure 3.2.a shows the curves of normalized equations 3.9.a, 3.10.a, and 3.12.a. These two figures show the following phenomena:

A. The leakage concentrated in the rear produces larger pressure drops. This is a consequence of the fact that the pressure drop in a pipe is proportional to the in-line mass flow and this in-line flow is larger in cars in front of the concentrated leakage.

B. There is no difference in the pressure drop of front cars when leakage is concentrated in cars further back. For example, the 50th car in an 150 car train has the same pressure drop whether the leakage is concentrated in the rear half or in the rear third. Thus, if the total leakage is not changed, any arbitrary concentration of leakage in rear position does not affect any cars in front of the leakage.

3.2.2 MODEL WITH FLOW SINK LEAKAGE, TURBULENT-COMPRESSIBLE FLOW

In this case, the series resistance is modelled by the turbulent-compressible relation. Equation 2.2 can be written for the i^{th} lump as:

$$P_i^2 - P_{i+1}^2 = K_2 m_i^2 \quad (3.13)$$

Now the total flow in the i^{th} car is equal to the sum of the leakage flows in all the cars that come after. Thus, equation 3.13 becomes:

$$p_i^2 - p_{i+1}^2 = K_2 \left[m_{L(i+1)} + m_{L(i+2)} + \dots + m_{Ln} \right]^2 \quad (3.14)$$

This equation may be put into summation form as:

$$p_i^2 - p_{i+1}^2 = K_2 \left[\sum_{j=1}^{n-i} m_{L(i+j)} \right]^2 \quad (3.15)$$

By summing up n sections of the type given in equation 3.15, the locomotive-rear pressure relation is:

$$p_0^2 - p_n^2 = K_2 \left[\left(\sum_{j=1}^n m_{L(n+1-j)} \right)^2 + \left(\sum_{j=1}^{n-1} m_{L(n+1-j)} \right)^2 + \dots + \left(\sum_{j=1}^1 m_{L(n+1-j)} \right)^2 \right] \quad (3.16)$$

Equation 3.16 can be written in a compact form as:

$$p_0^2 - p_n^2 = K_2 \sum_{j=1}^n \left(\sum_{k=1}^j m_{L(n+1-k)} \right)^2 \quad (3.17)$$

where k is a summation index.

After some factoring, the relation between the pressure at any car and the locomotive pressure can be expressed as:

$$p_0^2 - p_i^2 = K_2 \left[\sum_{j=1}^n \left(\sum_{k=1}^j m_{L(n+1-k)} \right)^2 - \sum_{j=1}^{n-i} \left(\sum_{k=1}^j m_{L(n+i-k)} \right)^2 \right] \quad (3.18)$$

Now, one may consider the case of uniform or concentrated leakage by specializing equation 3.18.

A. UNIFORM LEAKAGE

If all the leakage flow are the same, equation 3.18 can be simplified as:

$$p_0^2 - p_i^2 = K_2 m_L^2 \left[\sum_{j=1}^n j^2 - \sum_{j=1}^{n-i} j^2 \right] \quad (3.19)$$

Equation 3.19 can also be expressed algebraically as:

$$p_0^2 - p_i^2 = \frac{K_2 m_L^2 \left[n(n+1)(2n+1) - (n-i)(n-i+1)(2n-2i+1) \right]}{6} \quad (3.20)$$

An approximate normalized form of equation 3.20 is:

$$\frac{P_0^2 - P_i^2}{K_2 m_L^2 n^3} = \frac{1 - (1 - \alpha)^3}{3} \quad (3.20.a)$$

B. LEAKAGE DISTRIBUTED IN REAR HALF

When the same total leakage is distributed uniformly over the rear half of the train, equation 3.17 may be applied, and after some manipulation yields:

$$P_0^2 - P_i^2 = 4K_2 m_L^2 \left[\left(\frac{n}{2} \right)^2 i \right], \quad 0 < i \leq n/2 \quad (3.21.1)$$

$$P_0^2 - P_i^2 = 4K_2 m_L^2 \left[\left(\frac{n}{2} \right)^3 + \frac{n/2 \left(\frac{n}{2} + 1 \right) (n+1) - (n-i)(n-i+1)(2n-2i+1)}{6} \right]$$

$$n/2 < i \leq n \quad (3.22.2)$$

An approximate normalized form of equation 3.21 is:

$$\frac{P_0^2 - P_i^2}{K_2 m_L^2 n^3} = \alpha, \quad 0 < \alpha \leq 1/2 \quad (3.21.1.a)$$

$$\frac{P_0^2 - P_i^2}{K_2 m_L^2 n^3} = \frac{2}{3} \left[1 - 2(1 - \alpha)^3 \right], \quad 1/2 < \alpha \leq 1 \quad (3.21.2.a)$$

C. LEAKAGE CONCENTRATED IN REAR THIRD

In this case, the total leakage is distributed uniformly on the rear third of the train, and equation 3.18 becomes:

$$p_0^2 - p_i^2 = 9 K_2 m_L^2 \left[\left(\frac{1}{9} n^2 \right) i \right], \quad 0 < i \leq \frac{2n}{3} \quad (3.22.1)$$

$$p_0^2 - p_i^2 = 9 K_2 m_L^2 \left[\frac{2}{27} n^3 + \frac{\frac{n}{3}(\frac{n}{3}+1)(\frac{2n}{3}+1) - (n-i)(n-i+1)(2n-2i+1)}{6} \right]$$

$$\frac{2n}{3} < i \leq n \quad (3.22.2)$$

An approximate normalized form of equation 3.22 is:

$$\frac{p_0^2 - p_i^2}{K_2 m_L n^3} = \alpha, \quad 0 < \alpha \leq \frac{2}{3} \quad (3.22.1.a)$$

$$\frac{p_0^2 - p_i^2}{K_2 m_L n^3} = \frac{9}{6} \left[\frac{14}{27} - 2(1-\alpha)^3 \right], \quad \frac{2}{3} < \alpha \leq 1$$

(3.22.2.a)

Figure 3.3 shows the pressure drop versus car position for the flow sink shunt, turbulent-compressible flow model.

The figure was calculated from equations 3.20, 3.21, and 3.22 with $p_0 = 80$ psig and $K_{2L}^2 = 0.34(10)^4$ psi. For the nonlinear model leakage concentrated in rear is even more heavily weighted than in the linear in-line resistance model. It also shows that there is no difference in the pressure drop in front cars when leakage is concentrated in cars further back. Figure 3.3.a shows the curves plotted with the same normalized equations.

3.3 RESISTANCE LEAKAGE MODELS

Figure 3.4 shows a network model in which the shunt element is a linear resistance, R_i . In this model, the leakage flow depends on the car pressure and the shunt resistance. From a physical point of view each shunt resistance represents a particular hole and such hole size may be treated as the total leakage area of an individual car in relation to the actual brake pipe.

It should be noted that the absolute pressure must be used in the following models since the leakage resistance linearity is based on absolute pressure.

The laminar-incompressible and turbulent-compressible in-line relations are also applied in the following models.

3.3.1 MODEL WITH RESISTANCE LEAKAGE, LAMINAR-INCOMPRESSIBLE FLOW

In this case, equation 3.1 and 3.2 are still valid to model the linear resistance, that is:

$$p_i - p_{i+1} = K_i m_i \quad (3.23)$$

$$m_i = m_{i+1} + m_{L(i+1)} \quad (3.24)$$

However, the leakage flow in equation 3.24 must be related to car pressure, so that equation 3.24 becomes:

$$m_i = m_{i+1} + \frac{p_{i+1}}{R_{i+1}} \quad (3.25)$$

Where the subscripted resistance, R_i , refers to the shunt resistance of a car in position i . Because both the series and shunt elements are linear resistances, the model can be treated as an electrical network with resistances in ladder arrangement as shown in appendix 3 (figure a.1). By means of z transformation technique for solving linear system, one can come up with an exact solution in which potential between series resistances are related to the inlet potential (see appendix 3). With this convenience, one can easily obtain the pressure gradient of the brake pipe model with different leakage distributions.

A. UNIFORM LEAKAGE RESISTANCE

In this case, all the shunt resistances in the model are the same. This is equivalent to placing a fixed bleed hole in each car $R_1 = R_2 = R_3 \dots R_i$. From the relation derived in appendix 3,

$$\frac{P_i}{P_0} = \frac{\cosh b (n - i + 1/2)}{\cosh b (n + 1/2)} \quad (3.26)$$

where

$$b = \cosh^{-1} y/2$$

$$y = 2 + \frac{K_1}{R_i}$$

Since the denominator in equation 3.26 is a constant, the pressure gradient curve will be of hyperbolic nature.

B. LEAKAGE RESISTANCE IN REAR HALF

The condition here is $R_1 = R_2 \dots = R_{n/2} = \infty$ and the rear half resistances R_c are 1/2 of those in the previous case. With this leakage distribution, another exact solution for the equivalent electrical circuit is given in figure a.2. Referring the notations to the circuit, one gets:

$$P_i = P_0 - m i K_1, \quad 0 < i \leq n/2 \quad (3.27.1)$$

$$P_i = \frac{P_{1/2} \cosh b \left[n/2 - (i - n/2) + 1/2 \right]}{\cosh b \left[n/2 + 1/2 \right]} \quad (3.27.2)$$

$$n/2 < i \leq n$$

$$p_{n/2} = \frac{p_0}{1 + \frac{1}{2}n \left[\frac{\cosh b(n/2 + 1/2) - \cosh b(n/2 - 1/2)}{\cosh b(n/2 + 1/2)} \right]}$$

$$m = \frac{p_{n/2}}{K_1} \left[\frac{\cosh b(n/2 + 1/2) - \cosh b(n/2 - 1/2)}{\cosh b(n/2 + 1/2)} \right]$$

$$b = \cosh^{-1} y / 2, \quad y = 2 + \frac{K_1}{R_c}, \quad R_c = \frac{1}{2} R_i$$

C. LEAKAGE RESISTANCE IN REAR THIRD

The condition here is $R_1 = R_2 = \dots = R_{2n/3} = \infty$ and the rear third resistance R_d are $1/3$ of those in uniform resistance case. Thus one has:

$$p_i = p_0 - n i K_1, \quad 0 < i \leq \frac{n}{3} \quad (3.28.1)$$

$$p_i = \frac{p_{2n/3} \cosh b \left[\frac{n}{3} - (i - \frac{2}{3}n) + \frac{1}{2} \right]}{\cosh b \left(\frac{1}{3}n + \frac{1}{2} \right)},$$

$$\frac{1}{3}n < i \leq n \quad (3.28.2)$$

$$p_{2n/3} = \frac{p_0}{1 + 2^{n/3} \left[\frac{\cosh b (2^{n/3} + 1/2) - \cosh b (n/3 - 1/2)}{\cosh b (n/3 + 1/2)} \right]}$$

$$m = \frac{p_{2n/3}}{K_1} \left[\frac{\cosh b (n/3 + 1/2) - \cosh b (n/3 - 1/2)}{\cosh b (n/3 - 1/2)} \right]$$

$$b = \cosh^{-1} \frac{y}{1/2}, \quad y = 2 + \frac{K_1}{R_d}, \quad R_d = 1/3 R_i$$

Figure 3.5 shows the pressure drop versus car position for the linear resistance leakage network. The figure was calculated from equations 3.26, 3.27 and 3.28 with $K_1/R_i = 10^{-5}$ and $p_0 = 80$ psig. The trend of the results are similar to those shown in figure 3.2.

3.3.2 MODEL WITH RESISTANCE LEAKAGE, TURBULENT-COMPRESSIBLE FLOW

An analytical solution is difficult to obtain for this case. However, the problem is simpler if equation 2.2.a is applied to model the series nonlinear resistances.

$$p_i - p_{i+1} = \frac{K_2}{2 p_{i+1}} m_i^2 \quad (3.29)$$

the mass flow m_i is the sum of all leakage flow occurring after i^{th} car, that is:

$$m_i = \sum_{j=1}^{n-i} \frac{p_{j+i}}{R_{j+i}} \quad (3.30)$$

If equation 3.30 is substituted into equation 3.29, after some factoring, the result is:

$$p_i = p_{i+1} \left[1 + \frac{K_2}{2R_{i+1}^2} \left(1 + \sum_{j=1}^{n-i-1} \frac{p_{i+j+1}}{p_{i+1}} \frac{R_{i+1}}{R_{i+j+1}} \right)^2 \right] \quad (3.31)$$

as a shorthand notation, B_{i+1} is defined as:

$$B_{i+1} = \frac{p_i}{p_{i+1}} \quad (3.32)$$

Equation 3.32 can be used to express the ratios of non-adjacent car pressure as the product of terms. For example:

$$\frac{p_{i+j+1}}{p_{i+1}} = \prod_{k=1}^j \frac{1}{B_{i+k+1}} \quad (3.33)$$

Applying equation 3.32 and 3.33 to equation 3.31, one gets:

$$\beta_{i+1} = 1 + \frac{K_2}{2R_{i+1}^2} \left[1 + \sum_{j=1}^{n-i+1} \left(\prod_{k=1}^j \frac{1}{\beta_{i+k+1}} \right) \left(\frac{R_{i+1}}{R_{i+j+1}} \right) \right]^2 \quad (3.34)$$

The value of B_i can be calculated from B_n to B_1 if one specializes R_i from R_i to R_n . For example, from equation 3.34, one gets:

$$\begin{aligned} \beta_n &= 1 + \frac{K_2}{2R_n^2} \\ \beta_{n-1} &= 1 + \frac{K_2}{2R_{n-1}^2} \left[1 + \frac{1}{\beta_n} \frac{R_{n-1}}{R_n} \right]^2 \\ \beta_{n-2} &= 1 + \frac{K_2}{2R_{n-2}^2} \left[1 + \frac{1}{\beta_n} \frac{R_{n-2}}{R_{n-1}} + \frac{1}{\beta_n} \frac{1}{\beta_{n-1}} \frac{R_{n-2}}{R_n} \right]^2 \end{aligned} \quad (3.35)$$

Then the pressure at any car can be related to the initial pressure as:

$$\frac{P_i}{P_0} = \prod_{k=1}^i \frac{1}{B_k} \quad (3.36)$$

From the knowledge of the series resistance K_2 and the shunt resistance R_i , B_i can be calculated from B_n to B_1 . Then the pressure distribution along the train can be computed by applying equations 3.34 to 3.36. If one specifies the value of R_i these equations can also be applied to the cases of different leakage distribution. In general, the ratio $K_2/2R_i^2$ will be very small, and as a result, the powers of $K_2/2R_i^2$ will be second order small. If this approximation is made, equation 3.34 and 3.35 can be reduced to a simplified function particularly in the case of uniform leakage distribution.

If $K_2/2R_i^2 = 0$, and $R_1 = R_2 = \dots = R_n$, factoring on equation 3.35 gives:

$$\begin{aligned} B_n &= 1 + \frac{K_2}{2R_n^2} \\ B_{n-1} &= 1 + \frac{K_2}{2R_n^2} [2]^2 \\ B_{n-2} &= 1 + \frac{K_2}{2R_n^2} [3]^2 \end{aligned} \quad (3.37)$$

Substituting equation 3.37 into 3.33 and relating the i^{th} car and n^{th} car to the last car, one gets:

$$\frac{P_i}{P_n} = \frac{1}{\left[1 + \frac{K_2}{2R_n^2}\right] \left[1 + \frac{K_2}{2R_n^2} |2|^2\right] \cdots \left[1 + \frac{K_2}{2R_n^2} |i|^2\right]} \quad (3.38)$$

$$\frac{P_0}{P_n} = \frac{1}{\left[1 + \frac{K_2}{2R_n^2}\right] \left[1 + \frac{K_2}{2R_n^2} |2|^2\right] \cdots \left[1 + \frac{K_2}{2R_n^2} |n|^2\right]} \quad (3.39)$$

Again, the same approximation is applied, and equation 3.37, 3.38 are combined.

$$\frac{P_i}{P_0} = \frac{1 + \frac{K_2}{2R_n^2} \left[(n-i)(n-i+1)(2n-2i+1)/6 \right]}{1 + \frac{K_2}{2R_n^2} \left[n(n+1)(2n+1)/6 \right]} \quad (3.40)$$

An approximate normalized form of this equation is:

$$\frac{P_0 - P_i}{P_0 \left(\frac{K_2}{2R_n^2} \right) n^3} = \frac{1 - (1 - \alpha)^3}{3} \quad (3.40.a)$$

Figure 3.6 shows the results for 50, 100, and 150 cars in different leakage distribution with a specific value of $K_2/2R_i^2 = 10^{-7}$. The figure is calculated from equations 3.33 and 3.35. The results are similar in trend to those previously shown for the other three models, but there is one major difference. In this case, as the leakage is concentrated in the rear of the train, the pressure drop in the front becomes smaller. This is a consequence of the fact that the total leakage flow becomes smaller.

Figure 3.7 shows the difference between equation 3.34 and 3.30 and its simplified equation 3.40. It is seen that with the specific value of $K_2 = 6000.0 \text{ lbf}^2 \text{-sec}^4 / \text{lbm}^2 \text{-in}^2$ and $R_i = 175000.0 \text{ lbf-sec/in}^2 \text{-lbm}$, the maximum error is not more than 5%. Figure 3.7.a shows the approximate normalized form of equation 3.40. This figure apparently shows that the differential pressures at the cars near the rear of the train are very close to each other.

3.4 NUMERICAL TECHNIQUE FOR SOLVING THE MODELS

In this section, a re-iterative computer technique is introduced for the solution of brake pipe models. This technique is valid for all the four analytical models mentioned in this chapter.

The idea of the scheme is that if the leakage and pipe resistance are known, with a guessed value p_n for the end car pressure provided, the pressure gradient can be calculated backward from p_{n-1} to p_0 . Satisfactory approximation can be made by continuing the iteration with new value of p_n and checking with the known locomotive pressure p_0 . The computer results are almost the same as those obtained analytically if the iteration steps are made small enough. The computer program also provides the ability of calculating pressure gradient for different train lengths, leakage distributions, and pipe resistances.

The flow chart for this algorithm is given in appendix 4.

3.5 SUMMARY

The analytical results for all the models mentioned were shown in figures 3.2, 3.3, 3.5, 3.6. These figures are presented in the same form as figure 1.1 to provide a look at the trends of the curves for similar leakage conditions. However, we cannot make a direct comparison without using actual values of brake pipe resistance and leakage.

The four cases illustrated in this chapter are possible models for the brake pipe resistance network. It is believed that the resistance leakage, turbulent-compressible in-line flow model is the best model of the actual brake pipe. This is primarily because, in the actual system, the

flow source leakage model is inappropriate. In addition, except for the last few cars, the in-line flow will be in the turbulent condition.

Figure 3.8 shows the relation between the train length, taper and brake pipe leakage of this model. The figure is calculated from equation 2.2 and 2.3 by using re-iteration computer technique, and presented in the same form as figure 1.2 for comparison in trend. The curves are calculated with the specific values $K_2 = 6000.0$ $\text{lbf}^2\text{-sec}^2/\text{in}^4\text{-lbm}^2$, $R_1 = 105000.0$ and 175000.0 $\text{lbf-sec}/\text{in}^2\text{-lbm}$, and $p_0 = 80$ psig. These values are arbitrarily chosen as in previous figures.

LEAKAGE DETECTION AND LEAKAGE MEASUREMENTS

4.1 LEAKAGE DETECTION

In chapter 3, it has been analytically shown that the location of leakage is one of the factors that influence the pressure gradient and the taper. Thus, to improve the braking capacity or to keep the train satisfying the operational criteria, it is necessary to detect and remove the major leaks which occur from train to train.

In the existing leakage detection method in which a noise detector is used, there is a shortcoming in that it only detects the leaks to some degree. It does not indicate quantitatively the leakage size, and the amount of leakage flow. In this chapter, the resistance shunt, turbulent-compressible flow model is applied for leakage detection corresponding to a given pressure gradient.

From equation 2.2,

$$m_i = \sqrt{\frac{p_i^2 - p_{i+1}^2}{K_2}} \quad (4.1)$$

where m_i is the in-line flow in i^{th} car, p_i and p_{i+1} are brake pipe pressure in i^{th} and $i+1^{\text{th}}$ car. Referring to figure 3.4, the leakage flow at any leakage point is equal

to the difference in the in-line flows of two adjacent pipes. Thus

$$m_{L,i} = m_{i+1} - m_i$$

$$m_{L,i} = \sqrt{\frac{p_{i+1}^2 - p_i^2}{K_2}} - \sqrt{\frac{p_i^2 - p_{i-1}^2}{K_2}}$$

$$1 < i < n$$
(4.2)

and

$$m_{L,n} = \sqrt{\frac{p_{n-1}^2 - p_n^2}{K_2}}$$
(4.3)

To illustrate how equations 4.2 and 4.3 may be utilized to detect leakage, the pressure gradient curves in figure 4.1.a are reproduced from figure 3.6 for a 150-car train with $K_2 = 6000.0 \text{ lbf}^2\text{-sec}^2/\text{in}^4\text{-lbm}^2$ and $p_0 = 80 \text{ psig}$. The three curves shown in figure 4.1.b are the corresponding leakage flow curves obtained by applying equations 4.2 and 4.3. Similarly with the same equation applied to a brake pipe with random leakage distribution, the largest leaks can be determined in terms of mass flow rate. This will be shown later in chapter 5 (figure 5.12 and figure 5.13).

4.2 PRESSURE DROP MEASUREMENT

The leakage measurement introduced in the first chapter has been expressed in terms of "pressure drop" in psi per minute, or "leakage flow" in cubic feet per minute (CFM). These two quantities can be analytically related to the leakage condition for a given brake system. In the "leakage drop" measurement, a 15 psi pressure reduction is first made in order to isolate the car braking units from the brake pipe before measuring the rate of pressure drop. Thus, this measurement only deals with the leakage in the brake pipe. The actual behavior of this measurement is complicated by the fact that during a test like this, the pressure is not uniform throughout the brake pipe. However, the analysis can somewhat be simplified if one assumes that a uniform pressure exists throughout the pipe a few seconds after the 15 psi reduction. The brake pipe can then be treated mathematically as a volume, rather than a pipe with significant distributed properties.

Form the ideal gas law

$$p = \frac{M R T}{v}$$

one gets,

$$\frac{dp}{dt} = \frac{R T}{v} \frac{dM}{dt} \quad (4.4)$$

where v is the total volume of the brake pipe and where

isothermal condition are assumed to prevail. According to the above-mentioned assumption, $v = nAl$, where n is the number of cars in a train, A is the cross-section area of the brake pipe, l is the car length, plus an additional 10 ft. of coupling hose.

From section 2.2, equation 2.3 gives the coefficient of resistance for the leakage of the i^{th} car as:

$$R_i = \frac{4\sqrt{T}}{0.532\pi C_d d_{oi}^2} \quad (4.5)$$

where d_{oi} is a given value of the equivalent diameter of the leakage in each car. If all the cars have the same leakage area, lumping all the leakage together and representing the resistance for the total leakage of a train by R_T ,

$$R_T = \frac{4\sqrt{T}}{0.532\pi C_d n d_{oi}^2} \quad (4.6)$$

equation 2.2 can be written as:

$$m_{\text{total}} = \frac{p}{R_T} \quad (4.7)$$

Where m_{total} is a total leakage flow of a train and p in psia, is the (uniform) pressure in the brake pipe at time t . Hence for a discharging process equation 4.4 becomes:

$$\frac{dp}{p} = - \frac{Q_T}{v R_T} dt. \quad (4.8)$$

After integration, the equation becomes:

$$\Delta p = p' \left(1 - e^{\frac{-Q_T}{v R_T} t} \right) \quad (4.9)$$

where p' is the pressure in the brake pipe immediately after the 15 psi reduction is successfully made.

From the definition of v and equation 4.6, one gets,

$$v R_T = \frac{4 \sqrt{T} A l}{0.532 \pi C_d d_o^2}$$

It is noted that $v R_T$ is independent of n and dependent upon l and p_0 . If one assumes that the value of p_0 to be constant for each car independent of the length (since leakage occurs mainly at the joints of the ends of the brake pipe, and at the valve brackets leading to the car control valve, this assumption is considered to be valid), equation 4.9 can be written as:

$$\Delta p = p' \left(1 - e^{-\frac{c}{l} t} \right) \quad (4.10)$$

The value of c , according to the assumption mentioned above, is constant for all trains with any number of cars and with the same leakage per car uniformly distributed throughout the train.

Based on equation 4.9, one can plot the pressure drop in 1 minute ($t=60$) for different value of R_T for a train made up of all 50 ft. cars, and $p' = 65$ psig. The result is shown in figure 4.2. Using this curve, one can estimate approximately the value $R_T = 2400.0 \text{ lbf-sec/in}^2\text{-lbm}$ for 5 psi per minute pressure drop.

Note that the usefulness of equation 4.10 lies in its emphasis on the pressure drop (per minute) as a function of l , the length of each car. The purpose of this equation is to establish whether a single pressure drop figure stipulated by the train handling regulation on the industry (namely 5 psi per minute) is universally adequate for all trains made up of cars of different lengths. Thus, equation 4.10 is plotted as shown in figure 4.3, which shows the pressure drop for trains of identical number of cars but of different car length. It shows that the pressure drop decreases significantly as the length of cars increases. This means that, for example, if a 150-car train made up of

50 ft. cars has 5 psi/min pressure drop, while a 150-car train made up of 100 ft. cars has only approximately 2.5 psi per min pressure drop. It shows that if a train made up of shorter cars satisfies the 5 psi per min criterion, than a train with longer cars but otherwise similar setup will satisfy lesser pressure drop rates. Thus a stipulation of a single pressure figure (5 psi/min) tends to be lenient for trains with larger cars, and too severe on those with shorter cars. The leakage criterion should take figure 4.3 into consideration.

4.3 LEAKAGE FLOW MEASUREMENT

As for the "leakage flow", it is a steady state measurement of the flow into the entire braking system to compensate for the system leakage. This flow is indicated on a flow indicator equipped on the pipe bracket in the locomotive. The resistance shunt, turbulent-incompressible analytical model provides a mathematical means to relate this leakage flow to the leakage condition of the system.

Equation 3.30 shows that the total leakage flow of the whole system equals to the in-line flow through the first pipe,

$$m_1 = \sum_{i=1}^n \frac{p_i}{R_i} \quad (4.11)$$

where n is the total car number, p_i is the pressure

at i^{th} car, psia. R_i is the coefficient for resistance leakage flow at i^{th} car as indicated in equation 2.3.

The pressure gradient of the brake pipe is given by equation 3.36:

$$P_i = P_0 \prod_{k=1}^i \frac{1}{B_k} \quad (4.12)$$

where B_k is as given in equation 3.32, P_0 is the inlet pressure, psia, P_i is the pressure at i^{th} car, psia.

If one assumes that the leakage area of each car is the same, (i.e. $R_1 = R_2 = R_3 \dots \dots \dots R_n$). Substituting equation 4.11 into 4.12, the total mass flow rate, lbm/sec, is given by:

$$\dot{m}_{\text{total}} = \frac{P_0}{R_n} \sum_{i=1}^n \left[\prod_{k=1}^i \frac{1}{B_k} \right] \quad (4.13)$$

Figure 4.4 shows how the total leakage flow varies with the car number. The specific values are arbitrarily chosen so that $K_2 = 6000.0 \text{ lbf}^2\text{-sec}^2/\text{in}^4\text{-lbm}^2$, $P_0 = 80.0 \text{ psig}$. It is seen that any train less than 150 cars with leakage $R_i = 160000.0 \text{ lbf-sec/in}^2\text{-lbm}$ has a total leakage of less than 60 CFM (see curve a). also, the same is true for a train with 70 cars eventhough its leakage is twice that of the 150 car train. (see curve b') this clearly shows that for a

different number of cars in a train, one needs a different indicated flow to ensure that the leakage is to the same degree.

Figure 4.5 is plotted based on the assumption that the leakage (value of R_1) in each car is the same for different car length. It is recalled from section 2.2 that the pipe resistance constant K_2 is proportional to car length. For example, in this figure, the value K_2 for 50 feet cars and 10 feet hoses is $6000.0 \text{ lbf}^2\text{-sec}^2/\text{in}^4\text{-lbm}^2$ and for 100 feet cars and 10 feet hoses is $1100.0 \text{ lbf}^2\text{-sec}^2/\text{in}^4\text{-lbm}^2$. The three lines on the figure shows that the leakage flow rate for three train length varies slightly with the car length. In an extreme case for a 150-car train, the difference in the leakage flows between a train made up of 50 ft. cars and 100 ft. car is approximately 5%. Thus, in contrast to the "leakage drop" measurement, the "flow measurement" is valid for a train made up of different car length, as long as they have the same number of cars each. Moreover, the leakage flow is approximately proportional to the total number of cars in a train. Thus a similar conclusion can be drawn as for the pressure drop criterion. A single leakage flow indication cannot be utilized as a universal criterion for all trains.

4.4 CORRELATION BETWEEN THE TWO LEAKAGE MEASUREMENTS

The train taper can be used to correlate the flow measurement and the pressure drop measurement. It can be obtained by substituting $i=n$ into equation 3.36,

$$p_o - p_n = p_o \left(1 - \prod_{k=1}^n \frac{1}{B_k} \right) \quad (4.14)$$

where B_k is a function of n , R_i and K_2 are as given in equation 3.36.

Figure 4.6. displays, for various car number, the relationship between the "pressure drop" (psi per minute), the taper (psi), and the leakage flow (CFM). The curves on the left-hand portion of the figure show how the air flow varies with the taper for 4 different train lengths. They are calculated from equations 4.13 and 4.14 with specific values $K_2 = 6000.0 \text{ lbf}^2\text{-sec}^2/\text{in}^4\text{-lbm}^2$, $p_o = 30.0 \text{ psig}$, and the R_i as a parameter varying from 2000.0 to 16000.0 $\text{lbf-sec}/\text{in}^2\text{-lbm}$. The curves on the right-hand portion show how the taper varies with the pressure drop rate. The curves are calculated from equations 4.9 and 4.14 with specific values $p' = 65 \text{ psig}$, $t = 60 \text{ sec}$, $T = 520^\circ\text{R}$, $\mathcal{Q} = 640.0 \text{ lbf-sec}/\text{lbm-}^\circ\text{R}$ for the same range of values of the parameter R_i . The figure shows, for example, 11 psi/min pressure drop produces a fully charge gradient of 12 psi on 150 cars and to maintain this level of gradient a flow of approximately 67 CFM is required. (see the chain-

dot curve ABCD)

Note that figure 4.6 is a somewhat simplification of the real situation since it is not possible at this stage to include leakage due to car control valves (e. g. ABD vales, quick servic valves, etc.). This consideration (called the system leakage) tends to increase the total leakage flow rate.

4.5 SUMMARY

In the leakage detection scheme introduced in the first section, equation 2.2 was used to calculate the leakage flow of each car. One should take into consideration that the in-line flow in the last few cars of a real train may be in laminar condition. In the case like that, the application of equation 2.1 in stead of 2.2 for those rear cars would improve the whole leakage detection scheme.

In section 2 and 3, it showed that in the "pressure drop" and "leakage flow" measurements, a single indication of pressure drop rate and leakage flow can not be universally utilized for all trains. To ensure that the train is operating under proper leakage condition, one should take into consideration the effects of the car length and total number of car respectively in the first and second measurement.

CHAPTER 5

EXPERIMENT INVESTIGATION

5.1 INTRODUCTION TO EXPERIMENTAL MODELS

Due to the unfeasibility of testing the actual brake pipe because of its huge size, a scaled down model is designed for the experimental laboratory set-up.

In the 1st and 3rd analytical models, it was assumed that the in-line flow of the brake pipe is in a laminar-incompressible condition. In order to maintain the brake pipe to perform as a linear resistance (Reynolds Number should be less than 2000), the brake pipe leakage has to be very small. This results in a slight pressure gradient which brings difficulties in the measurement. Since the mathematical models in this thesis were formulated by using circuit theory, they can be proven by electrical circuit rather than fluid models. In electrical circuits, electrical components provide good linearity in comparatively large current flow and are easily measured. An equivalent electrical circuit is therefore designed to demonstrate these two models..

Thus, in this chapter, two types of experiment are introduced to demonstrate the theory. They are the electrical experiments and brake pipe experiments on scaled down model.

5.2 EXPERIMENTS ON ELECTRICAL MODEL

In this experimental model, series resistances are used to model the resistive elements for brake pipe with laminar-incompressible flow. Other resistances are used to model the resistive elements for choked orifice in the first analytical model, while adjustable shunt resistances are used to model the flow sink for leakage flow in the second analytical model.

Figure 5.1.a shows the photograph of the electrical panel. It consists of 100 one-ohm resistances in series but divided into ten equal sections. The shunt resistances are made by inserting them across the terminal-pairs labelled AA. The arrangement of the resistances are shown in figure 5.1.b. Each section can be connected or disconnected to the next one by flipping a switch located at the top of the panel. Below each section, there is a 10-position selector (labelled as SS) to enable one to measure the voltage difference across any series resistance in the section by placing the switch in the required position and by applying a voltmeter to the terminals (labelled as TT).

5.2.1 TESTS ON ELECTRICAL EXPERIMENTAL MODEL

Two different types of test are performed:

1. "constant shunt resistance test"

2. "constant flow sink test"

In the constant shunt resistance test, 100 shunt resistances each 1000.0 ohms are inserted and the supply voltage is 10.0 volts. Voltage readings are taken from every 10th series resistance.

In the constant flow sink test, 10 adjustable shunt resistances with range from 500.0 to 10000.0 ohms are inserted in the first section of the model. The supply voltage is 10.0 volts. Before taking any readings, an ammeter is connected across the shunt resistances and they are adjusted in such a way that all the currents are the same (0.00635 amps). Data is taken from every measuring point.

5.2.2 RESULTS OF EXPERIMENTS ON ELECTRICAL MODEL

Figure 5.2 and 5.3 show the experimental results in comparison with the theoretical results which are calculated by referring the electrical notations and parameters to equation 3.8 and 3.26. All the experimental results from the electrical model are in excellent agreement with analytical predictions. The figures show that the data exactly fall on the theoretical curves.

5.3 EXPERIMENT ON BRAKE PIPE MODEL

This brake pipe experimental set up is designed for the 2nd and 4th analytical models. It consists of 10 pipe-bend

combinations and 10 same diameter orifices or adjustable orifices. Before assembly of the complete test set up, two types of experiment were run. These compared the pressure-flow characteristics of the basic elements in accordance with the mathematical description given in equations 2.2, 2.3 and 2.4. The test set-up and results for pipe-bend combinations and orifices, as well as the whole brake pipe experiment are given separately in the following sections.

5.3.1 TEST SET UP FOR PRESSURE-FLOW CHARACTERISTIC ON THE PIPE-BEND COMBINATION

Figure 5.4 shows the schematic drawing of the set up. In this experiment, the air is passed through a flowmeter and then to an individual pipe-bend combination. The pipe-bend combination consists of a galvanized pipe and a plastic tubing with a cross. The galvanized pipe is 10 ft. long and 0.25 in. inside diameter. It is connected by an 18 in. length of plastic tubing in an 180 degree bend with a cross placed down stream of the bend. The flow through the pipe-bend is varied by a valve placed at the end of the whole unit. The volume flow measurement is made with an FP-1/4-20 rotameter and is subsequently converted to mass flow. The pressure difference between the head end pressure and the pressure at the cross is measured with a differential manometer.

5.3.2 PIPE-BEND COMBINATION TEST AND RESULTS

During the test, the head end pressure is maintained at 60 psi. The flow through the combination is varied by the valve. The pressure drop due to different flow can be read on the manometer. Figure 5.5 shows the difference in the square of the absolute pressures before and after the pipe-bend combination. Data from 10 different pipes are shown. The data are presented in this form to demonstrate the agreement of the pipe-bend combination to equation 2.2. With the geometric parameters of the line, friction factor $f=0.052$, and neglecting the curvature of the bend, K_2 may be calculated from equation 2.2 as $10.5(10)^6 \text{ lbf}^2\text{-sec}^2/\text{in}^4\text{-lbm}^2$. The experiments were performed on ten different pipe-bend sections. The experimental data varied from one pipe-bend combination to another. The smallest experimental value of K_2 is $9.1(10)^6 \text{ lbf}^2\text{-sec}^2/\text{in}^4\text{-lbm}^2$, and the largest is about $13.0(10)^6 \text{ lbf}^2\text{-sec}^2/\text{in}^4\text{-lbm}^2$. Most of the data falls close to a value of K_2 equal to $9.2(10)^6 \text{ lbf}^2\text{-sec}^2/\text{in}^4\text{-lbm}^2$.

5.3.3 TEST SET UP FOR PRESSURE-FLOW CHARACTERISTIC ON THE ORIFICE

Figure 5.6 shows the schematic drawing for the set up. During the test, the air supplied from the regulator is passed through a FP-1/4-20 rotameter and to a cross. The openings of the cross, perpendicular to the flow direction are used to mount a pressure gauge and an orifice. The opening opposite to the flow direction is blocked by a plug.

The flow into the set up can be varied by the regulator and the pressure inside the cross is indicated on the pressure gauge. Two types of orifice which are used to model the resistance leakage and the flow sink leakage are tested or adjusted before experiments. They are the same diameters orifices drilled in pipe plugs and valves used as adjustable orifices.

5.3.4 ORIFICE TEST AND RESULTS

During the test, the head pressure can be varied by the regulator and the leakage flow from the orifice is indicated on the flowmeter. In the case of the resistance leakage experiment, all orifices of the same diameter yielded pressure-flow characteristics only marginally different. Figure 5.7 shows some typical experimental pressure-flow characteristics of the orifices. The theoretical characteristic calculated from equation 2.3 with $C_d = 1.0$ are superimposed on figure 5.7. These characteristics are shown dotted below 30 psia because the equation is valid only for choked flow. Theory and experiment are in good agreement in this case. Thus, the leakage resistance of the 0.023 orifice is $10.43(10)^4 \text{ lbf-sec/in}^2\text{-lbm}$ and of the 0.033 in. orifice is $5.07(10)^4 \text{ lbf-sec/in}^2\text{-lbm}$. In the case of the flow sink leakage experiment, using the same set-up, the section area of the orifices are adjusted so that all the flow are the same under different head pressures obtained from corresponding analytical models.

5.3.5 TEST SET-UP FOR THE BRAKE PIPE SCALED DOWN MODEL

Figures 5.8 and 5.9 show a schematic drawing and photograph of the brake pipe experimental model. The model consists of 10 pipe-bend combinations. They are connected and mounted parallel to one another 12 inches apart. The openings in each cross, perpendicular to the flow direction, are used to mount a quick disconnect fitting for static pressure measurements and an orifice to simulate flow leakage. Same diameter orifices will be used for the case of resistance leakage while adjusted orifices are used for the case of flow sink leakage. If no leakage is desired, a plug without orifice is used. The whole set-up is approximately 1/5 size of an actual brake pipe. At the head end of the experimental model, air is supplied to the composite line through a cylindrical tank 4 inches in diameter and 10 in. long. The flow into the tank is controlled by a pressure regulator (not shown in figure 5.8) and the pressure between head end pressure and pressure in the quick disconnect fitting is measured with a differential manometer. Before performing the experiment, all fittings were checked carefully for leakage. It should be noted that it is difficult to regulate the adjustable orifice as a flow sink elements during experiments. This regulation procedure can be simplified if the preliminary adjustment of the constant flow rate is made on the corresponding orifices according to the head pressure obtained from the

theoretical prediction.

5.3.6 BRAKE PIPE LEAKAGE TEST AND RESULTS

Two different types of tests are performed:

1. pressure gradient tests
2. brake pipe taper tests

In the pressure gradient tests, both the flow resistance and flow sink leakage condition are applied. In the set-up for flow resistance leakage, an orifice (0.023 in.) is placed in the cross of all ten pipes. The head end pressure is maintained at either 30 psig or 60 psig by the regulator. Pressure differential measurements between adjacent pipe-bend combinations are measured with a manometer. Figures 5.10 and 5.11 show the results of the pressure gradient tests made with all the orifices of 0.023 in. diameter. The pressure given by the manometer data are indicated at each car position by symbols. Superimposed on the experimental results are the results obtained from the analytical models. The resistance leakage model (equation 3.36) is shown by the solid line. In this case the resistance of the 0.023 in. leakage orifice $R_1 = 10.43(10)^4$ lbf-sec/in²-lbm and the resistance of the pipe-bend combination $K_2 = 9.2(10)^6$ lbf²-sec²/lbm⁴-in² are used. In the case of flow sink model, the theoretical pressure gradient curves are first obtained by using equation 3.19. The leakage flow chosen to

use in this equation is the flow through a 0.023 in. orifice at the head end pressure (0.000746 lbm/sec at 60 psig and 0.00043 lbm/sec at 30 psig). Before the experiment, all corresponding orifices are adjusted by the set-up mentioned in section 5.3.3 in such a way that the leakage flow are read the same under different head pressures obtained from theoretical pressure gradient curves (the dashed curves in figure 5.10 and 5.11). During the test, the experimental pressure gradient was measured in the same manner as for the previous case. This pressure gradient data is indicated by symbols in figure 5.10 and 5.11. In both case for resistance and flow sink leakage experiments, the data and model diverge gradually as the car position is further from the head end. Towards the rear of the composite pipe the weighting effect of rear cars becomes significant. A rear car error in brake pipe coefficient K_2 , leakage resistance R_i , or flow sink leakage m_L is weighted and therefore its effect is magnified. Any error will show up more pronounced in the rear. In addition one must remember that the models were calculated with equal values of R_i and K_2 for each pipe. The data from figures 5.5 and 5.7 show that this is not the case. Much closer agreement between experiment and theory may result if one applies equation 3.36 with the individual values measured for R_i and K_2 on each pipe and orifice.

Figure 5.12 shows two graphs, the upper graph shows the theoretical curve and experimental data of the pressure gradient obtained in the same manner as in figure 5.11. for the case of resistance leakage. All the orifices are 0.023 in. diameter except the last car is 0.033 in.. The lower curves show the leakage in terms of mass flow rate corresponding to the car number. The solid line is calculated by equation 4.3 with data from theoretical gradient curve while the dotted line is calculated by the same equation with data from experimental pressure gradient. Recalling from section 4.1, this figure is used for the purpose of leakage detection. It shows that if one of the 10 orifice (number 10) is relatively larger than the other, then this leakage can be detected by comparing all the leakage flow of different orifices. In this figure, it is seen that the flow of the 10th orifice is approximately twice the average flow. Figure 5.13 shows the same curves as in figure 5.12 except the larger orifice (0.033 in. diameter) is placed at 7th pipe. The major leak of this test can also be detected in the same manner.

In the pipe taper tests the experimental set-up was used to determine the difference between head end and last pipe pressure as a function of the number of cars. Both the resistance and flow sink leakage were applied. In the resistance leakage case, all the crosses had 0.023 in. orifices. The pressure difference between head end and

last pipe is measured as the taper of 10 pipes when the head end pressure is maintained at either 60 psig or 30 psig. To simulate a 9 car assembly the orifice in cross number 10 is replaced by a plug. This effectively shortens the assembly by one pipe. A pressure difference measurement is made between head end and rear. Proceeding in this way the orifice is removed from the end cross and a plug inserted until only two cars remained with leakage. In the case of flow sink leakage, the experimental procedure are the same except the same diameter orifices are replaced by adjustable orifices and they were adjusted to have the same flow rate under corresponding theoretical pressures. These pressures (dashed curves in figure 5.14 and 5.15) were calculated from equation 3.20 with n varying from 2 to 10, $m_L = 0.000746$ lbm/sec at 60 psig and $m_L = 0.00043$ lbm/sec at 30 psig. Figure 5.14 and 5.15 show the taper for both resistance leakage and flow sink leakage models as function of car number. One observes that the longer the assembly, the larger the discrepancy between theory and experiment. The error between experiment and resistance leakage model is always less than 0.17 percent of the taper.

CHAPTER 6

CONCLUSION AND SUGGESTION ON FURTHER WORK

6.1 CONCLUSION

Two groups of models were analytically introduced in chapter 3. They are the resistance and flow sink leakage models. Both groups are used in conjunction with the compressible-turbulent and incompressible-laminar series elements representing the fluid resistance of the brake pipe.

Referring these models to the actual brake pipe, in the pressure gradient curve they all demonstrate that leakage in rear cars has a larger effect on pressure gradient and pipe taper than those located at the front end of the train. One may interpret the models as assigning the weighting factors to each car. In the incompressible models the weighting factors are proportional to the car position from the head end (section 3.2.1 and 3.3.1). In the compressible flow models the weighting factor are approximately proportional to the square of the car position (section 3.2.2 and 3.3.2).

Leakage detection and leakage measurement were analytically described in chapter 4 based on the compressible-turbulent, resistance shunt model. With the

introduced leakage detection scheme in which degree of leakage in each car is represented by the amount of leakage flow, one can detect the major leaks throughout the entire train by the comparison of such leakage flows. In section 5.3.6, this 'leakage' detection scheme was applied to compare the leakage flows in the experimental set-up according to the data of the pressure gradient. The results showed that the largest leak could be determined by its prominent position in the leakage flow versus leakage position curves.

The mathematical expressions of both the "pressure drop" and "leakage flow" measurements reveal the fact that to ensure all trains operating in proper leakage condition (all cars have the same degree of leakage in a train made up of any numbers of cars), one single indication of pressure drop rate or total leakage flow can not be universally utilized in the safe road operation certeria. Since the "pressure drop" measurement involves only the brake pipe leakage and what affects the whole braking activities is the leakage in all brake units, the "leakage flow" measurement seems to provide more sufficient information for the braking condition. In addition to its simple testing procedure and less time required, this measurement is believed to be more adaptable compared to the "pressure drop" measurement. Furthermore, this measurement can be improved by marking different indications on the flow indicator for trains made up of different numbers of car.

In chapter 5, the experiment for all the analytical models were introduced. The incompressible-laminar models were in excellent agreement with the experiments in the electrical circuit. It was because the electrical components behave exactly as they were prescribed mathematically. In the brake pipe experimental model, both the resistance shunt and the flow sink leakage are applied. The maximum errors between the analytical and experimental results are always occurring at the rear. This is a consequence of the weighting and cumulative effect of rear car leakage. Another source of error is caused by differences in the series pipe characteristics K_2 . It was assumed that in the analytical models all the cars had the same brake pipe characteristic K_2 . The tests for pressure-flow characteristics on pipe-bend combinations show that there is a considerable discrepancy between the pipes. In fact, the results have been improved by substituting the different pipe characteristics K_2 of each into the analytical model. In addition, there is a general problem with these models that some of the rear cars in an actual train are operating in laminar flow while the front cars are in turbulent flow. The present experiments were designed to minimize this effect by using relatively large leakage orifices. Thus, in the experiments possibly only the last car had a laminar flow condition. Even for the long trains, there is no significant change in pressure gradient between those having all cars operating in turbulent flow and those

having a few rear cars in laminar flow. The large discrepancies between the analytical models and experimental model occur in the rear are less than 17 % of the brake pipe taper. Despite the discrepancies, the analytical models provide a basis for quantitatively understanding brake pipe leakage.

It should be pointed out that, besides the physical size, there are differences between the actual brake pipe and the experiment set-up. Firstly, in our analytical and experimental models, the leakage is concentrated at one point while the leakage in an actual freight car is distributed at random. Secondly, the flow through the connecting hose of a freight car may have more restriction than the experimental model. In a real train arrangement, the in-line flow first goes through a 45 degree angle cock to a cutout cock where the flow has two 90 degree direction changes before it goes into the next car through another angle cock. Thirdly, the brake pipe in a real car has some degree of curvature depending on location of other devices equipped on the car.

6.2 FURTHER SUGGESTION

The experimental work in this thesis has proven that in order to formulate these models, certain experimental data is required. It is encouraged that this data be obtained from the actual brake pipe. Tests should be directed to the

investigation of the pressure-flow characteristics of the pipe, hose and leakage.

So far the steady state of the brake pipe leakage was successfully modelled with the network theory. But this concept will still be valid if the research is extended to the dynamic nature of the brake pipe. With the addition of storage-elements to the present models, it is possible to form new models which can also provide simulation to the charging and discharging process in the brake pipe.

It should be noted that it is not possible to determine quantitatively the tolerable leakage for a train just from the knowledge of the brake pipe or any other local components. The quantity of such allowable leakage can only be established through the optimization of the entire brake system behavior.

REFERENCES

1. "Management of Train Operation and Train Handling." The Air Brake Association Handbook 1972.
2. Blaine, D.G and M.F. Hengel "Brake-System Operation and Testing Procedures and Their Effects on Train Performance." ASME paper 71-WA/RT-9, 1971.
3. "Brake Pipe Leakage" the Air Brake Association Committee on Brake Pipe Leakage. Proceedings of 33rd annual convention of the Air Brake Association, 1926, PP 133-211.
4. Rlein, W.F. "Characteristics of Air Flow in Automatic Train Braking". Proceeding of Annual Meeting of Air Brake Association, 1950, PP 162-173.
5. Hart, C.E. "analysis of Brake system Leakage Surveillance". Proceeding of Annual Meeting of Air Brake Association, 1967, PP 33-57.
6. Central Air Brake Club "Effect of Higher Brake Pipe Pressures on Leakage and the Testing of Freight Cars". Proceedings of Annual Meeting of Air Brake Association, 1968.
7. Wright, C.D. "Effective Brake Pressure for Brake

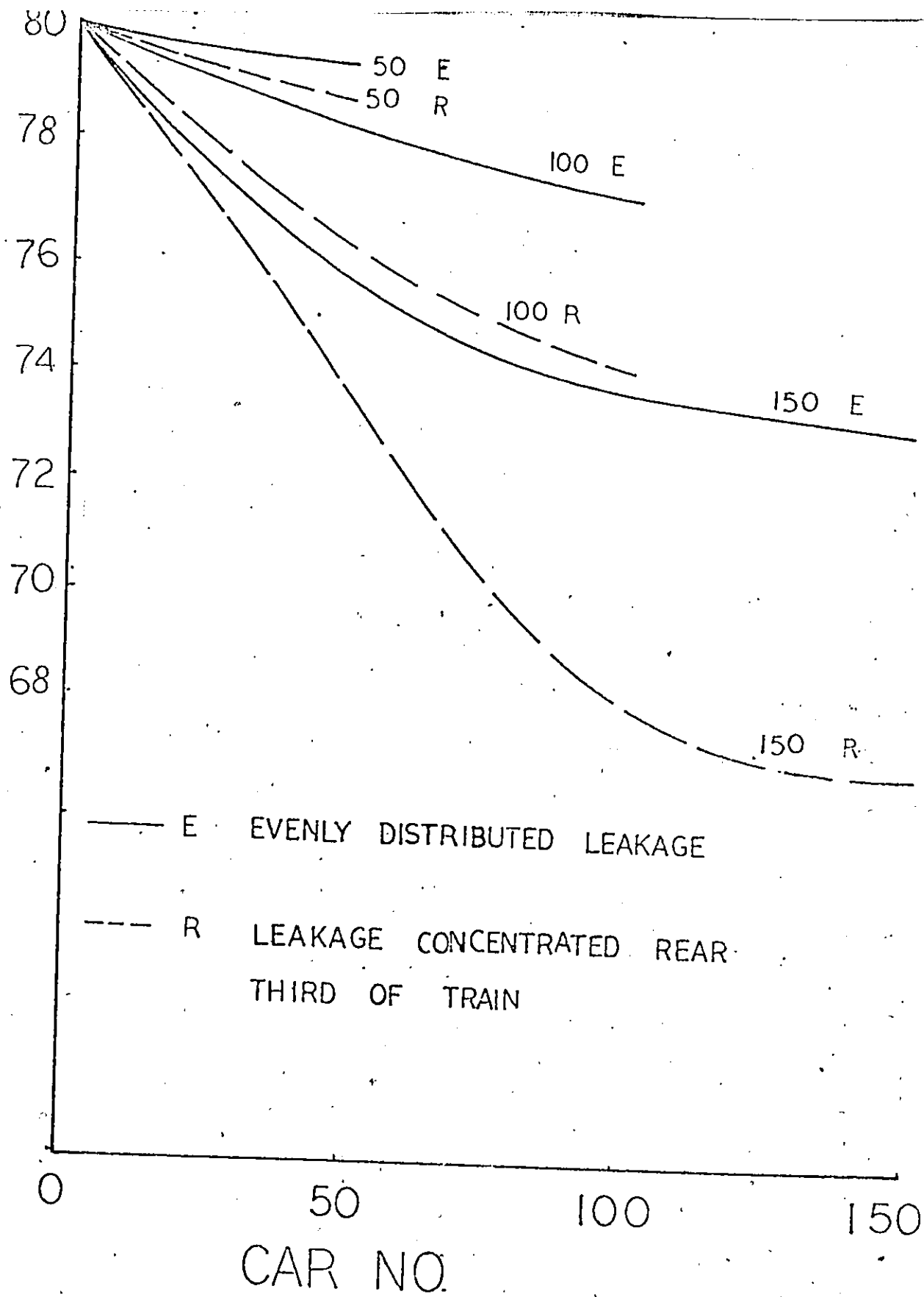
- Performance". Proceedings of Annual Meeting of Air Brake Association, 1967.
8. Wichham, D.J. "Informing the driver of Brake-pipe Flow and Leakage Parameters". Rail Engineering International, May 1974, vol. 4 No. 4.
 9. Hart, C.E. "Expediting the Measurement of Brake System Leakage". Proceeding of Annual Meeting of Air Brake Association 1970.
 10. Palmer, D.E "Brake system Leakage". Proceeding of Annual Meeting of Air Brake Association, 1975.
 11. Wilson, R.L. "leakage and Gradient Considerations in Train Braking". The Air Brake Association Annual Meeting, Chicago, Illinois, September 28, 1976.
 12. Wilson, J.T. "Braking System Research Needs". Railroad Research Study Transportation Research Board Presentation at National Academy of Sciences, Woods Hole, Massachusetts, July, 1975.
 13. Kirshner Joseph M. "A Definition of the Mechanical Potential Necessary to a Fluid Circuit Theory". HDL Fluid Amplification Symposium, Vol. 1, PP 245-250, oct. 1965.

14. Schaedel, H.M. and G. Kessel "The D-C Equivalent Circiut of Fluidic Line Branchings", Fluidics Quarterly, Vol. IV, No. 2, April 1972.
15. Schaedel, H.M. "Signal Analysis of Fluidic Networks", HDL Fluidic State-of-the-art Symposium. Vol. III, PP 189-301, September 1974.
16. Iseman, Josepn M. "A Circuit Analysis approach to the Solution of Passive Pneumatic Fluidic Compensation Networks". HDL Fluidic State-of-the-art Symposium, Vol. IV, PP 77-177, September 1974.
17. Blackburn, J.F., G. Reethof, and J.S. Shearer "Fluid Power Control". M.I.T. Press and John Wiley, Jan. 1960.
18. Binder, R.C. "Fluid Mechanics" Third Ed. Prentice-hall, 1955.
19. Streeter, V.L., and E.B. Wylie "Fluid Mechanics" Six Ed., M. C. Graw Hill, 1975.
20. Andersen Blaine W. "The Analysis and Deisgns of Pneumatic System". John Wiley Sons Incorp., 1967.
21. McIlroy M.S. "Pipe Networks Studied by Non-linear Resistors". Transaction ASCE, Vol. 118, PP. 1055-1067,

1953.

22. Kesavan, H.K. And M. Chandrasheker "Graph-theoretic Models for Pipe Network Analysis". Journal of the Hydraulic Division, Proceedings of the A.S.C.E., Vol. 98, HY2 February 1972, PP. 345-364.

BRAKE PIPE PRESSURE, PSIG



— E EVENLY DISTRIBUTED LEAKAGE
--- R LEAKAGE CONCENTRATED REAR
THIRD OF TRAIN

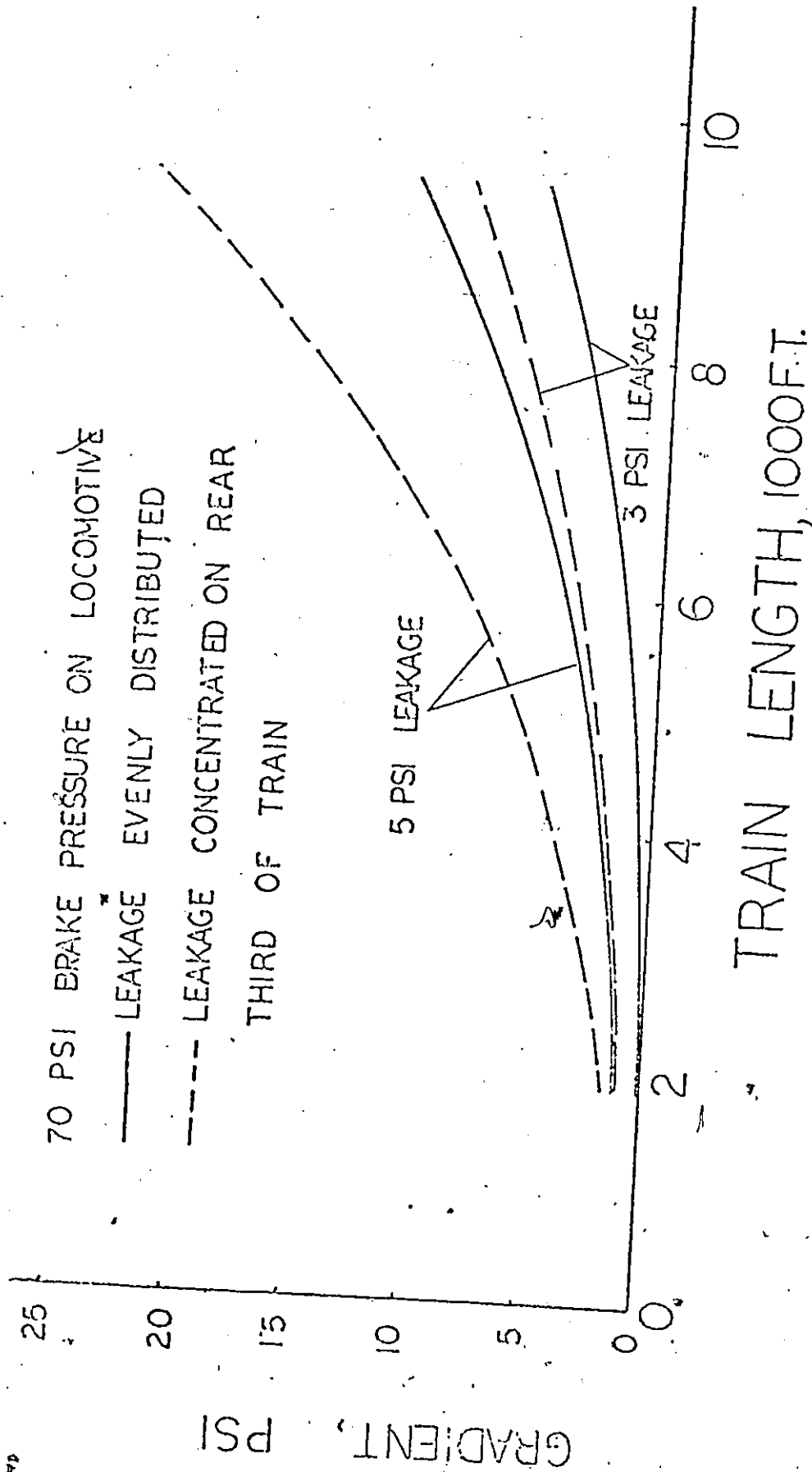


Fig. 1.2: Brake Pipe Gradient vs. Train Length
 Reproduced from: C.D. Wright, "Effective
 Brake Pressure for Brake Performance",
 Air Brake Association Annual Meeting,
 September 1965.

	BASED ON LEAKS			BASED ON TOTAL CARS		
	1925	1950	1975	1925	1950	1975
Hose & Gaskets	17.0%	19.8%	31.8%	71.0%	16.7%	11.1%
Angle Cocks	21.6%	4.0%	18.3%	92.3%	3.4%	6.3%
Brake Pipe	20.8%	12.8%	3.2%	87.4%	9.3%	1.1%
Branch Pipe	20.4%	40.1%	14.8%	85.4%	33.3%	5.1%
Triple Valve	17.1%	1.2%	19.4%	84.8%	1.0%	3.9%
Reservoir	3.1%	22.1%	12.5%	18.0%	18.6%	7.4%
Base (total number of leaks or cars)	10634 (leaks)	169 (leaks)	249 (leaks)	2424 (cars)	204 (cars)	741 (cars)

Fig. 1.3: Comparison of three leakage tests conducted in 1925, 1950, 1975 by Air Brake Association

Reproduced from "Brake System Leakage"
Presented at the Air Brake Association
Annual Meeting, September 15, 1975.

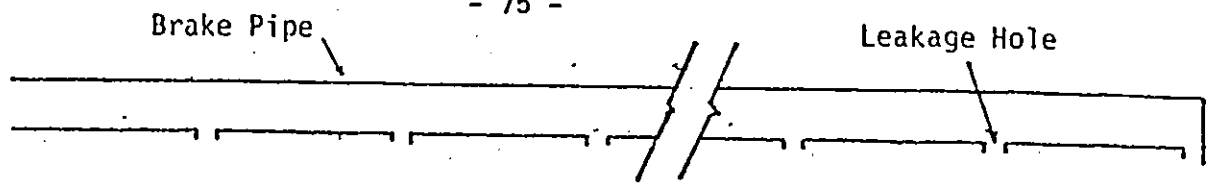


Fig. 2.1.a: Simplified Brake Pipe Model

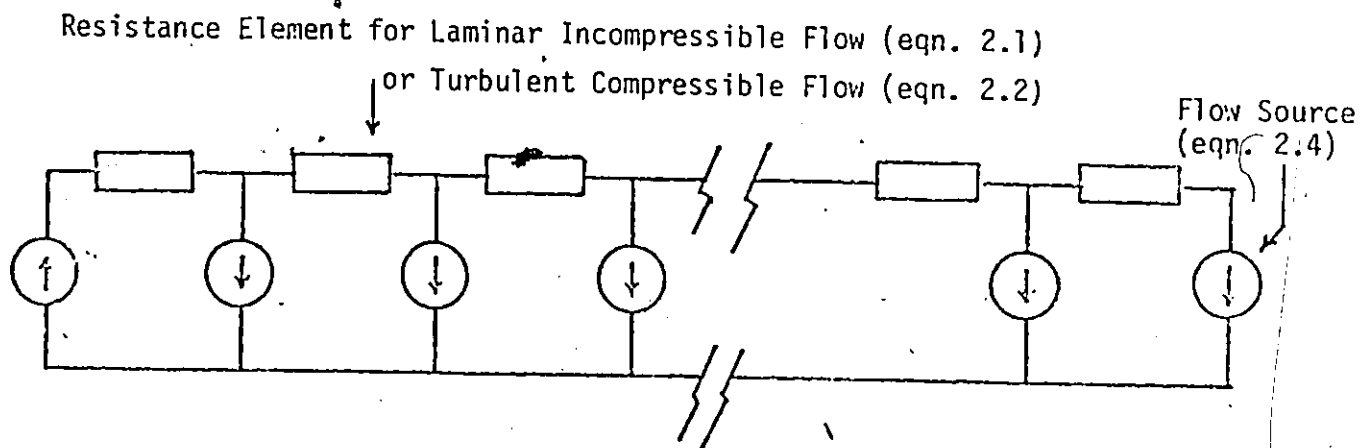


Fig. 2.1.b: Flow Sink Leakage Model

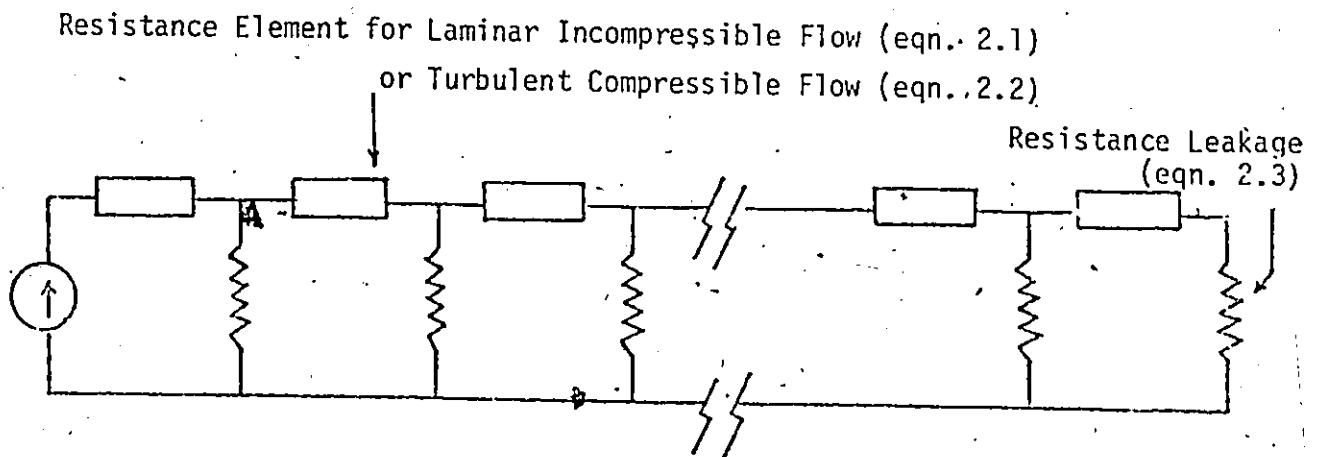


Fig. 2.1.c: Resistance Leakage Model

Fig. 3.1: Flow sink leakage model

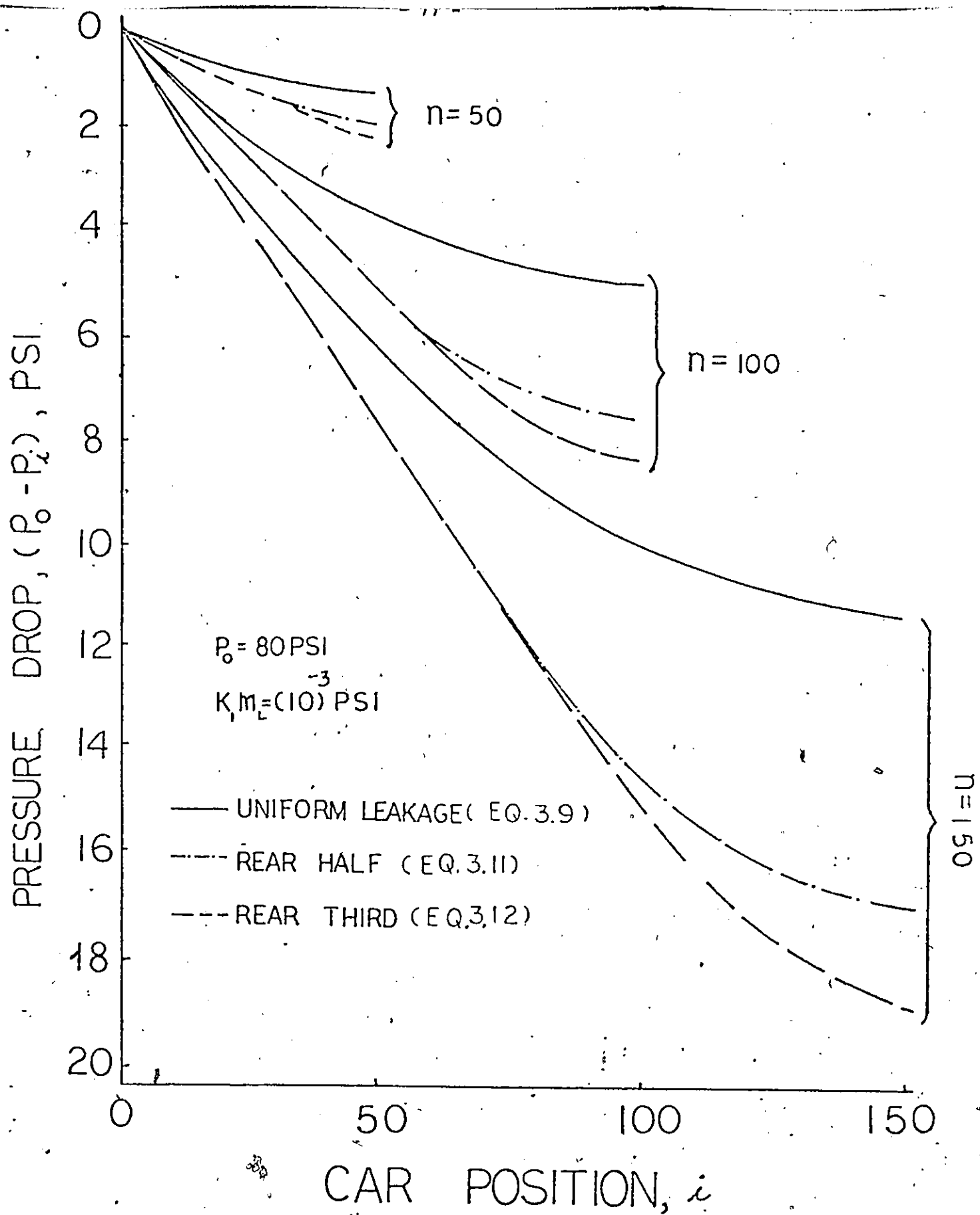


Fig. 3.2: Pressure gradient curves for flow sink leakage, laminar-incompressible flow model

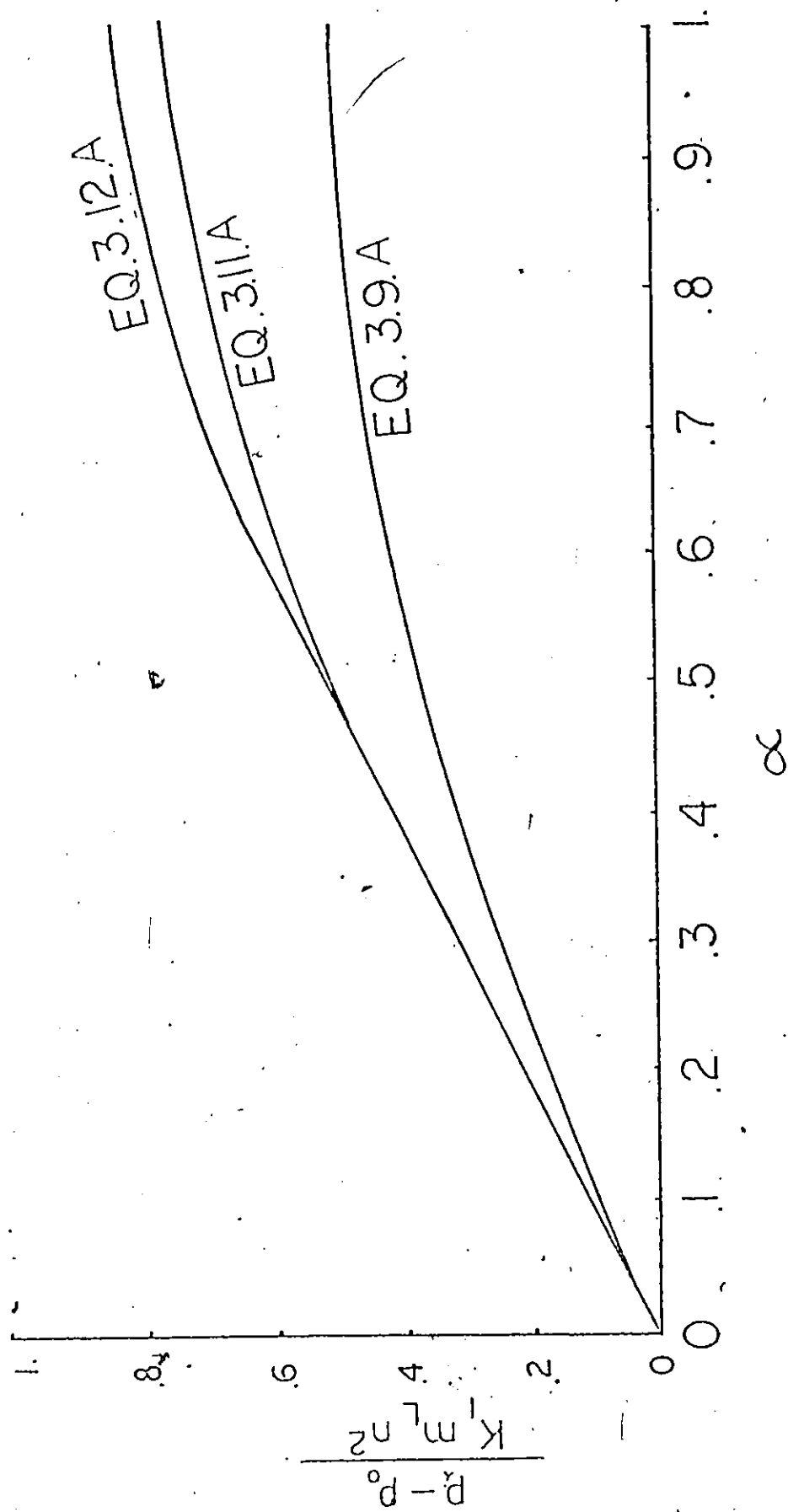


Fig. 3.2.a: Dimensionless pressure gradient curve for flow sink
leakage, laminar-incompressible flow model

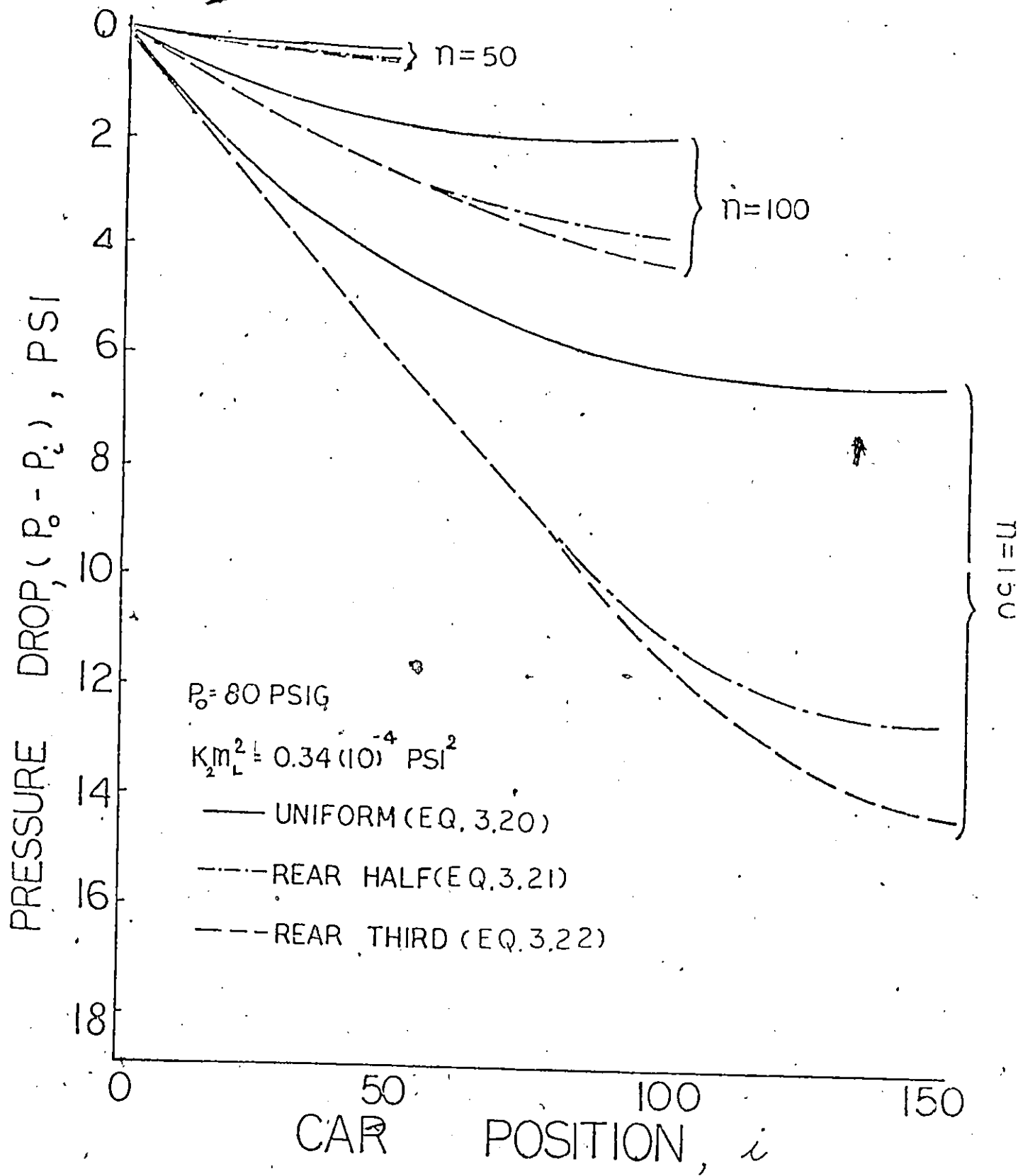


Fig. 3.3: Pressure gradient curves for flow sink leakage, turbulent-compressible flow model

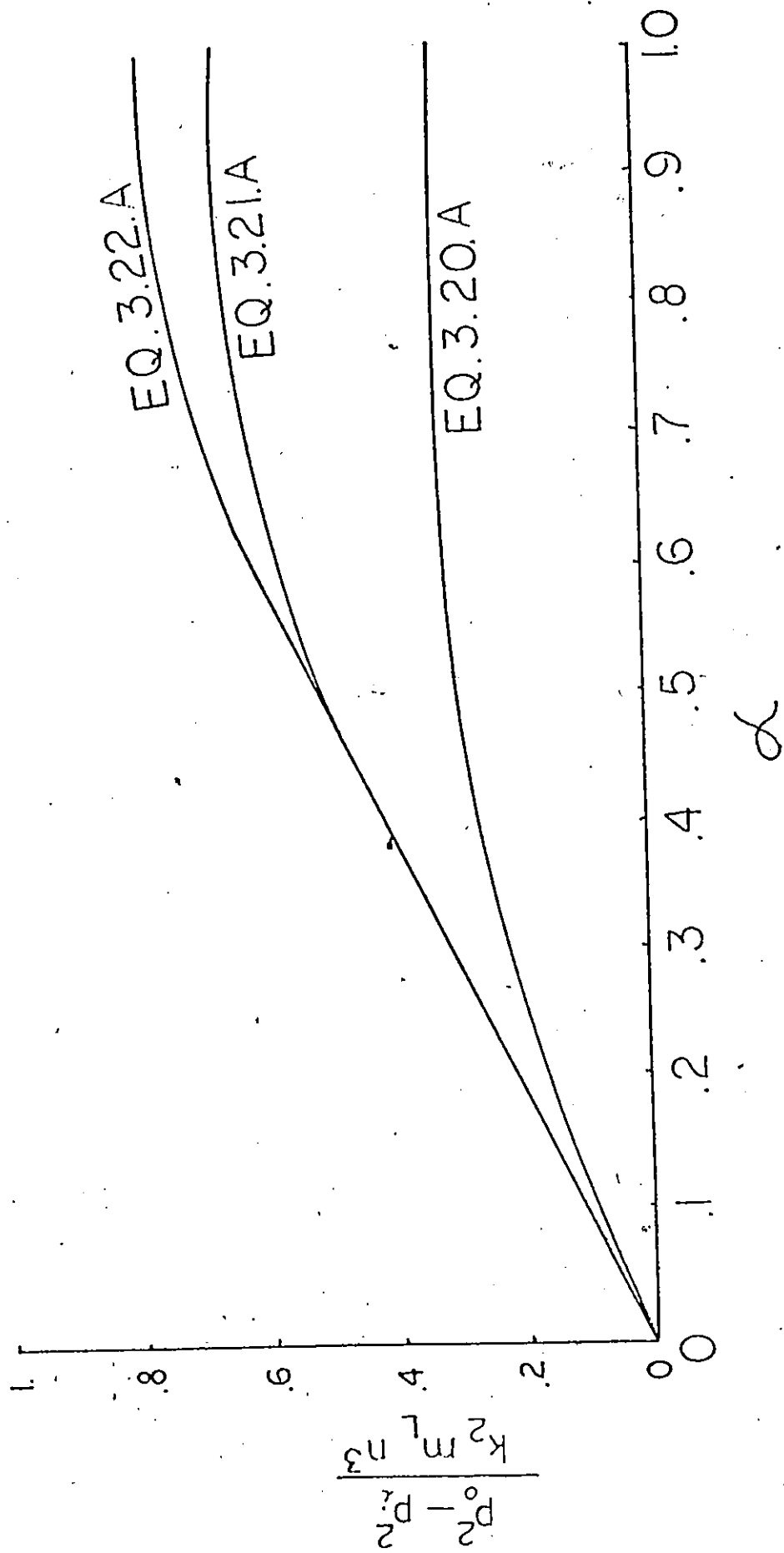


Fig. 3.3.a: Dimensionless pressure gradient curves for flow sink leakage, turbulent-compressible flow model

RESISTIVE ELEMENT

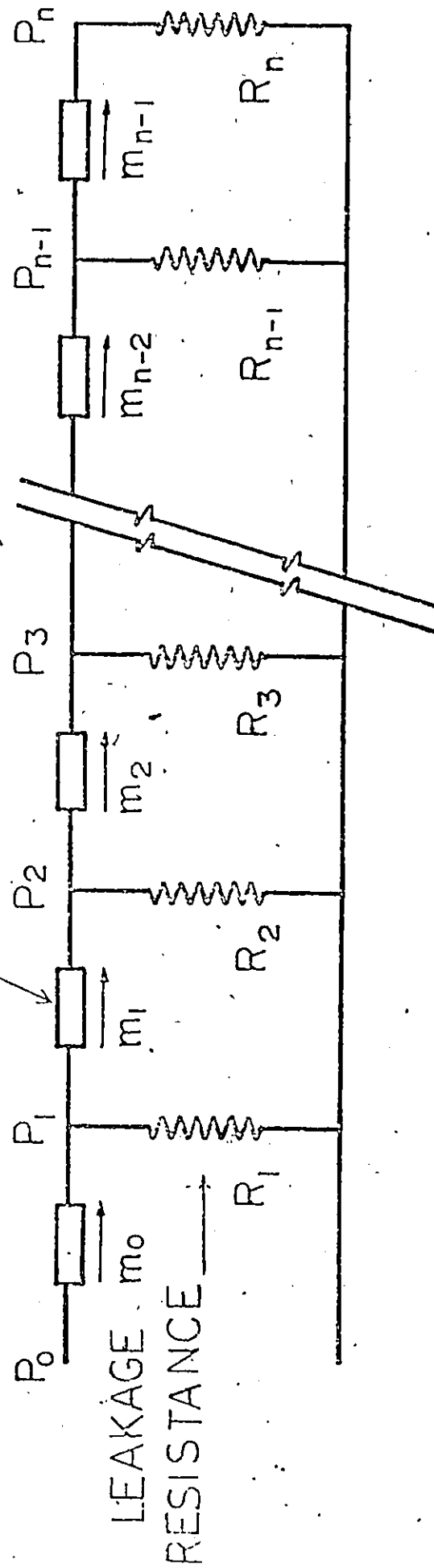


Fig. 3.4: Resistance leakage model

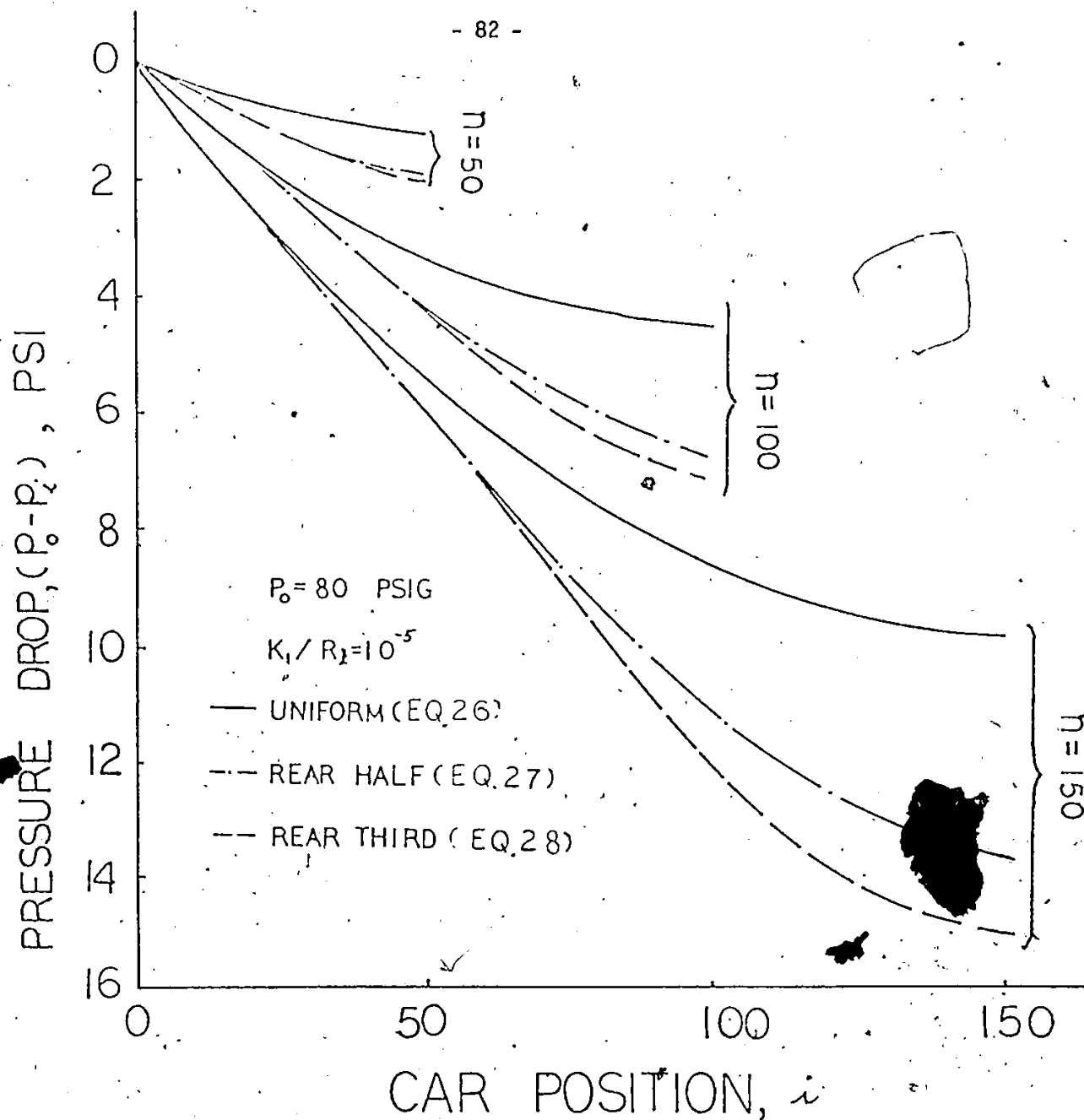


Fig. 3.5: Pressure gradient curves for resistance leakage, laminar-incompressible flow model.

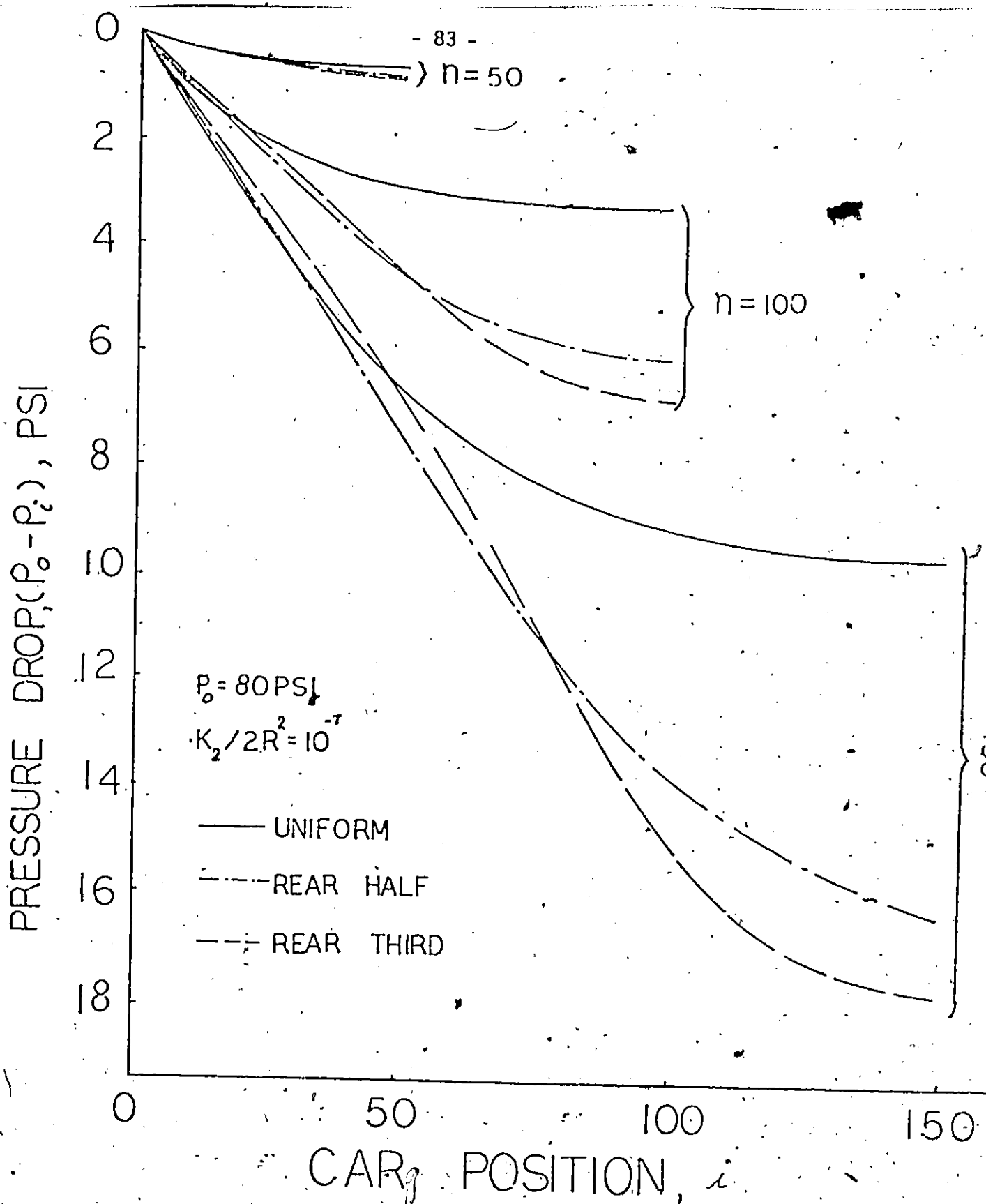


Fig. 3.6: Pressure gradient curves for resistance leakage, turbulent-compressible flow model

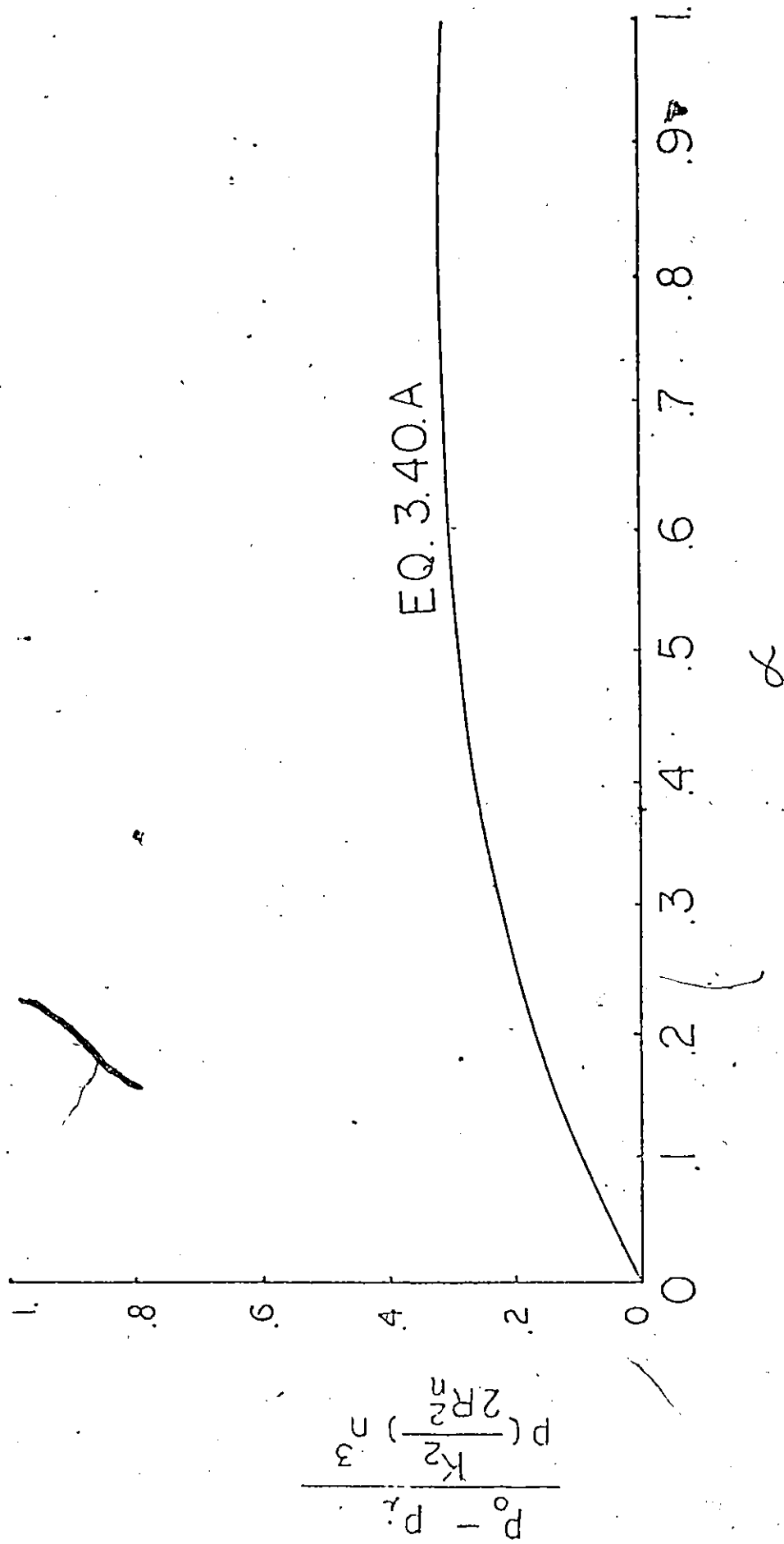


Fig. 3.6.a: Dimensionless pressure gradient curves for resistance leakage, turbulent-compressible flow model

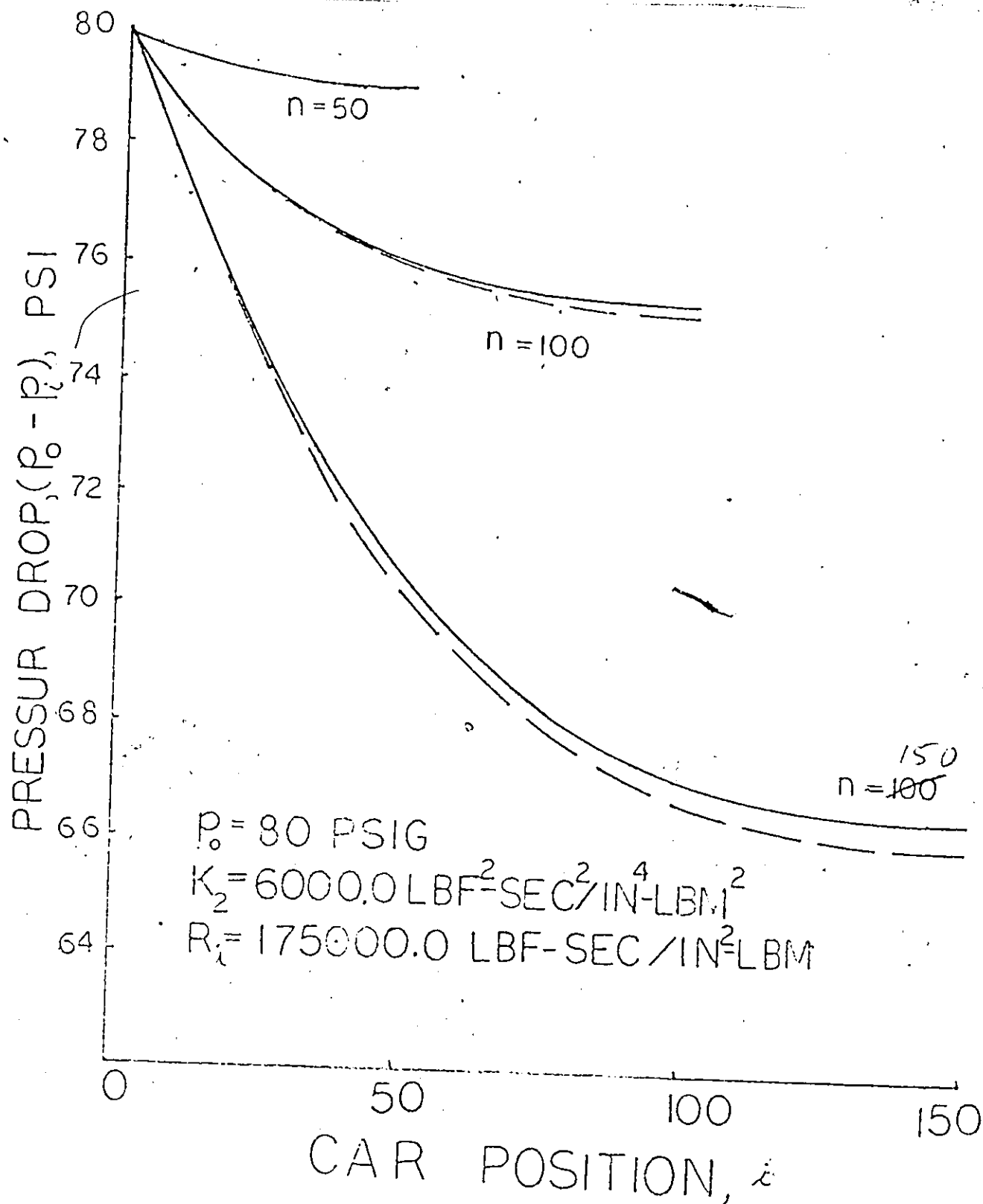


Fig. 3.7: Pressure gradient curves for the simplified equation of the resistance leakage, turbulent-compressible flow model

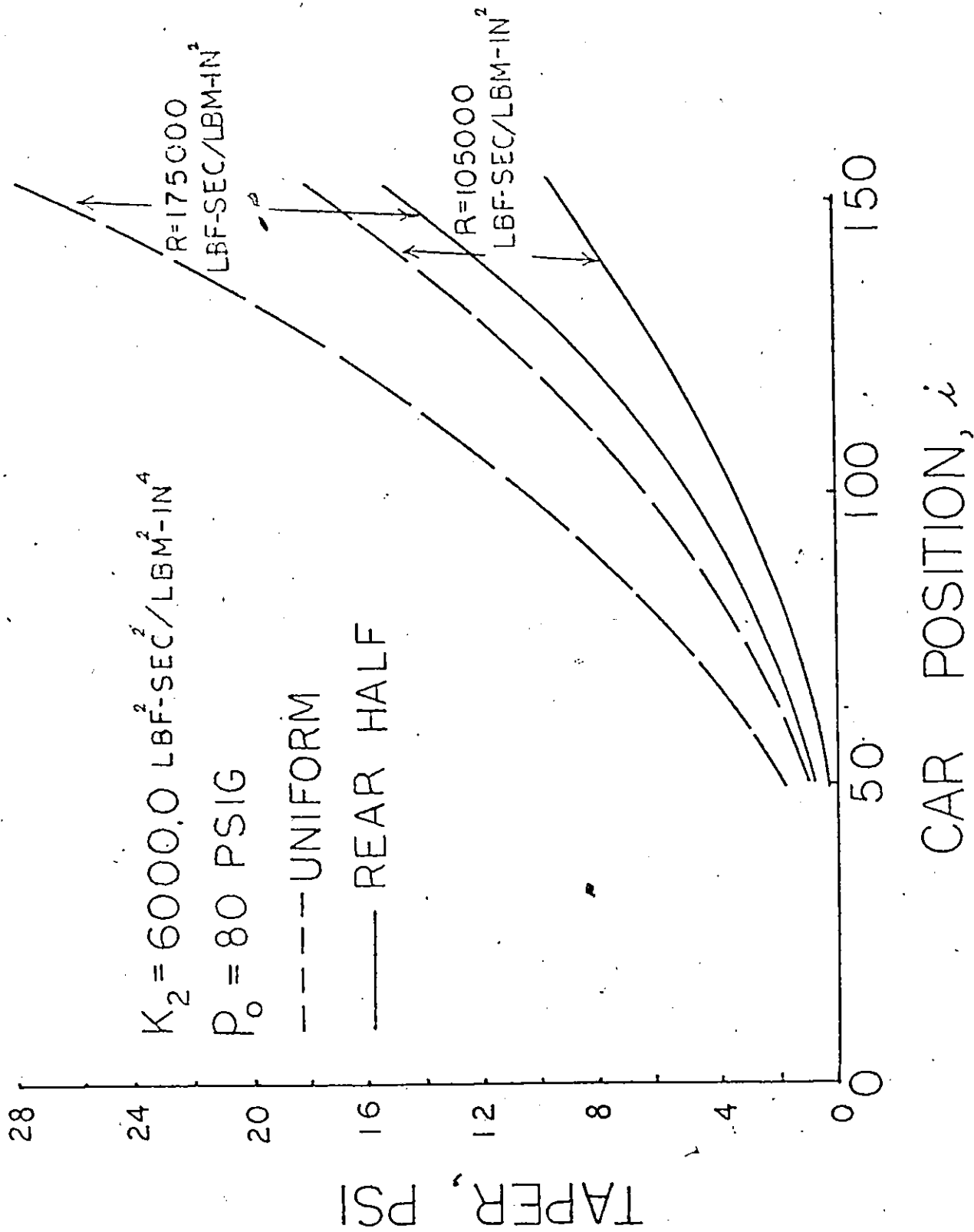


Fig. 3.3: Brake pipe gradient VS train length

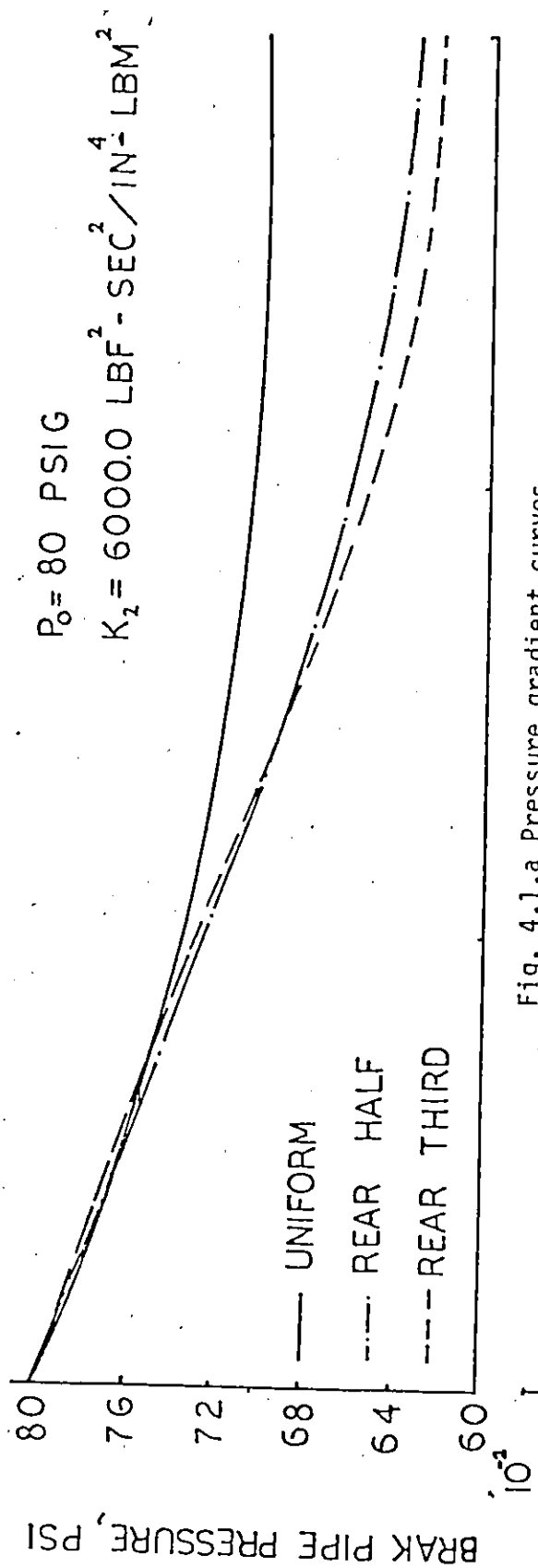


Fig. 4.1.a Pressure gradient curves

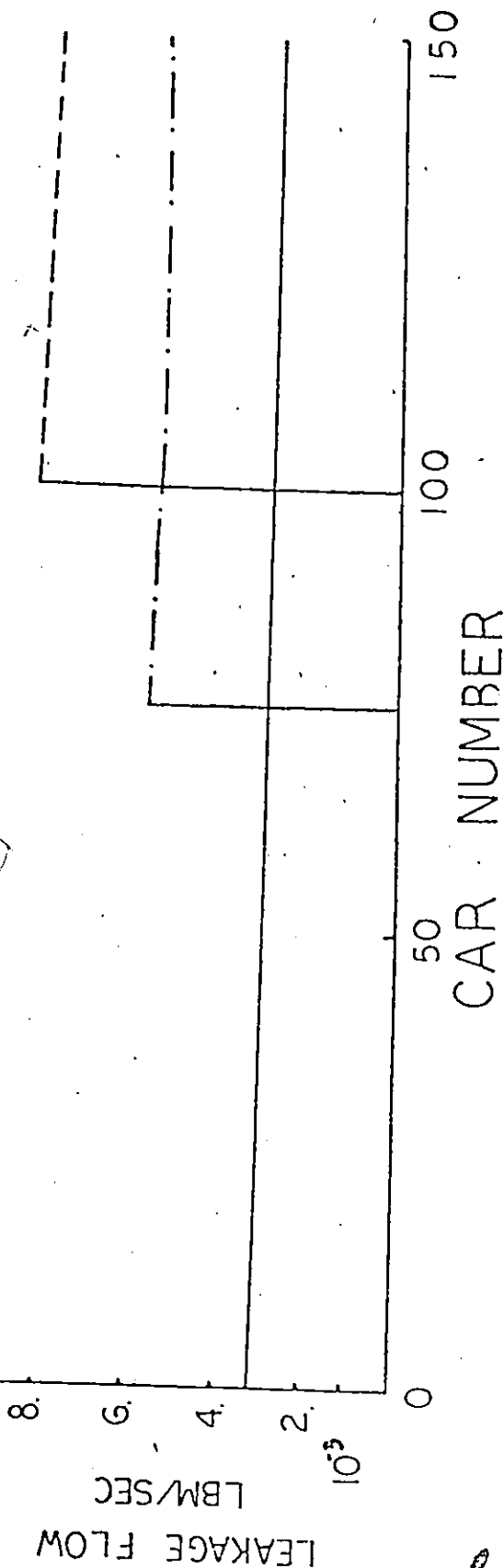


Fig. 4.1.b leakage flow VS car number

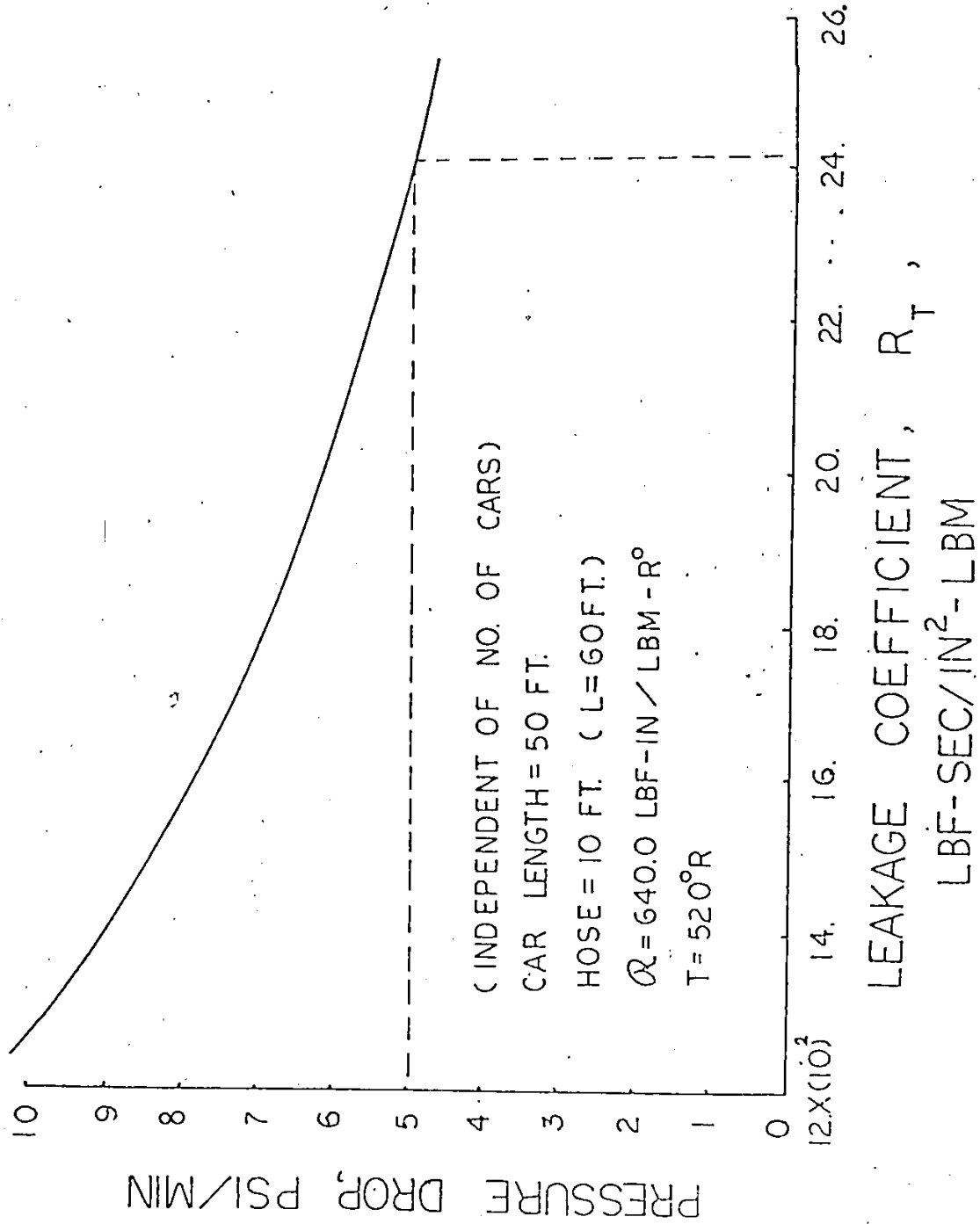


Fig. 4.2: Pressure drop VS leakage

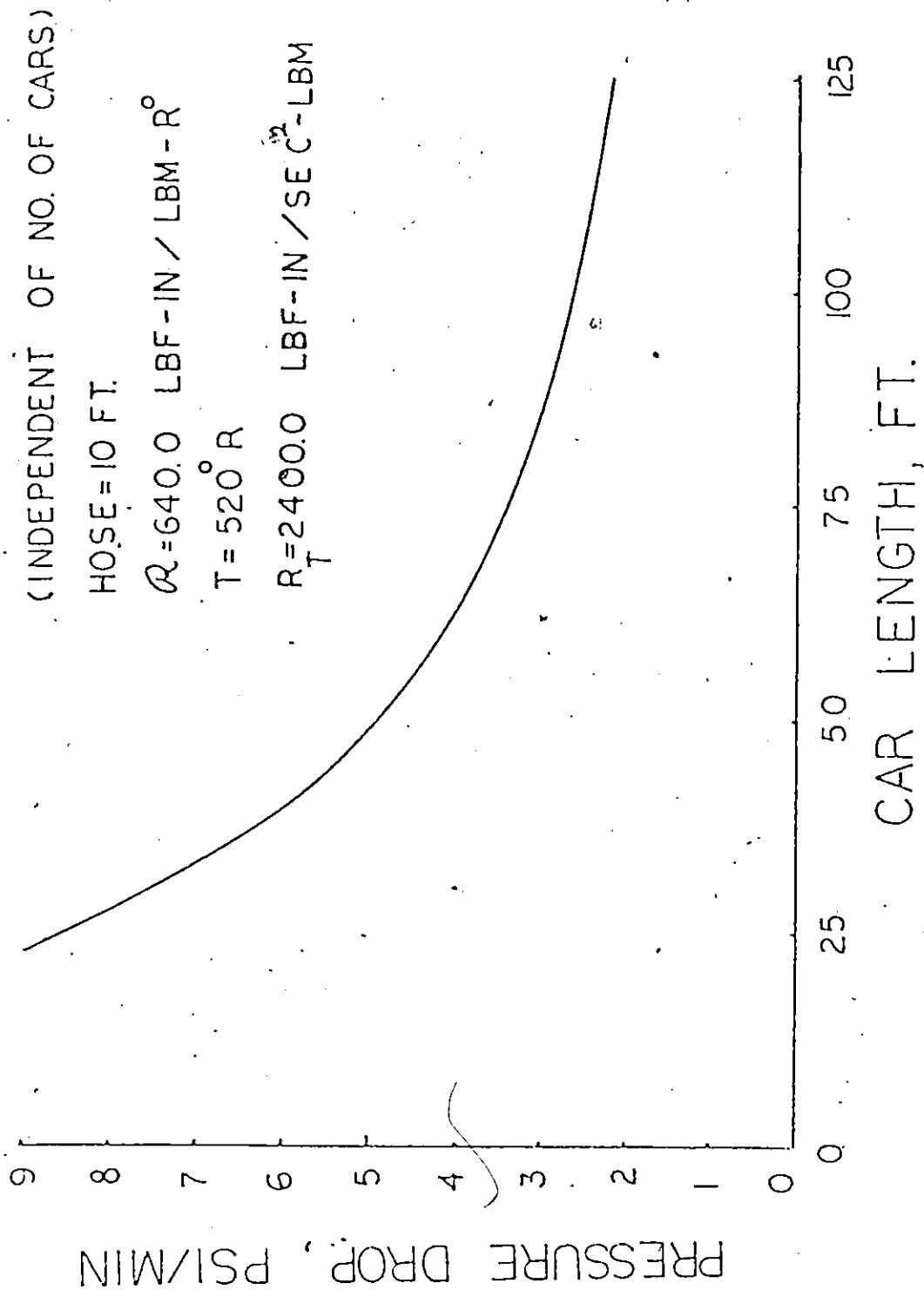


Fig. 4.3: Pressure drop VS car length

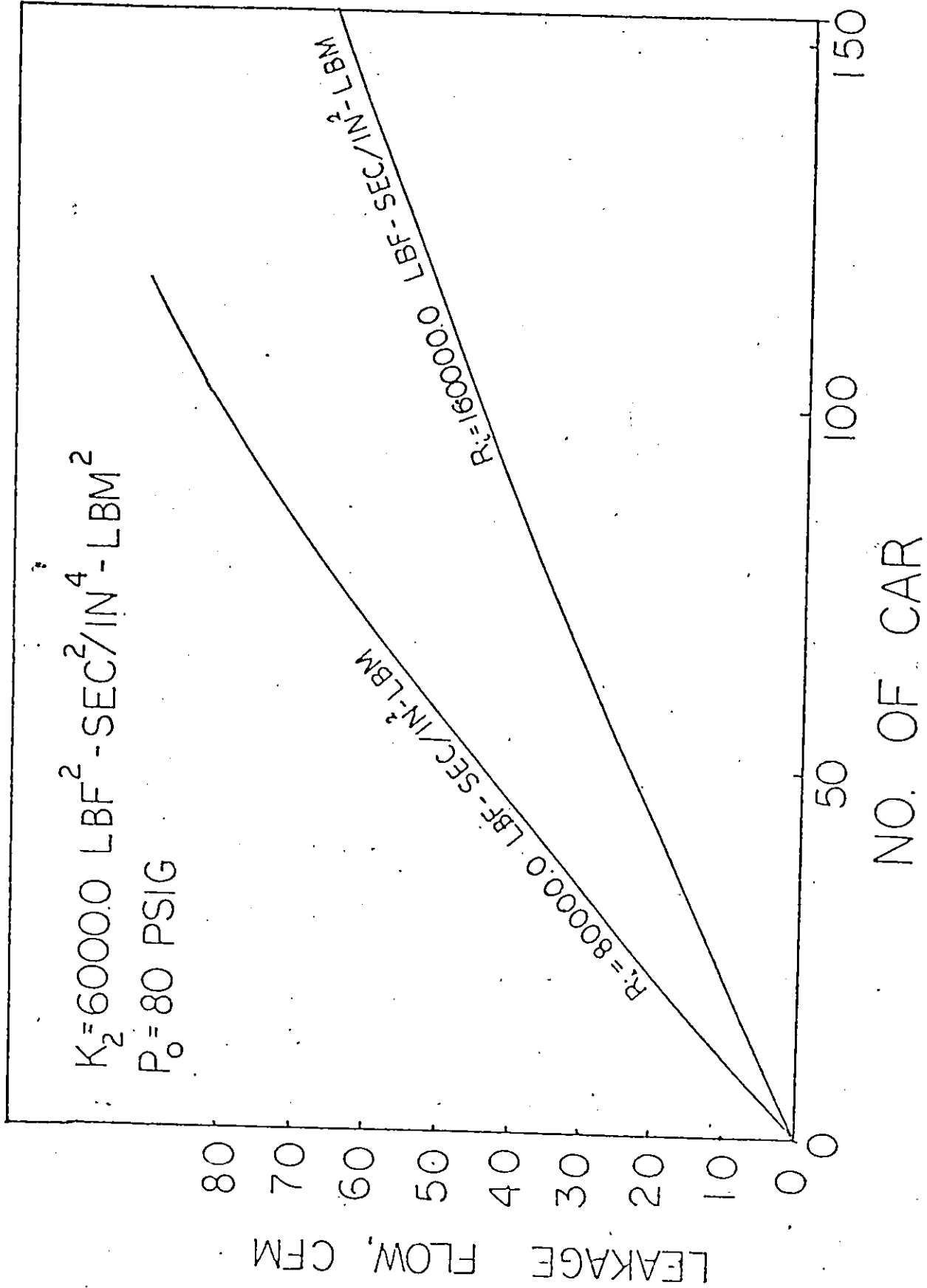


Fig. 4.4: Leakage flow VS no. of car

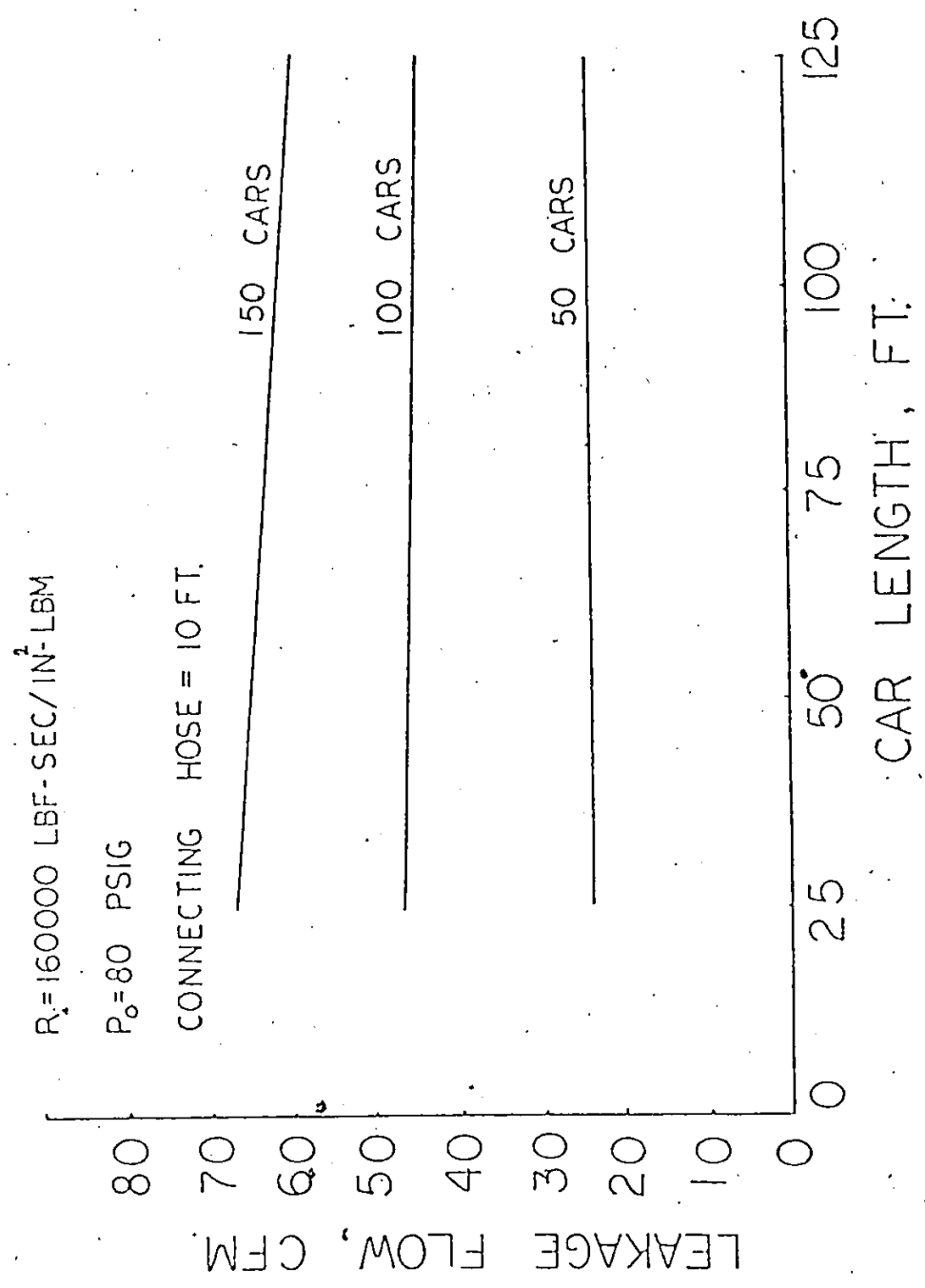


Fig. 4.5: Leakage flow VS car length

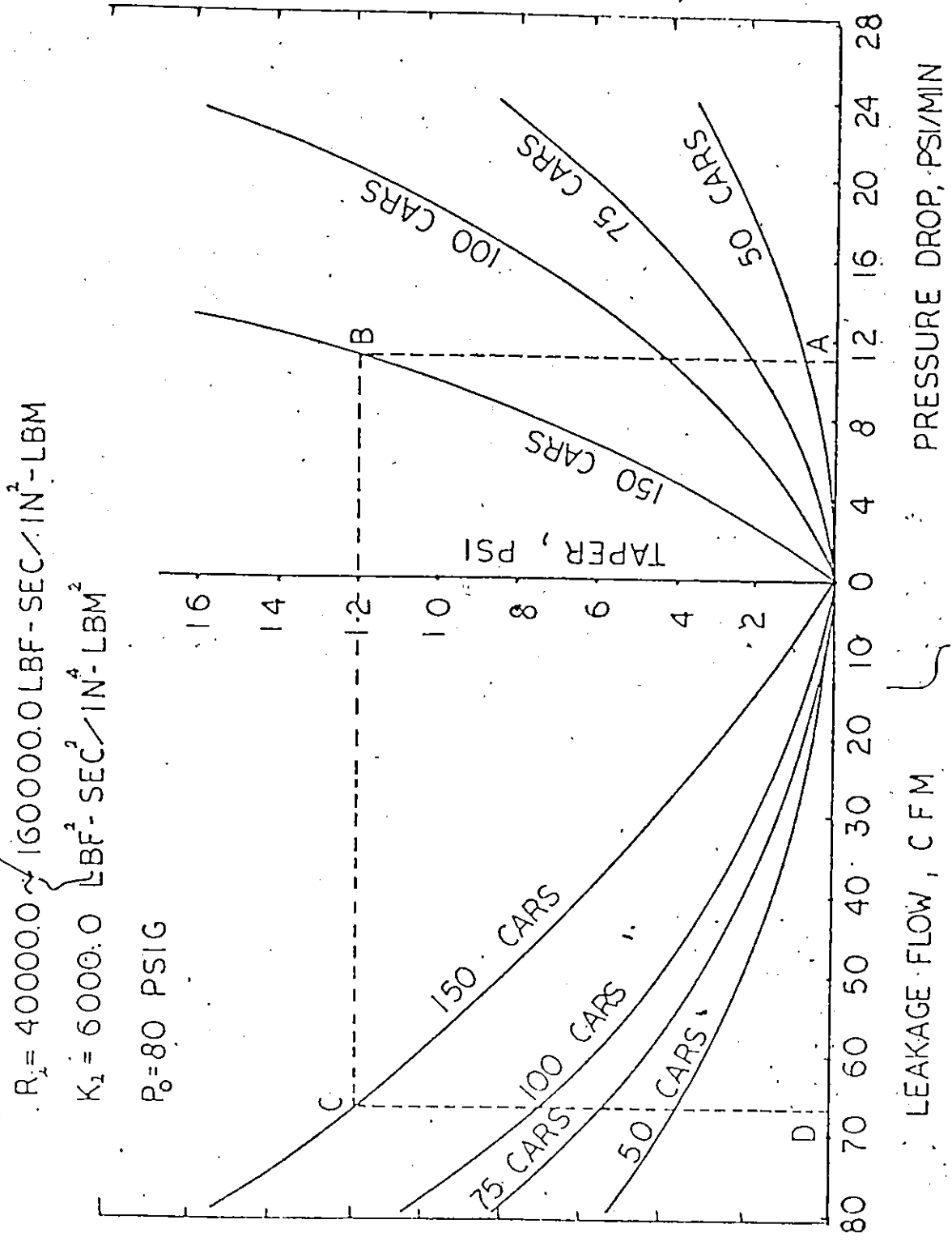


Fig. 4.6: Pipe taper VS leakage and pressure drop

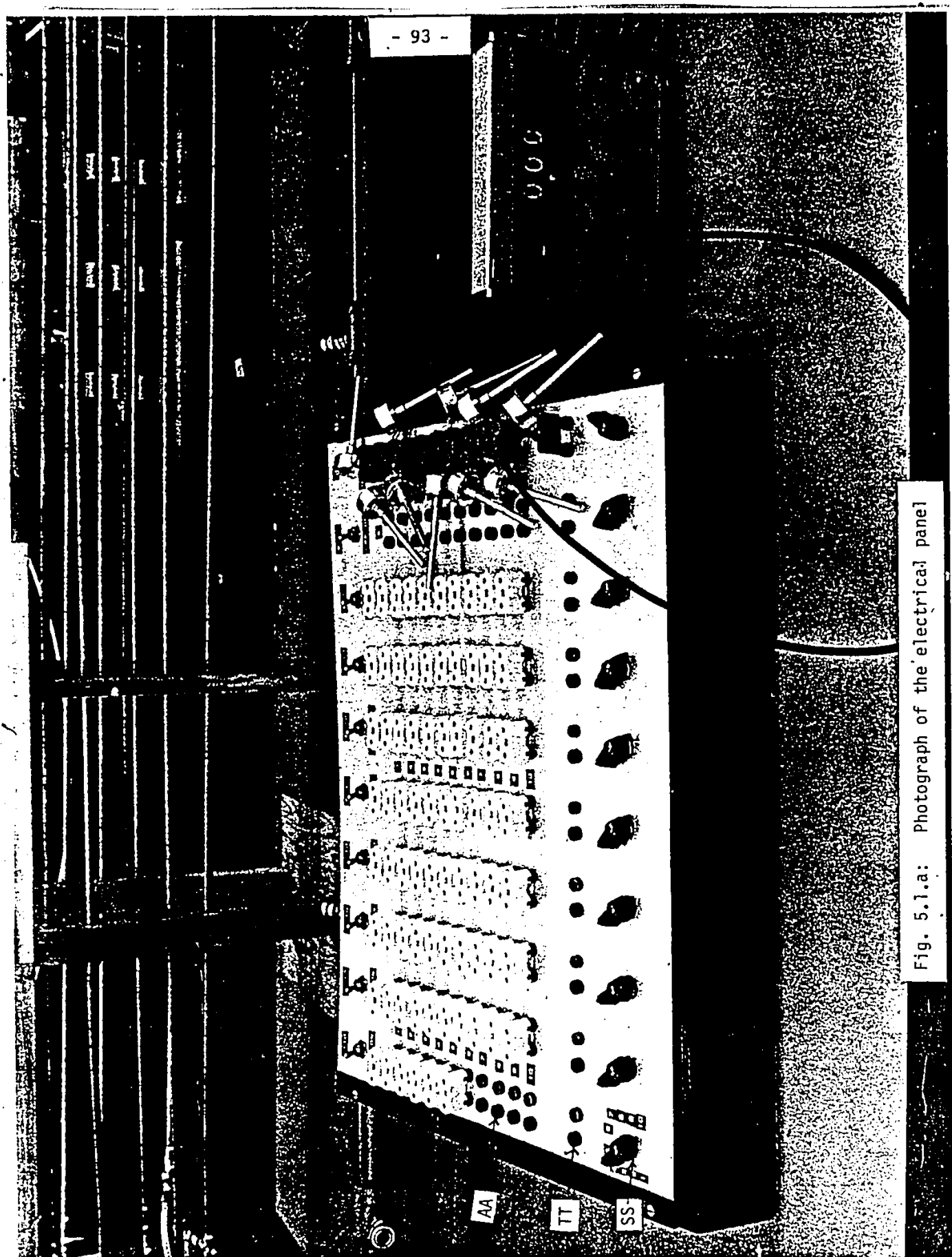


Fig. 5.1.a: Photograph of the electrical panel

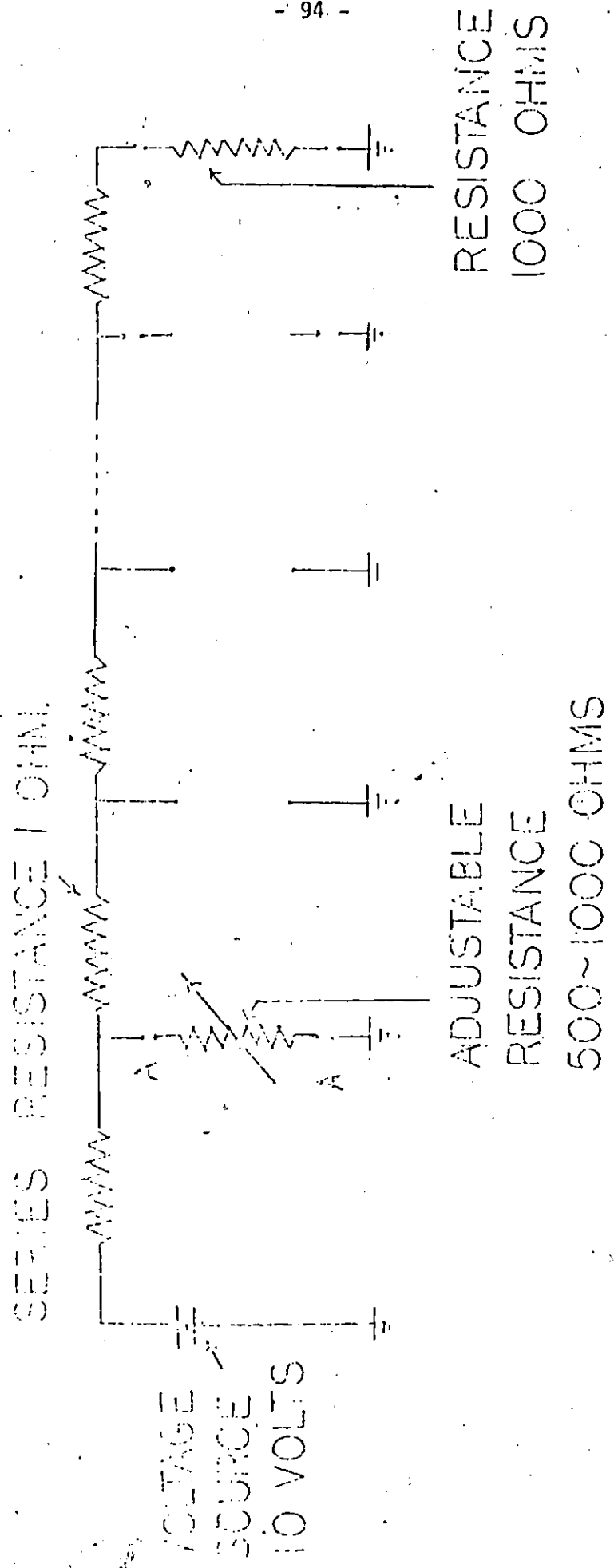
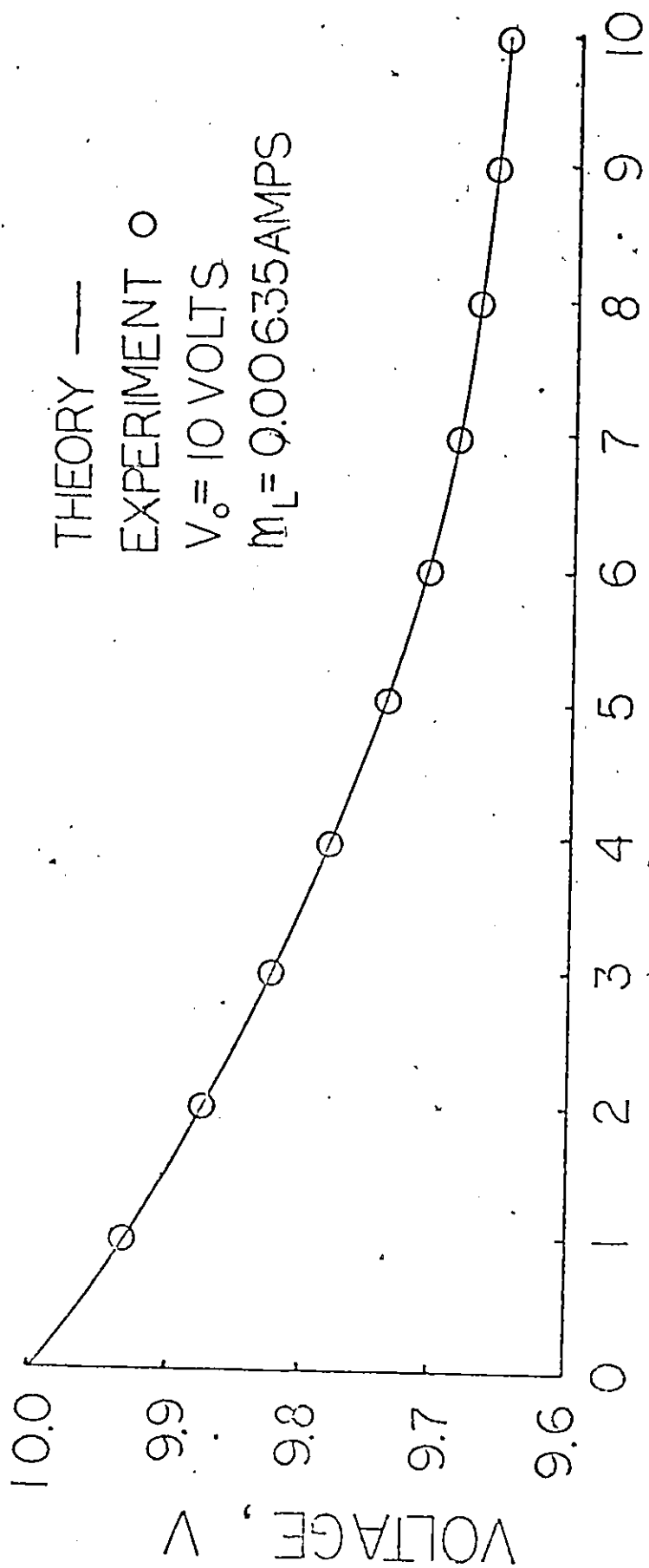


Fig. 5.1.b: Circuit of the electrical panel



NO. OF MEASURING POINT, z

Fig. 5.2: Flow sink leakage, laminar-incompressible model
 experiment on electrical panel.

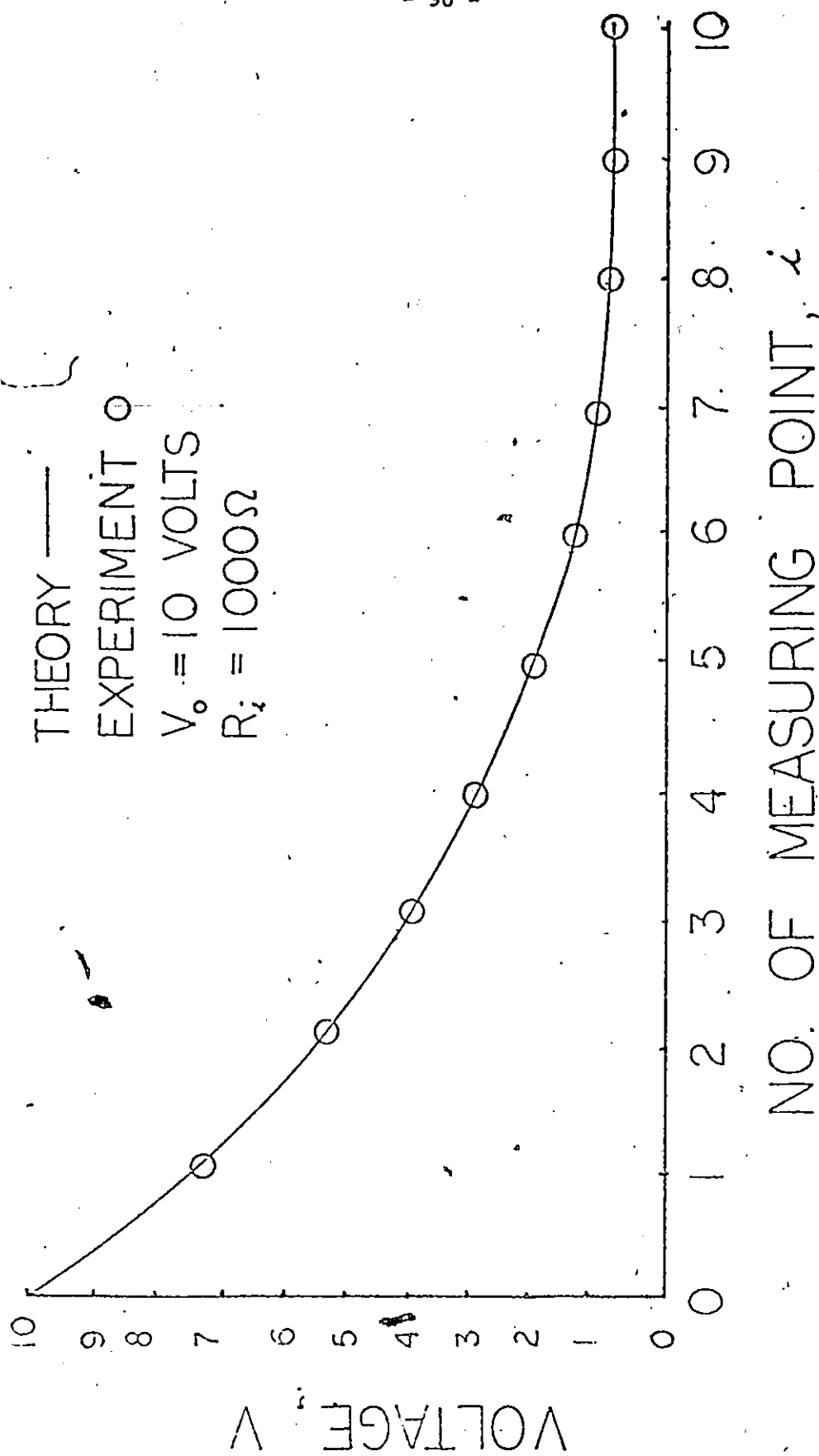


Fig. 5.3: Resistance leakage, laminar-incompressible model
experiment on electrical panel

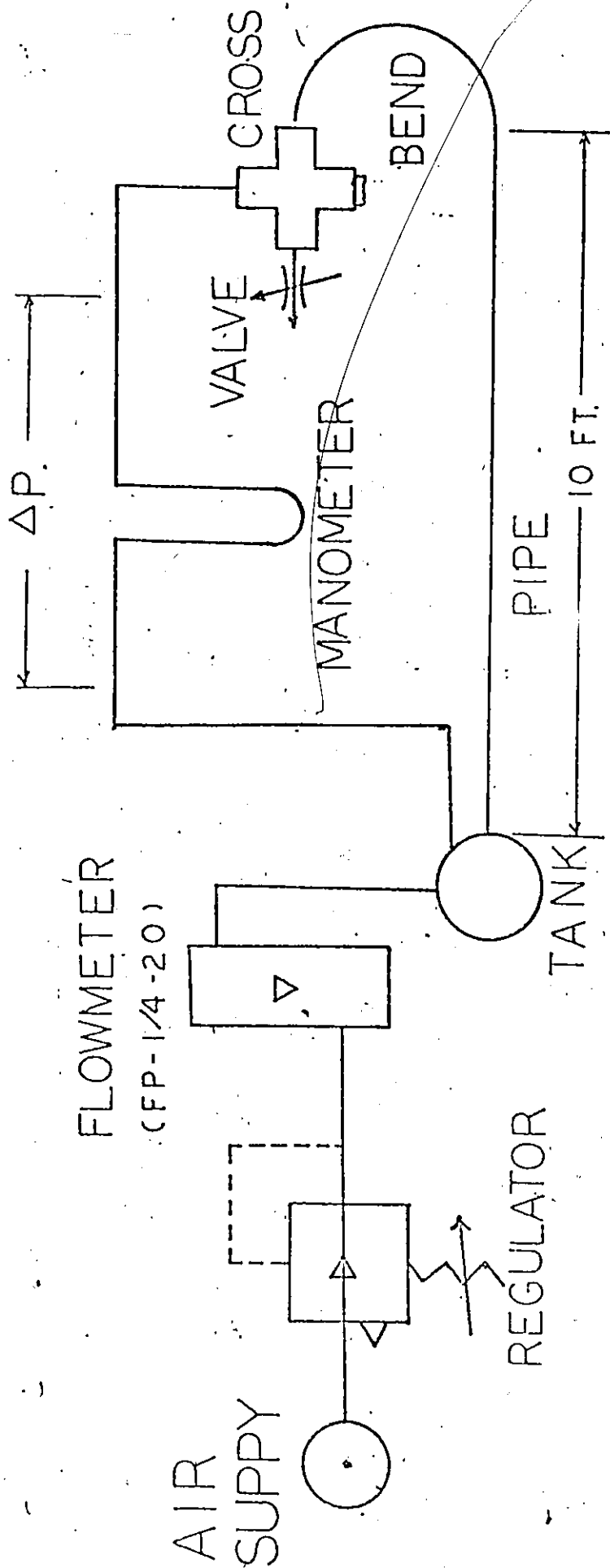


Fig. 5.4: Set-up for the pipe-bend combination test

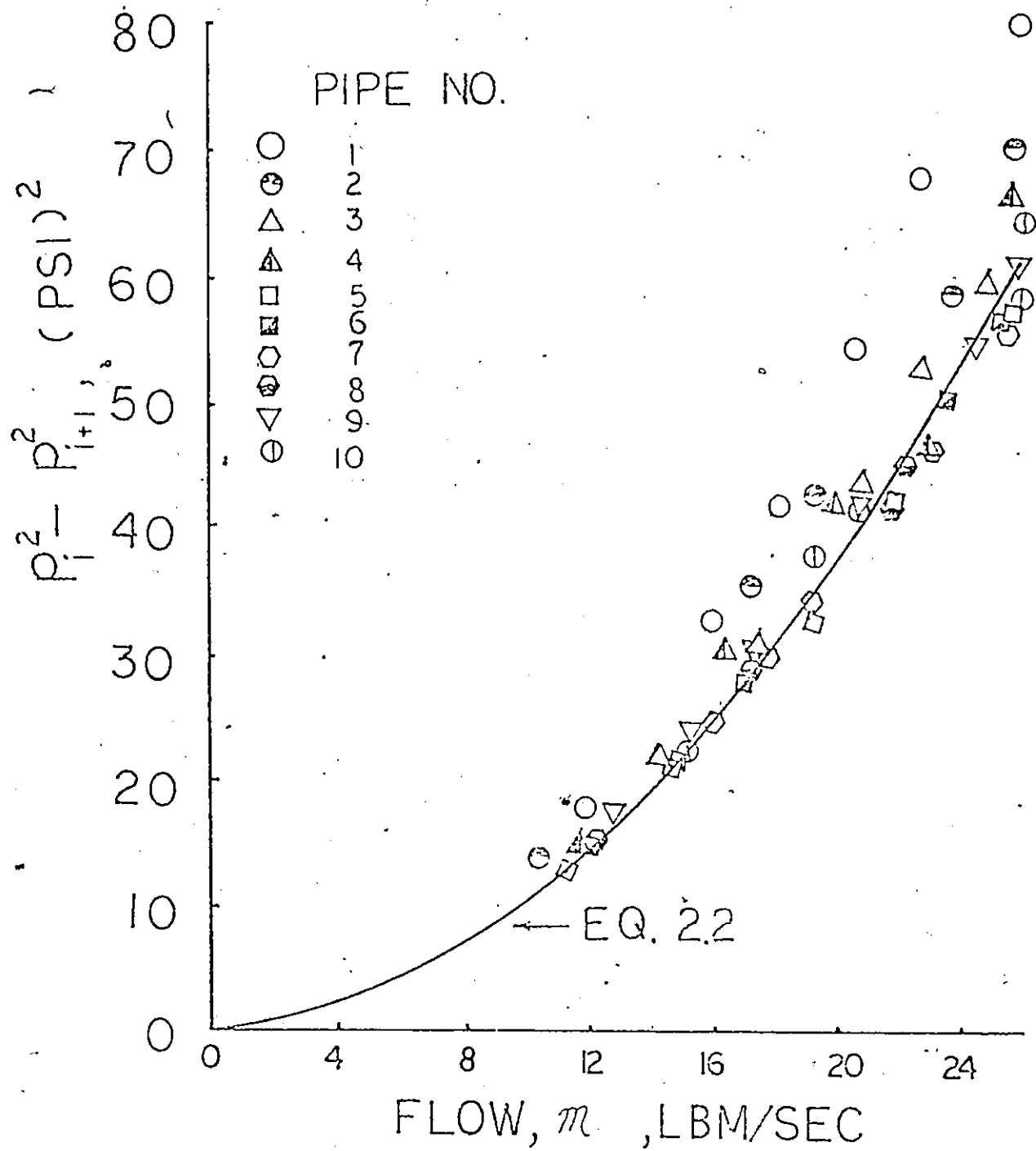


Fig.5.5: Mass-flow characteristics of the pipe-bend combinations

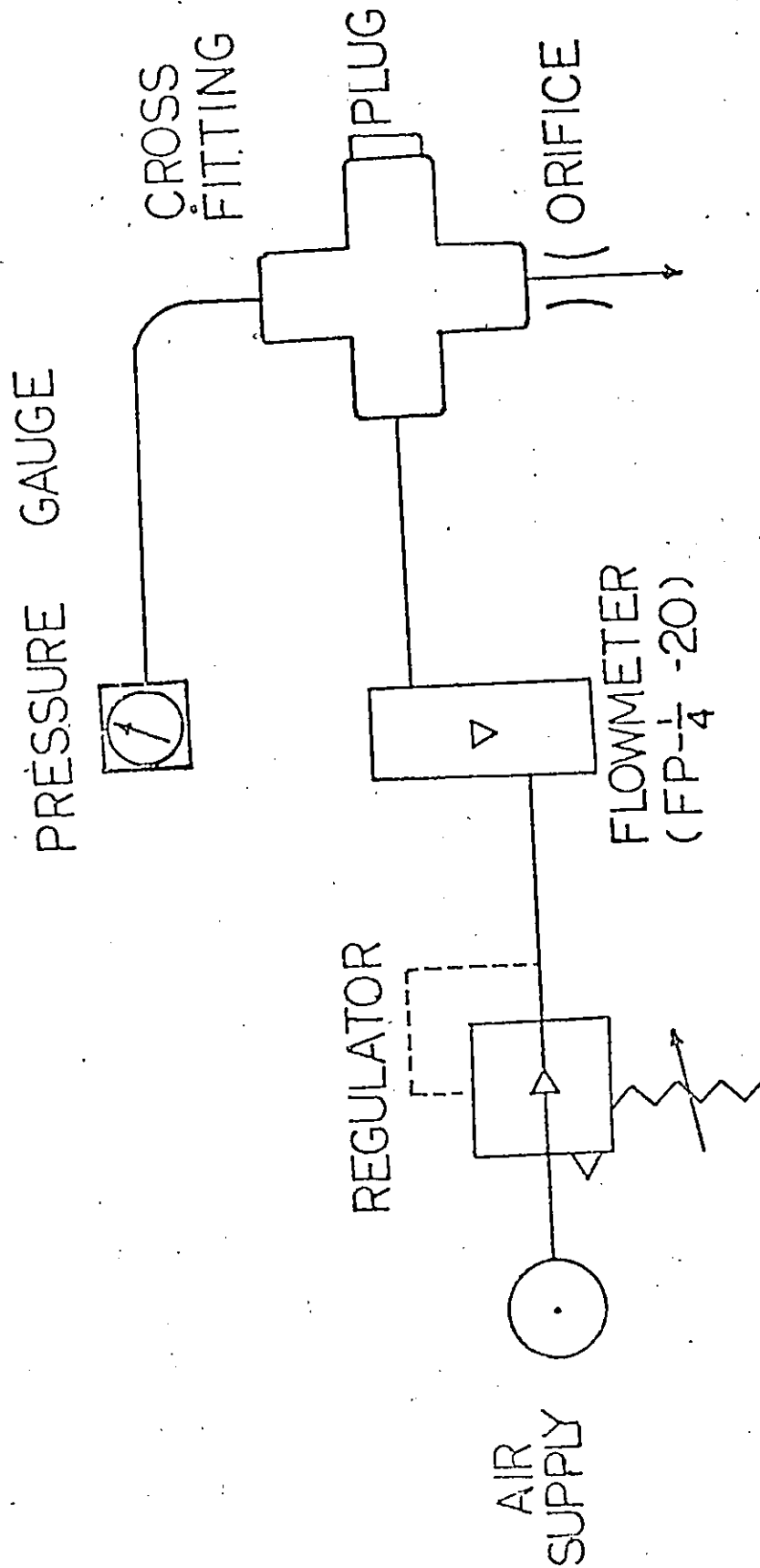


Fig. 5.6: Set-up for the orifice test

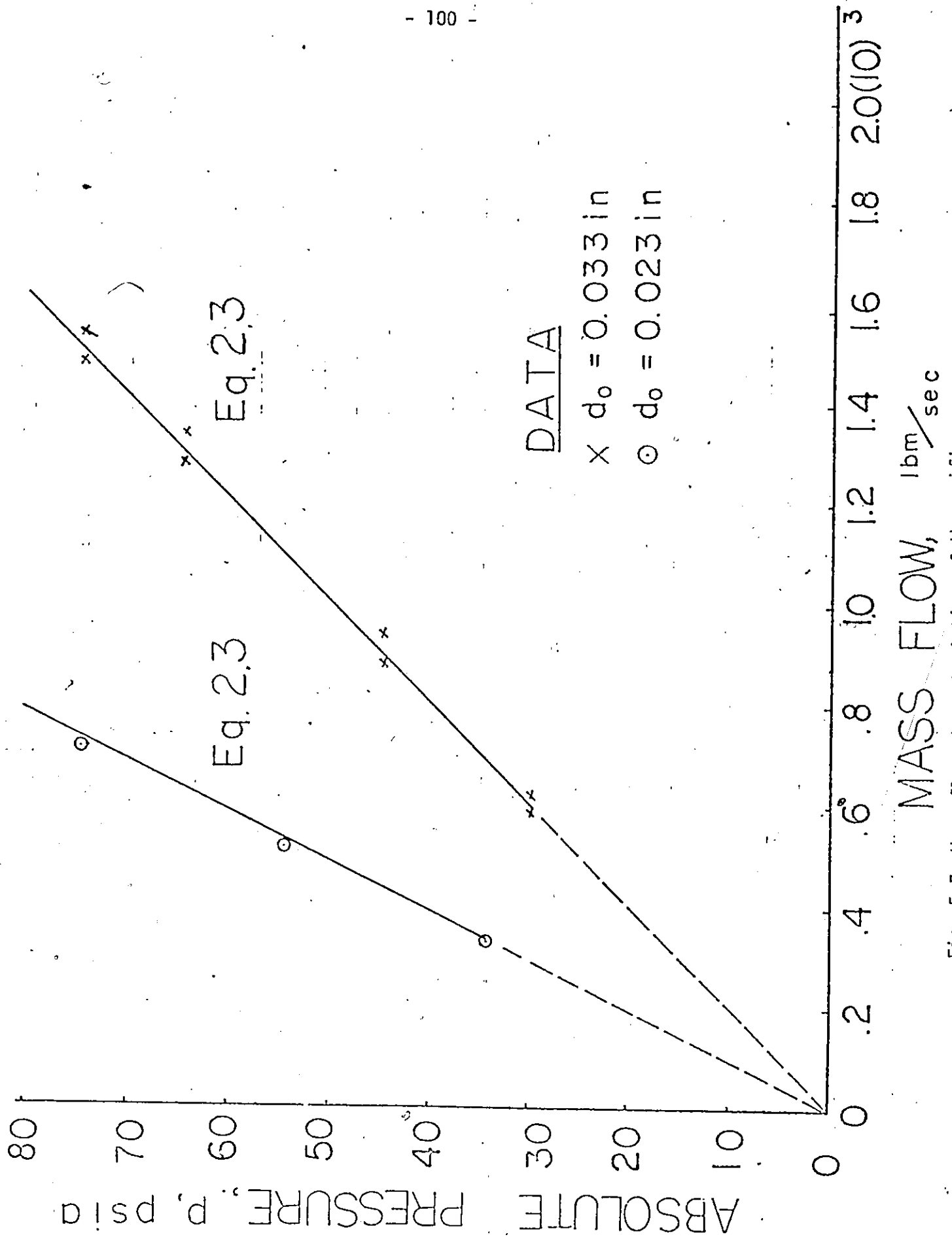


Fig. 5.7: Mass-flow characteristics of the orifices

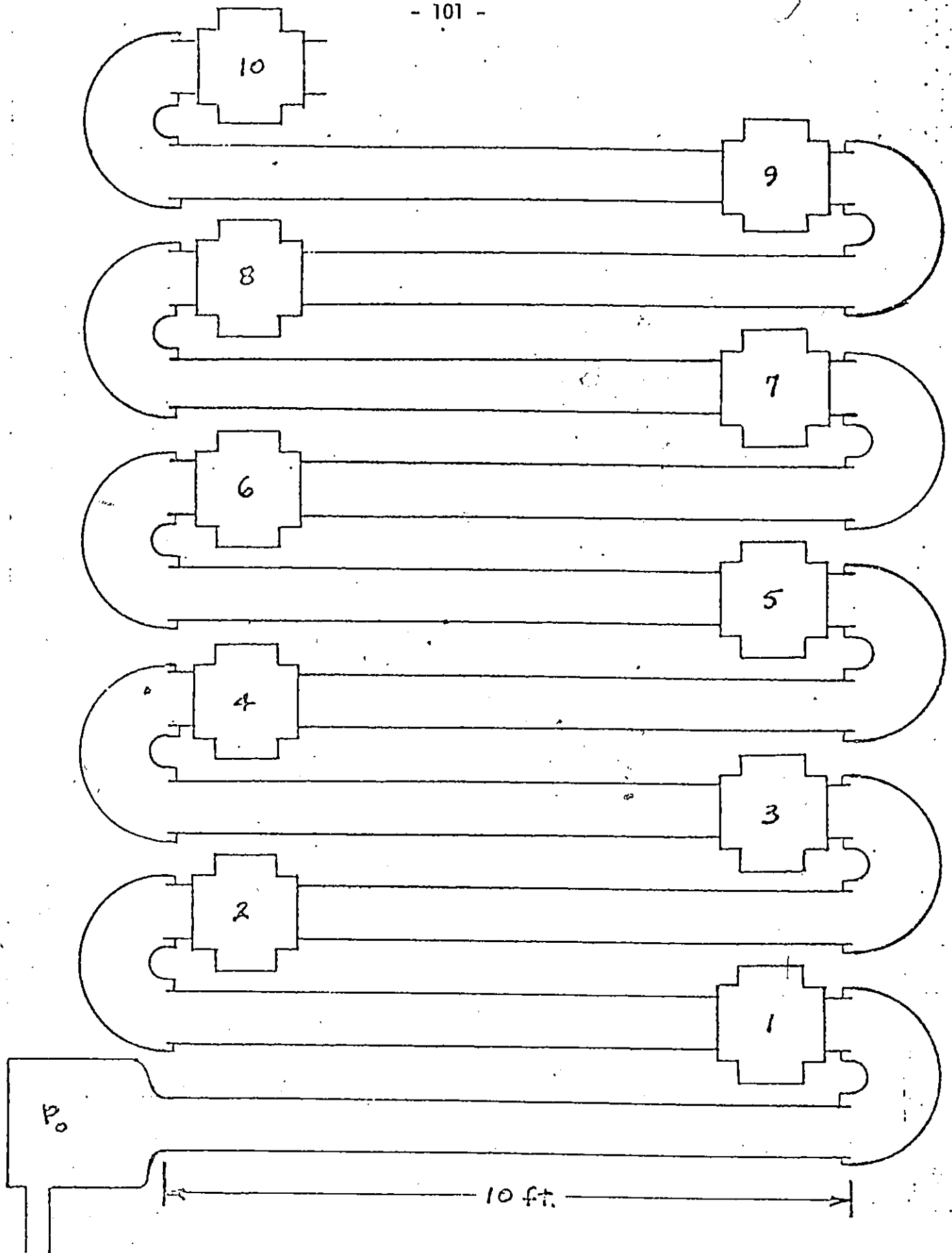
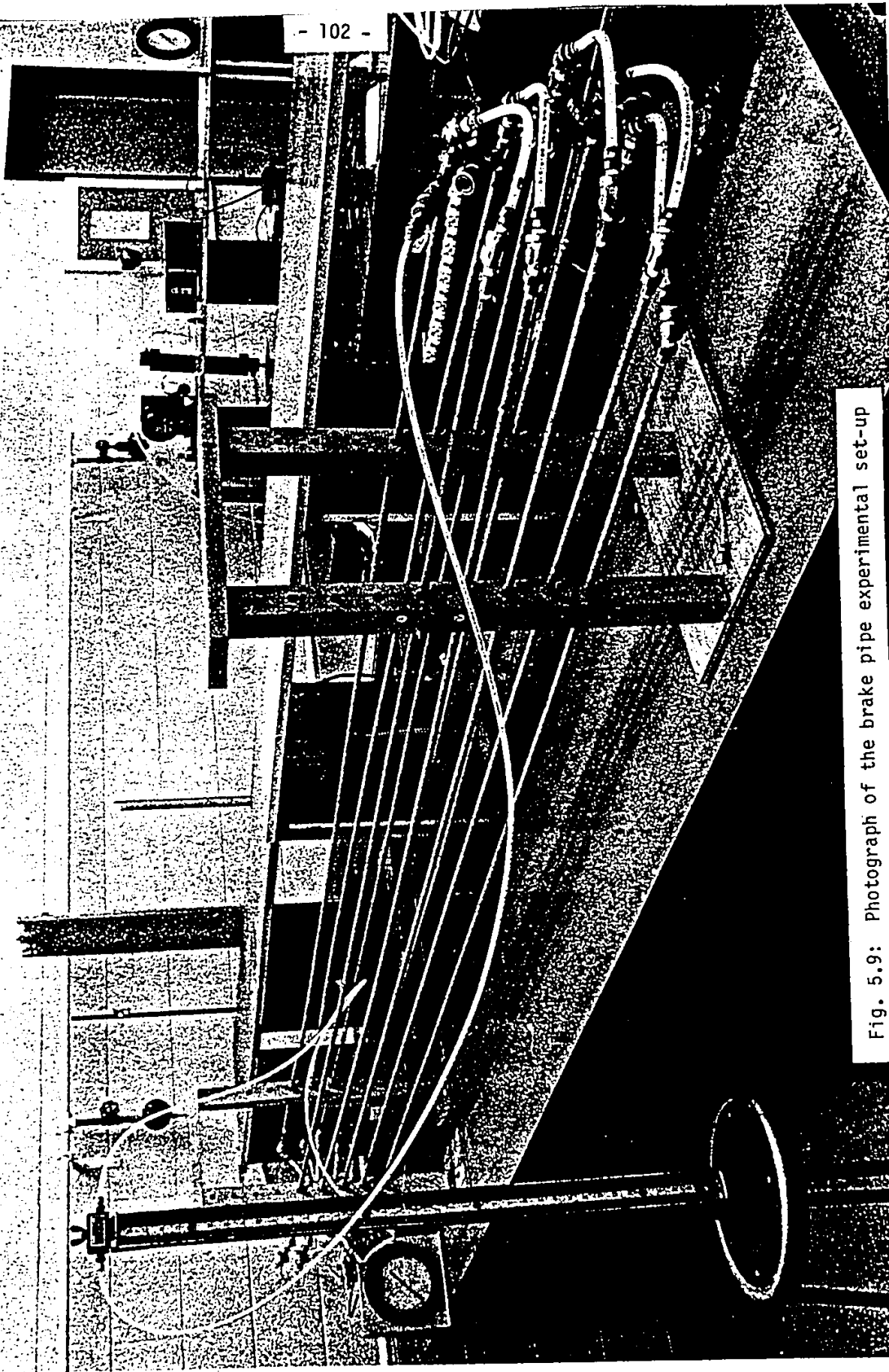


Fig. 5.8: Schematic drawing of brake pipe experiment model

NO SMOKING
OR ALCOHOL
IN THE AREA

- 102 -

Fig. 5.9: Photograph of the brake pipe experimental set-up



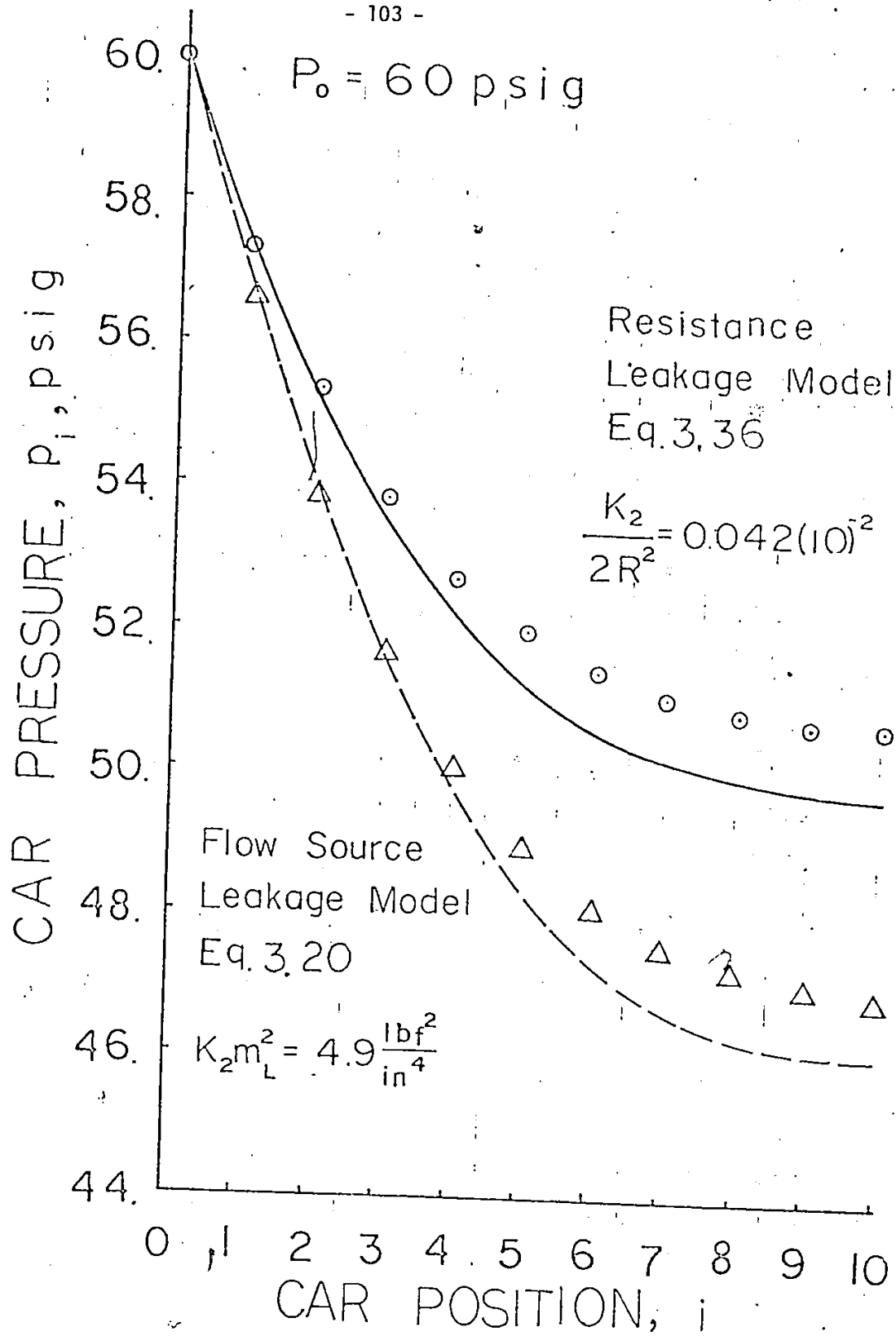


Fig. 5.10: Pressure gradient curves ($P_0 = 60 \text{ psig}$)

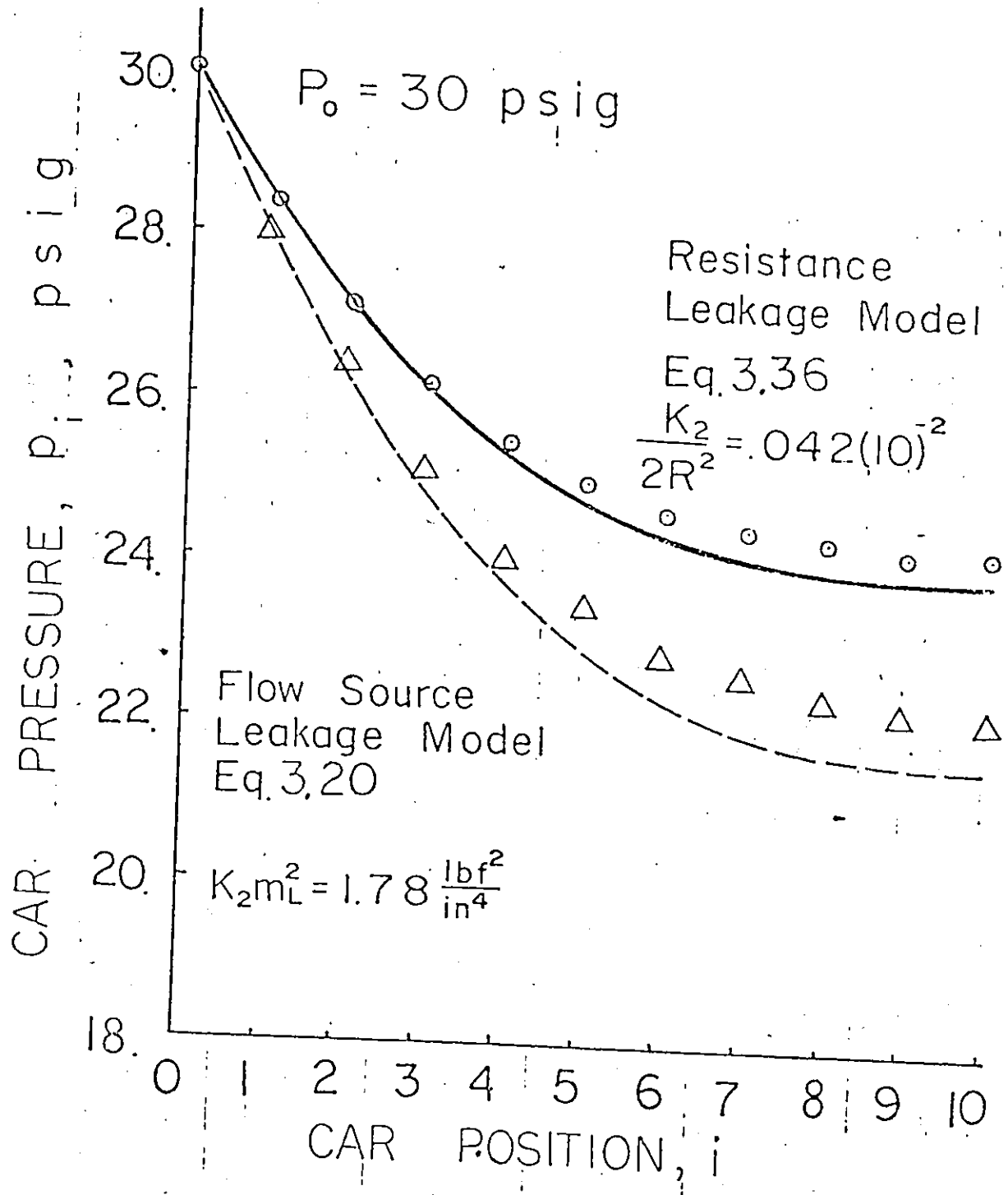


Fig. 5.11: Pressure gradient curves ($P_0 = 30$ psig)

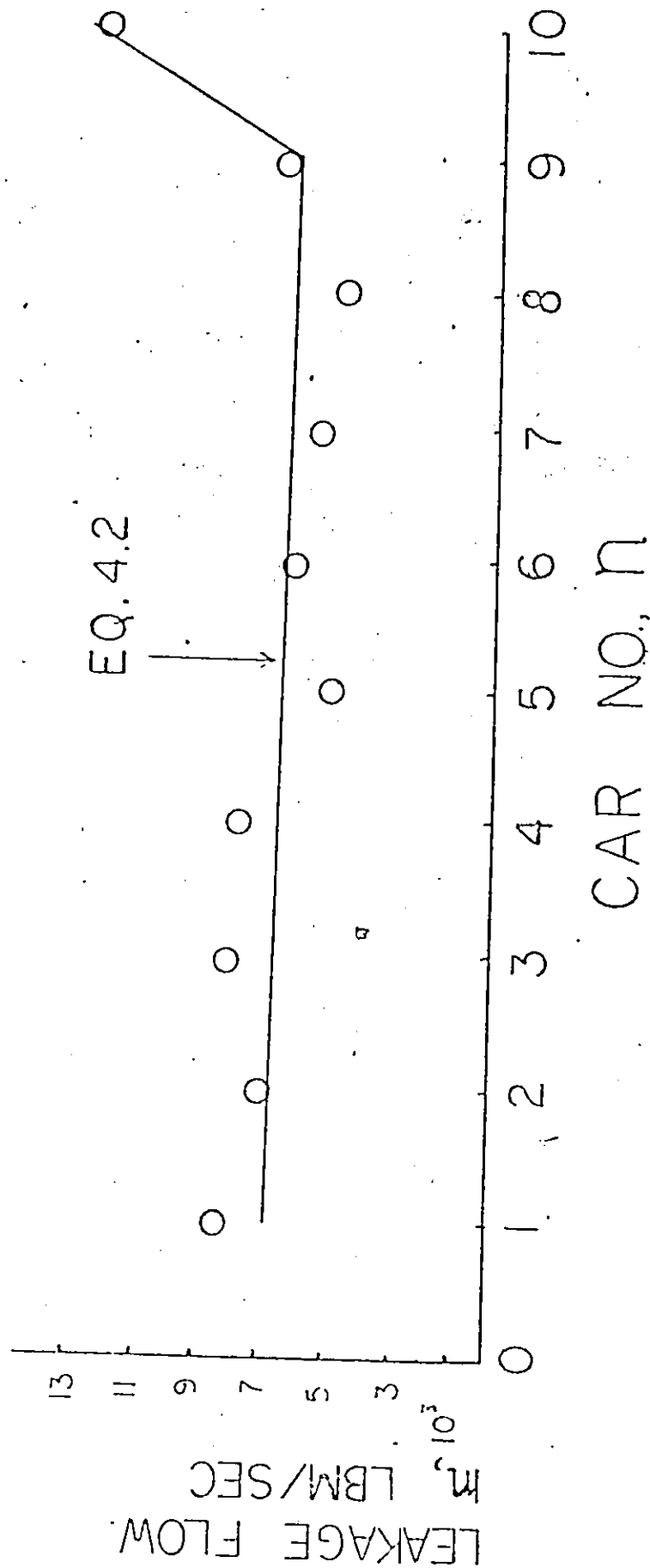
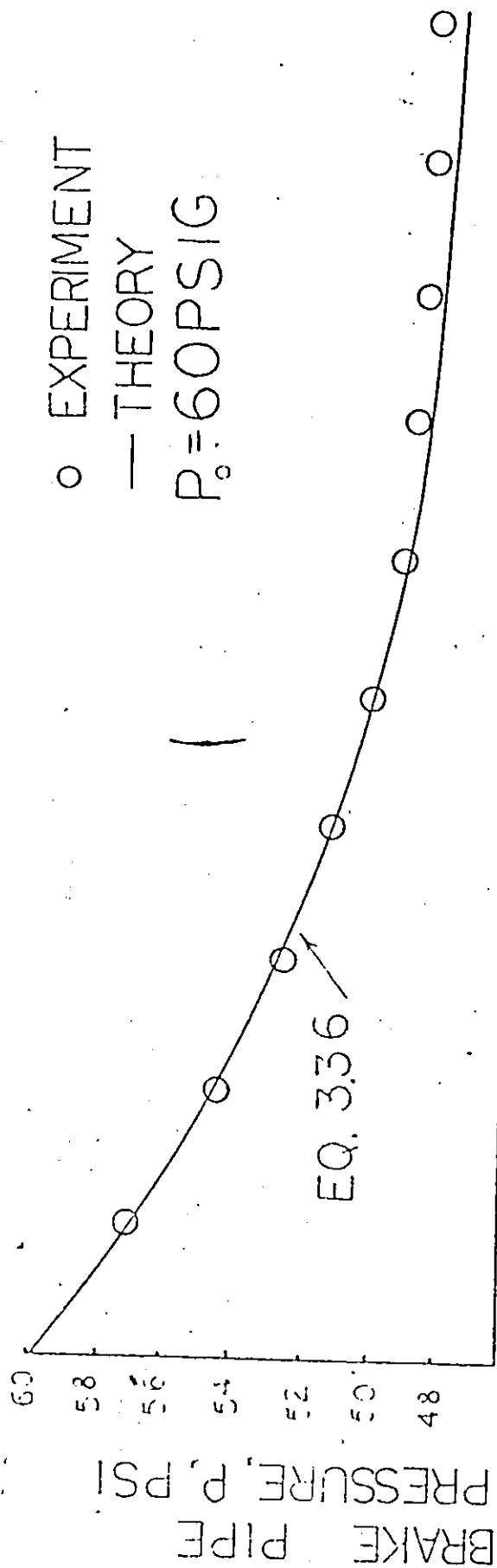


Fig. 5.12: Leakage detection (largest orifice at 10th pipe)

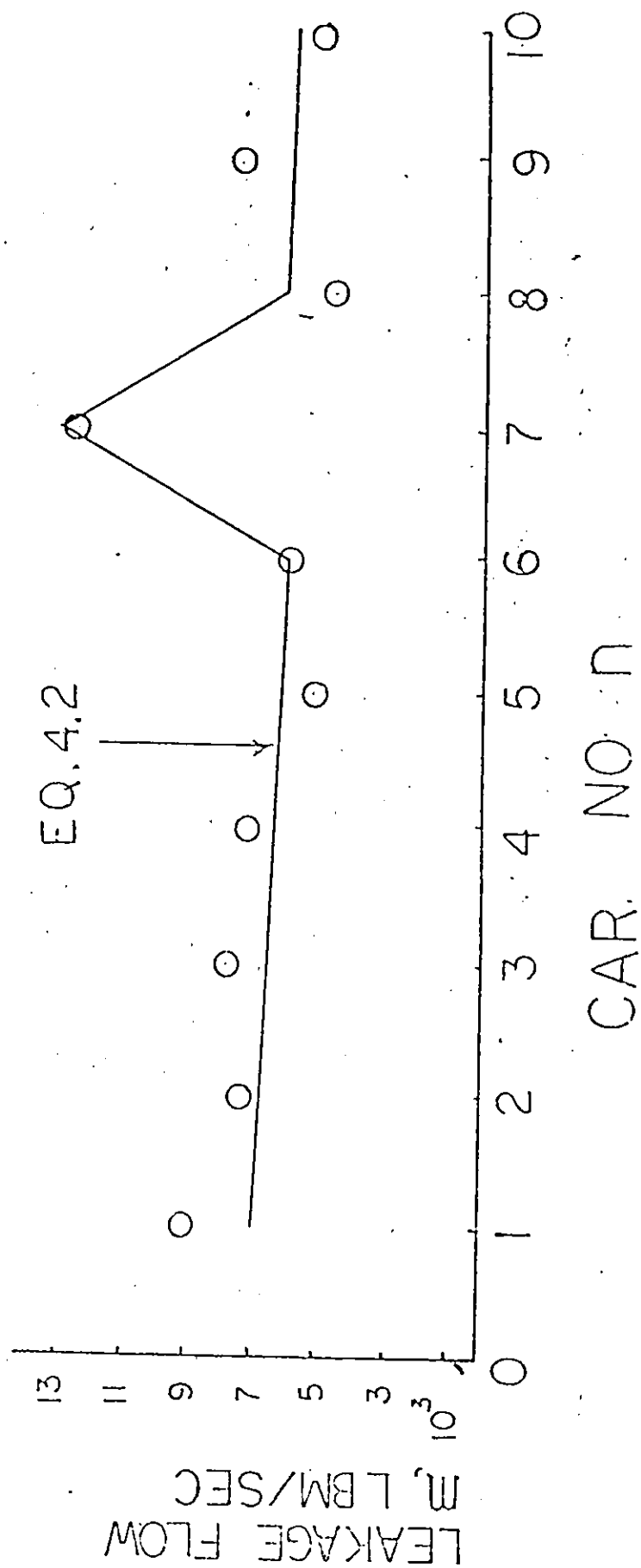
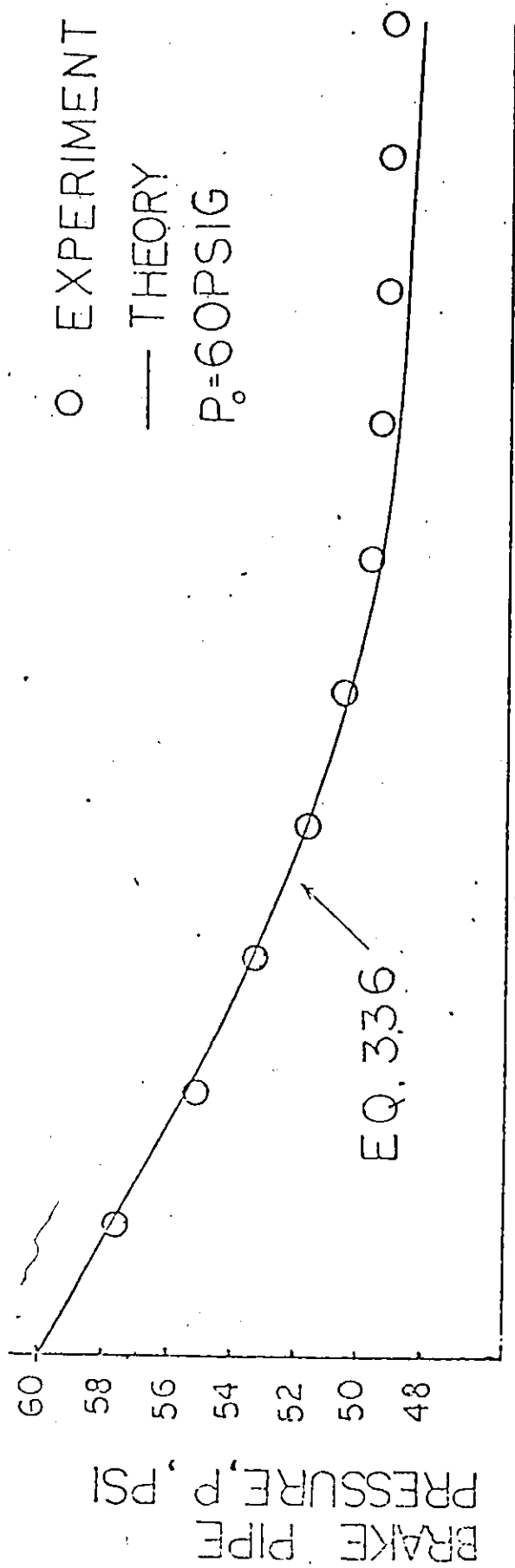


Fig. 5.13: Leakage detection (largest orifice at 7th pipe)

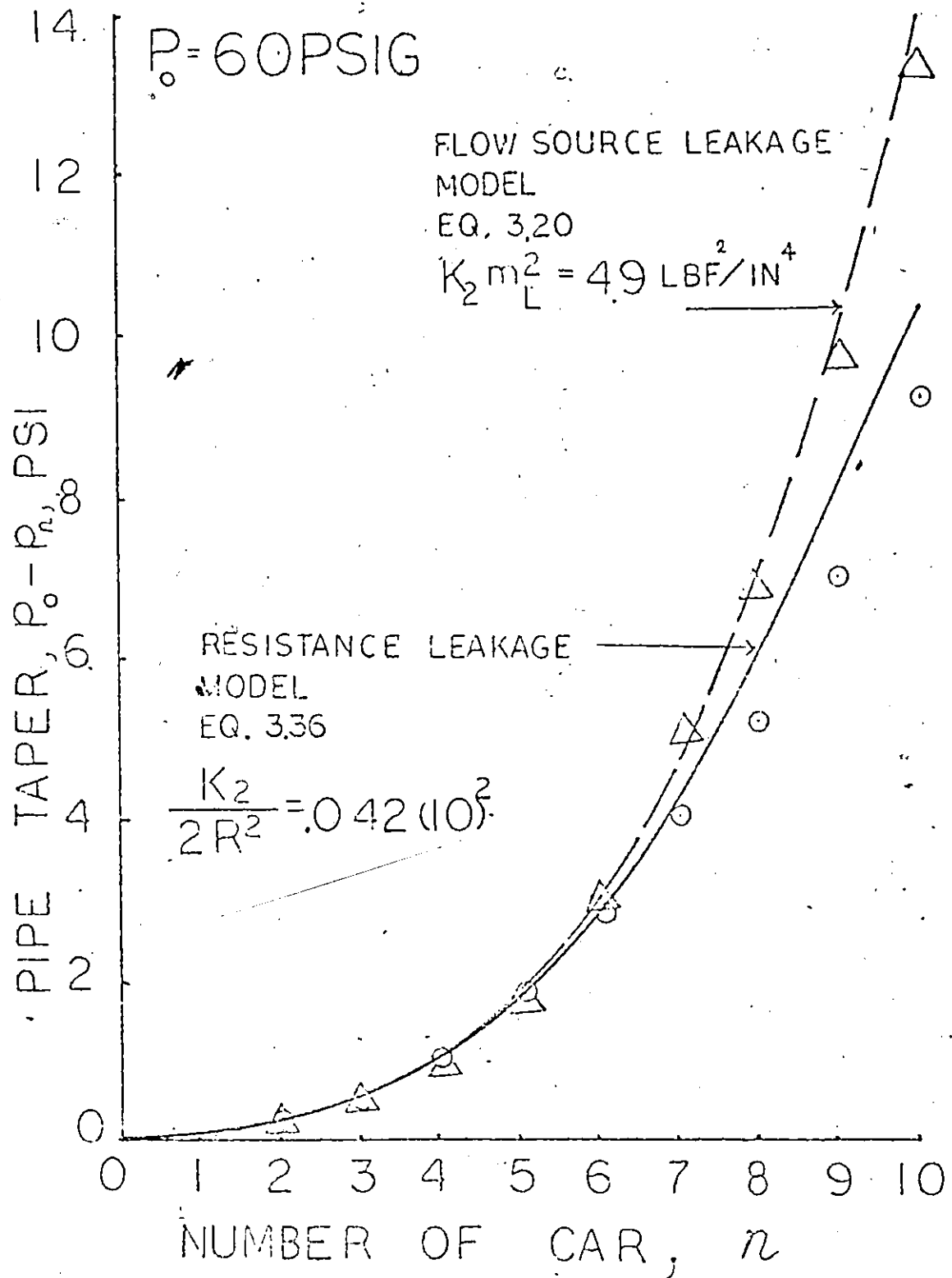


Fig. 5.14: Taper VS no. of cars ($p_0 = 60$ psig)

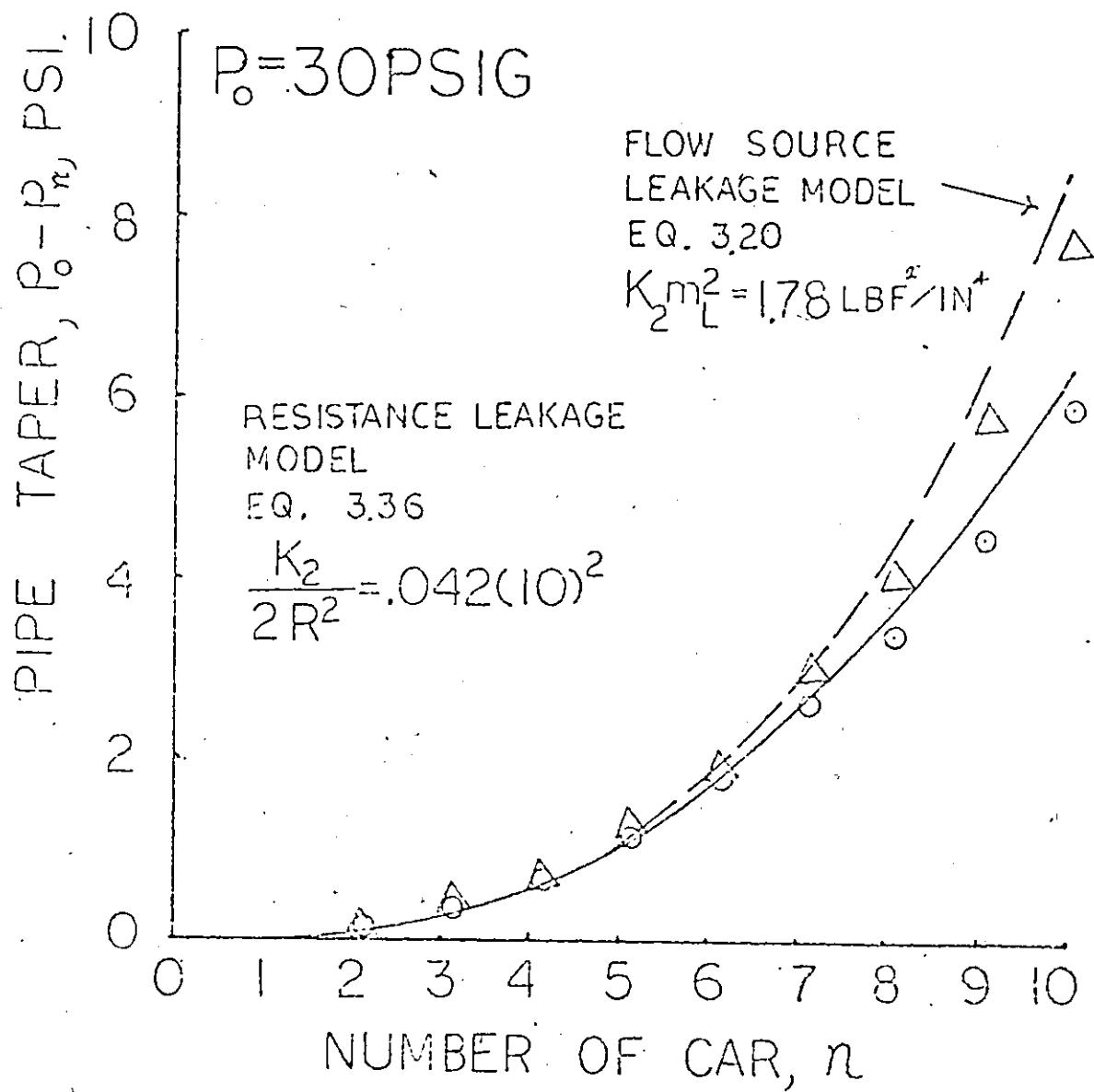


Fig. 5.15: Taper VS no. of cars ($P_0 = 30 \text{ psig}$)

APPENDIX ONE

From Darcy's formula, head loss through a pipe is:

$$h_L = 72 f \frac{l}{d} \frac{v^2}{g_c} \quad (A.1.1)$$

Thus, the pressure drop between 2 points along a pipe is:

$$p = 72 f \frac{l}{d} \frac{\rho v^2}{g_c} \quad (A.1.2)$$

for laminar flow $f = \frac{64}{R_e}$ (A.1.3)

R_e is the Reynolds number of the flow,
and

$$R_e = \frac{12 v d \rho}{\mu g} \quad (A.1.4)$$

$$m = 3 \pi d^2 v \rho \quad (A.1.5)$$

substituting A.1.3, A.1.4, A.1.5 into A.1.2, one gets:

$$p_i - p_{i+1} = K_1 m \quad (A.1.6)$$

where i refers to points along a pipe and

$$K_1 = \frac{128 \mu l}{\pi \rho d^4}$$

For compressible flow, the ρ appears in equation A.1.2 is not a constant. One can approximate the density as :

$$\rho = \frac{P_i - P_{i+1}}{2 R T} \quad (A.1.7)$$

Substituting A.1.7, A.1.5 into A.1.2 yields

$$P_i^2 - P_{i+1}^2 = K_2 m^2 \quad (A.1.8)$$

where

$$K_2 = \frac{16 f L R T}{\pi^2 d^5 g_c}$$

APPENDIX TWO

When a flow through an orifice to atmosphere, if the upstream pressure is p_1 , and the pressure ratio p_2/p_1 is less than 0.528, the flow is a ~~chuck~~ ^{choked} flow. The mass through the orifice will be proportional to the upstream pressure:

$$\dot{m} = \frac{K P_1 a \sqrt{T}}{\sqrt{T}} \quad (A.2.1)$$

The factor K is given by :

$$K = \left[\frac{\gamma g_c}{R} \left(\frac{2}{\gamma+1} \right)^{\frac{\gamma+1}{\gamma-1}} \right]^{\frac{1}{2}}$$

for air, if $\gamma = 1.4$ and $R = 639 \text{ in}^2/\text{lb} \cdot \text{R}$ then $K = 0.5318$,

If A is the effective area, equation A.2.1 may be written as

$$P_1 = \frac{4 \sqrt{T}}{0.5318 \pi C_d d_o^2} \dot{m} \quad (A.2.2)$$

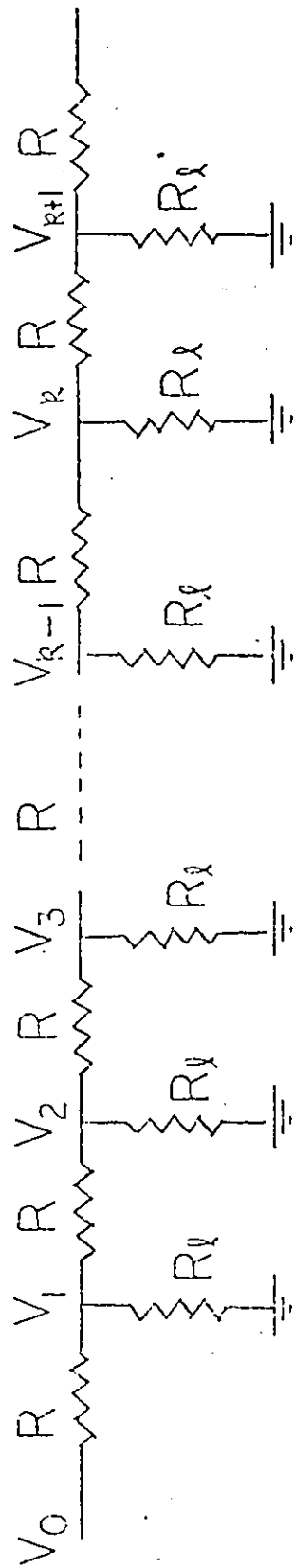


Fig. A.1: Shunt resistances uniformly distributed

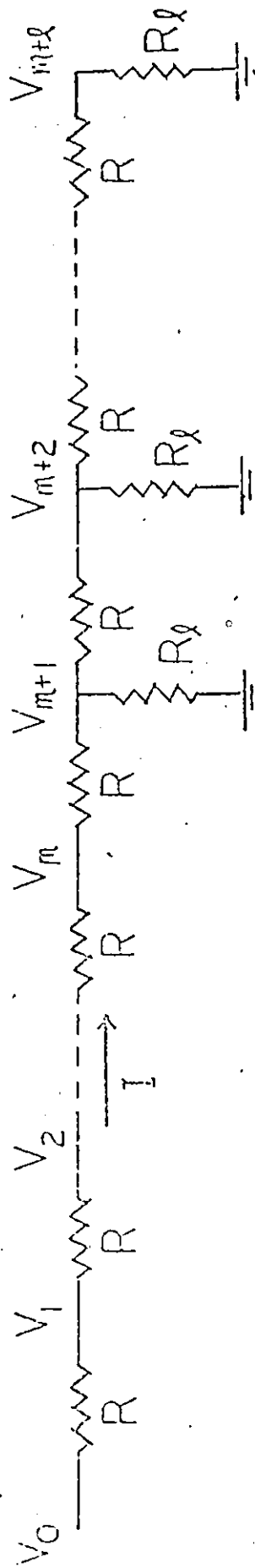


Fig. A.2: Shunt resistances concentrated at the rear

APPENDIX THREE

Figure A.1 shows the ladder network formed by series resistances R and shunt resistances R_1 . The node equation for typical section is given as :

$$\frac{V_{k-1} - V_k}{R} = \frac{V_k}{R_1} + \frac{V_k - V_{k+1}}{R} \quad (A.3.1)$$

Let $y = 2R/R_1$, $k=n+1$, one gets:

$$P(n) - y P(n+1) + P(n+2) = 0 \quad (A.3.2)$$

transformation of equation A.3.2 yields

$$V(z) - y z [V(z) - V(0)] + z^2 [V(z) - V(0)] - z V(1) = 0 \quad (A.3.3)$$

After some factoring, equation A.3.3 becomes :

$$V(z) = \frac{V(0) z (z - y/2)}{z^2 - yz + 1} + \frac{(V(1) - V(0) y/2) z}{z^2 - yz + 1} \quad (A.3.4)$$

Inverting equation A.3.4, one gets :

$$V(i) = V(0) \cosh bi - \frac{2}{\sqrt{y^2 - 4}} \left[\frac{V(0)y}{2} - V(1) \right] \sinh bi$$

(A.3.5)

$$b = \cosh^{-1} \frac{y}{2}, \quad y = 2 \cosh b$$

Given the boundary condition that there is no flow from rear car, one gets :

$$\left[\frac{p_i}{p_0} \right] = \frac{\cosh b (n - i + 1/2)}{\cosh b (n + 1/2)}$$

(A.3.6)

where

$$b = \cosh^{-1} \frac{y}{2}, \quad y = 2 \frac{R}{R_l}$$

The circuit shown in Figure A.2 is divided into two portions. They are the front portion and the rear portion. The front portion is formed by series resistances representing brake pipes without leakage. The rear portion, is formed by series resistances and shunt resistances, represents brake pipes and resistance leakage, and also has the same mathematical formulations as circuit in Fig. A.1.

$$\frac{V_{m+1}}{V_m} = \frac{\cosh b (l - j + 1/2)}{\cosh b (l + 1/2)} \quad (A.3.7)$$

where :

$$b = \cosh^{-1} y/2, \quad y = 2 + R/R_l$$

Applying eq. A.3.7 to the first series resistance of the rear portion, one gets:

$$\frac{V_{m+1}}{V_m} = \frac{\cosh b (l - 1/2)}{\cosh b (l + 1/2)} \quad (A.3.8)$$

$$V_m - V_{m+1} = V_m \left[\frac{\cosh (l + 1/2) - \cosh (l - 1/2)}{\cosh b (l + 1/2)} \right] \quad (A.3.9)$$

Let I be the flow through series resistances in front portion, and it is the same flow through the first series resistance of the rear portion.

$$V_m - V_{m+1} = IR \quad (A.3.10)$$

Since there are M resistances in the front portion, one can relate V_a to V_m by

$$V_a - V_m = IMR \quad (A.3.11)$$

Substituting A.3.10 and A.3.11 into A.3.9, one has

$$V_m = \frac{V_a}{1 + M \left[\frac{\cosh b(l + \frac{1}{2}) - \cosh b(l - \frac{1}{2})}{\cosh b(l + \frac{1}{2})} \right]} \quad (A.3.12)$$

and from A.2.9 and A.2.10, one also gets

$$I = \frac{V_m}{R} \left[\frac{\cosh b(l + \frac{1}{2}) - \cosh b(l - \frac{1}{2})}{\cosh b(l + \frac{1}{2})} \right] \quad (A.3.13)$$

If the voltage gradient is related to each series resistance in the circuit, from the front portion, one obtains

$$V_a - V_i = I i R \quad \text{for } 0 < i \leq m$$

$$V_i = V_a - I i R$$

(A.3.14)

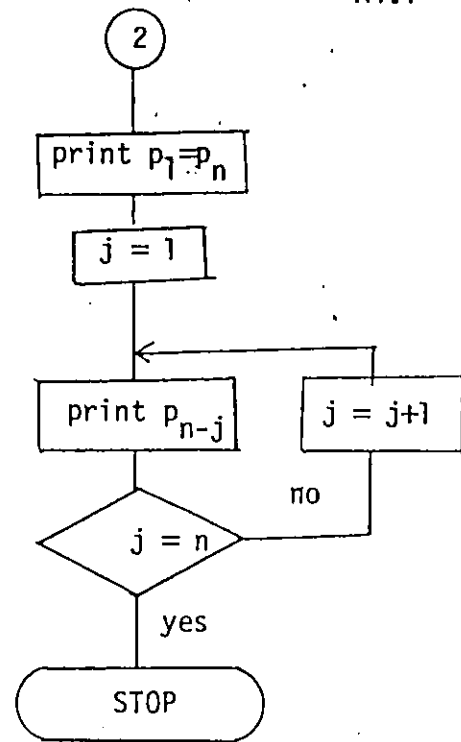
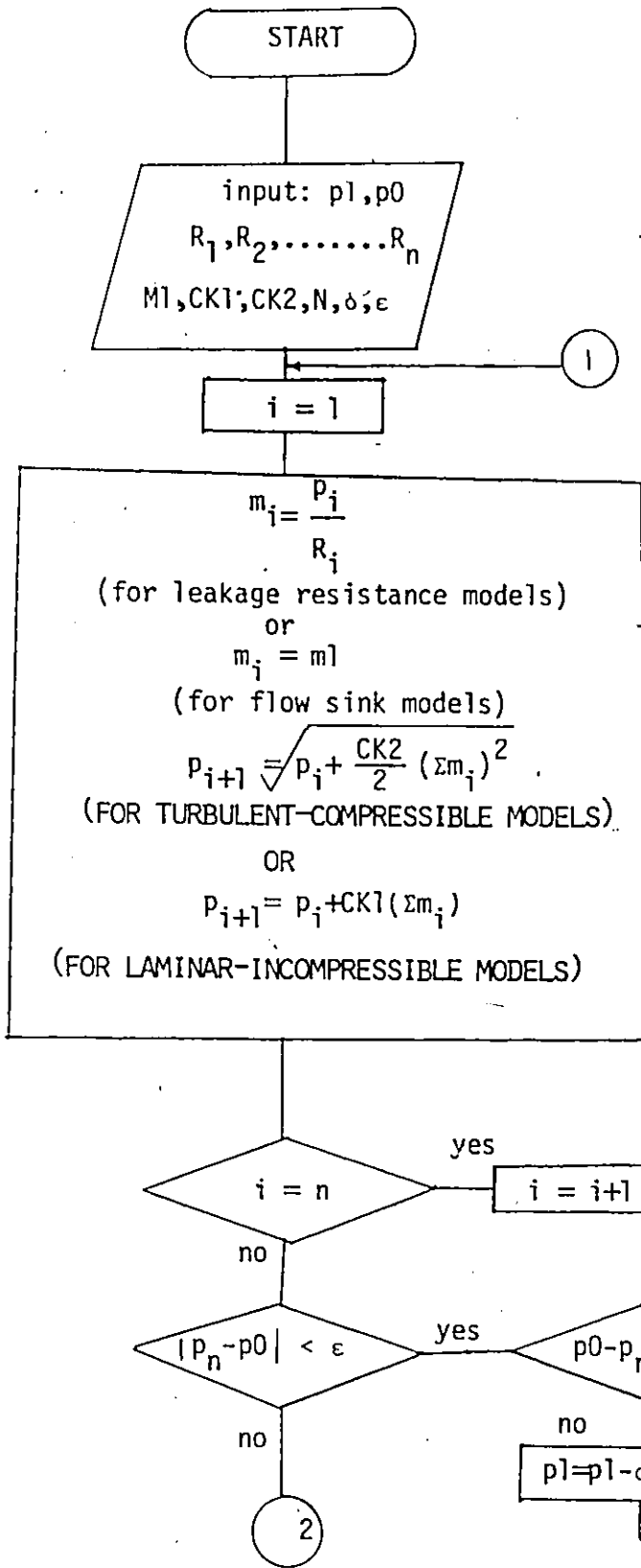
In the rear portion, one obtains

$$\frac{V_i}{V_m} = \frac{\cosh b (l - (i - m) + 1/2)}{\cosh b (-1 + 1/2)}$$

(A.3.15)

for $m < i < n$

where $n = m + 1$



$p1$ first gussed value
 for the pressure at last
 car
 $p0$ locomotive pressure
 $R_1 \dots R_n$ resistance for
 turbulent-compressible
 flow
 $m1$ flow from flow sink elements
 $CK1$ pipe constant for
 laminar-impressible flow
 $CK2$ pipe constant for
 turbulent-compressible flow
 ϵ maximum error for $p0$
 σ step for the new $p1$